Diffusion Coefficients in Multicomponent Mixtures

Medvedev, Oleg

Publication date:
2005

Document Version
Publisher's PDF, also known as Version of record

Diffusion Coefficients in Multicomponent Mixtures

Oleg Medvedev

2005

Ph.D. Thesis

DTU

TECHNICAL UNIVERSITY OF DENMARK
DEPARTMENT OF CHEMICAL ENGINEERING

Preface

This thesis is submitted as partial fulfillment of the requirements for obtaining the Ph.D. degree at the Technical University of Denmark. The work was carried out at the IVC-SEP, Department of Chemical Engineering, from November 2001 to November 2004 under the supervision of Associate Professor Alexander A. Shapiro. The project was financially supported by the Danish Technical Research Council as a part of the Talent Project, granted to Alexander A. Shapiro.

First of all, I am very grateful to Associate Professor Alexander A. Shapiro for his supervision throughout the project, for sharing his knowledge and experience, and for interesting and pleasant non-professional communications. I would like to acknowledge all staff of the IVC-SEP research group for creating the friendly and highly professional environment. It has been a big pleasure to work in the IVC-SEP.

I feel grateful to Professor Pavel Bedrikovetsky for spending 6 months in his group in Laboratory of Petroleum Engineering and Exploration (LENEP), State University of Norte Fluminense (UENF). These 6 months were very interesting in both professional and non-professional aspects. Dr. Adriano dos Santos and Dr. José Eurico Altoé Filho have shared their knowledge and helped me a lot during my stay in Brazil. I am also grateful to them for pleasant communications and time we spent together.

The participation of Dr. Guillaume Galliero in the last stages of project was very helpful. It provided a better insight onto the conducted work and showed the directions for further development. I am grateful to Guillaume for this and for many interesting conversations.

The great time, spent together, and constant support from my friends and colleagues: Roman Berenblyum, Petr Zhelezny, Sergey Artemenko, Dasha Khvostitchenko and Thomas Lindvig should be definitely mentioned here. I am very grateful to my friends in Ukraine and Russia, for keeping in touch and supporting me.

My everlasting gratitude goes to my parents and my sister – for loving and supporting me. The last, but not the least, is my wife Natasha, who was always really or virtually beside me during past years, sharing my feelings and supporting me.

Copenhagen. November, 2004

Oleg Medvedev

Summary

Diffusion is the process of relative motion of different components in a mixture. Diffusion mass transfer commonly appears in various industrial processes, including the processes of chemical and petroleum engineering, as well as natural processes related to ecological applications. Knowledge of diffusion coefficients is important for proper description of such processes. Diffusion is normally a slow process and is a rate determining factor in many cases of mass transfer. The hydrodynamic theory of diffusion mass transfer is well developed. However there is no rigorous theory for estimation of the constituting parameters in this theory, the diffusion coefficients.

For binary liquid mixtures, extensive databases of experimental values of diffusion coefficients are available. A number of models and correlations for their evaluation is developed. Since these models and correlations are built on empirical or semi-empirical grounds, their predictive capacity is limited. This is a strong limitation, especially because of the limited amount of experimental data available for verification of the models. Lack of rigorous physical theory for diffusion coefficients in liquids and a scarce amount of experimental data for multicomponent mixtures makes it difficult to predict the values of binary diffusion coefficients, and impossible to determine the values of the multicomponent diffusion coefficients outside the ranges of the experimental data available.

In the present work, an extensive overview of the mass transfer theory and existing methods for estimation of diffusion coefficients is presented. A large number of experimental data for diffusion coefficients in binary and ternary mixtures is collected, and the most widely used experimental methods are analyzed. Existing models for the diffusion coefficients are also analyzed in detail. It is shown that the existing situation with regard to estimation of the diffusion coefficients requires further development of the theory and a search for more theoretically grounded approaches.

Recent developments of the fluctuation theory for diffusion coefficients may provide a rigorous theoretical framework for modeling the diffusion coefficients. The fluctuation theory (FT) for diffusion coefficients is based on the principles of the general statistical fluctuation theory and non-equilibrium thermodynamics, and contains no model assumptions. An expression for the matrix of diffusion coefficients, obtained in the framework of the FT approach, contains several contributions responsible for different physical mechanisms forming these coefficients. Separation of the thermodynamic, kinetic and resistance factors, contributing to the matrix of diffusion coefficients, makes it possible to obtain a fundamental and physically interpretable description of the diffusion coefficients. The thermodynamic contribution is evaluated on the basis of an appropriate thermodynamic model (equation of state) for the mixture, but, unlike many previous approaches, it is not related to a specific

model. The resistance contribution depends on the newly introduced parameters, *the penetration lengths.* Choice of a specific expression for the penetration lengths may be considered as development of a specific model in the framework of the FT approach.

The present study has aimed at developing a specific, practically applicable approach to modeling diffusion coefficients in the framework of the fluctuation theory.

Two different ways for modeling the penetration lengths (and correspondingly the diffusion coefficients) are considered. The first way is based on the phenomenological considerations and is focused on relating the penetration lengths to the physical properties of the components in the mixture. The particular expressions for the penetration lengths are adjusted to a large number of the experimentally measured diffusion coefficients in binary liquid mixtures. Excellent description of the experimental binary diffusion coefficients over wide temperature and concentration range is obtained. The influence of the choice of a thermodynamic model, used for estimation of thermodynamic contribution, is analyzed. A clear physical meaning of different parameters entering the penetration lengths is demonstrated. Some of these parameters (the so-called penetration volumes) are correlated with the parameters of the equations of state for individual components.

The second way is based on molecular dynamics (MD) simulations, which are used to estimate the penetration lengths. A combination of the molecular dynamics and the FT theory creates a new, “mixed” approach to prediction of the diffusion coefficients. While the thermodynamic and kinetic factors are found from thermodynamic modeling, the resistance factor is estimated on the basis of MD simulations. It is shown that penetration lengths, obtained in the framework of the thermodynamic modeling, agree very well with the penetration lengths obtained by MD simulations.

The prediction capabilities of both proposed approaches are discussed. It is shown that objective physical reasons make it difficult to make the phenomenological approach fully predictive (at least with a reasonable degree of accuracy). This is related to the high sensitivity of the transport properties, like diffusion coefficients, to the volumetric properties in the liquid state.

In the final chapter of the thesis, a procedure for verification of the experimental diffusion coefficients in multicomponent mixtures is developed. The procedure is based on the utilization of the Onsager reciprocal relations, which impose the symmetry of the phenomenological coefficients in multicomponent mixtures. The four experimentally measured Fick diffusion coefficients in ternary mixtures may be reduced to the Onsager phenomenological coefficients by means of thermodynamic transformations. Verification of the experimentally measured diffusion coefficients makes it possible to evaluate both the quality of experimental information and applicability of the thermodynamic models to the modeling of diffusion coefficients.

Resumé

Diffusion er processen bestående af forskellige komponenters relative bevægelse i en blanding. Diffusionsmasseoverførelse forekommer almindeligvis i forskellige industrielle processer, inklusive processerne i kemi- og olieteknik, såvel som naturlige processer med relation til økologiske anvendelser. Viden om diffusionskoefficienterne er vigtig for at kunne beskrive sådanne processer rigtigt. Diffusion er normalt en langsom proces og en hastighedsbestemmende faktor i mange tilfælde af masseoverførsel. Den hydrodynamiske teori om diffusionsmasseoverførsel er veludviklet. Der er imidlertid ingen rigoristisk teori til beregning af de grundlæggende parametre, diffusionskoefficienterne, i denne teori.

Med hensyn til binære væskeblandinger findes der omfattende databaser med eksperimentelle værdier for diffusionskoefficienter. En række modeller og korrelationer til evaluering af disse udvikles. Siden disse modeller og korrelationer bygger på et empirisk eller semi-empirisk grundlag, er deres forudsigende evne begrænset. Dette er en stærk begrænsning, især på grund af den begrænsede mængde eksperimentelle data der er til rådighed for verificering af modellerne. Mangel på rigoristisk fysisk teori for diffusionskoefficienter i væske og knap mængde af eksperimentelle data for multikomponentblandinger gør det vanskeligt at forudsige værdierne af binære diffusionskoefficienter og umuligt at bestemme værdierne af multikomponentdiffusionskoefficienterne uden for området af til rådighed værende eksperimentelle data.

I dette værk gives et omfattende overblik over masseoverførselsteorien og eksisterende metoder til beregning af diffusionskoefficienterne. Et stort antal eksperimentelle data for diffusionskoefficienter i binære og ternære blandinger indsamles, og de mest anvendte eksperimentelle metoder analyseres. Eksisterende modeller for diffusionskoefficienterne analyseres også detaljeret. Det påvises, at den eksisterende situation med hensyn til beregning af diffusionskoefficienterne kræver videreudvikling af teorien og søgen efter mere teoretisk funderede fremgangsmåder.

En nylig udvikling i fluktuationsteorien for diffusionskoefficienter kan give en rigoristisk teoretisk ramme for modellering af diffusionskoefficienterne. Fluktuationsteorien (FT) for diffusionskoefficienter er baseret på principperne for generel statistisk fluktuationsteori og ikke-ligevægtstermodynamik og indeholder ingen modelantagelser. Et udtryk for diffusionskoefficientsmatricen, der er nået inden for rammerne af FT-fremgangsmåden, indeholder adskillige bidrag, der er årsag til forskellige fysiske mekanismer, som danner disse koefficienter. En adskillelse af termodynamiske, kinetiske og modstandsfaktorer, der bidrager til diffusionskoefficientsmatricen, gør det muligt at få en fundamental og fysisk udlagt beskrivelse af diffusionskoefficienterne. Det termodynamiske bidrag evalueres på

grundlag af en egnet termodynamisk model (tilstandsligning) for blandingen, men, til forskel fra mange tidligere fremgangsmåder, er den ikke relateret til en specifik model. Modstandsbidraget afhænger af de nylig introducerede parametre, penetrationslængderne. Valget af et specifikt udtryk for penetrationslængderne kan ses som udvikling af en specifik model inden for rammerne af FT-fremgangsmåden.

Nærværende afhandling har haft som mål at udvikle en specifik, praktisk anvendelig fremgangsmåde til modellering af diffusionskoefficienter inden for rammerne af fluktuationsteorien.

To forskellige måder at modellere penetrationslængderne på (og tilsvarende diffusionskoefficienterne) tages i betragtning. Den første måde er baseret på fænomenologiske betragtninger og fokuserer på at relatere penetrationslængderne til komponenternes fysiske egenskaber i blandingen. De specifikke udtryk for penetrationslængderne tilpasses til et stort antal eksperimentelt målte diffusionskoefficienter i binære væskeblandinger. En fremragende beskrivelse af de eksperimentelle binære diffusionskoefficienter i et bredt temperatur- og koncentrationsområde fås. Den indflydelse analyseres, som valget af termodynamisk model anvendt til beregning af termodynamisk bidrag har. En klar fysisk betydning af forskellige parametre, der indgår i penetrationslængderne, påvises. Nogle af disse parametre (de såkaldte penetrationsvoluminer) korreleres med tilstandsligningernes parametre for individuelle komponenter.

Den anden måde er baseret på molekylærdynamik (MD) simulationer, som bruges til at beregne penetrationslængderne. En kombination af molekylærdynamikken og FT-teorien skaber en ny, ”blandet” fremgangsmåde til forudsigelse af diffusionskoefficienterne. Medens de termodynamiske og de kinetiske faktorer findes ud fra termodynamisk modellering, beregnes modstandsfaktoren på grundlag af MD-simulationerne. Det påvises, at penetrationslængderne, opnået inden for rammerne af termodynamisk modellering, stemmer meget godt overens med de penetrationslængder, der er opnået ved MD-simulationerne.

Begge de foreslåede fremgangsmåders forudsigelsesevne diskuteres. Det vises, at objektive fysiske årsager gør det vanskeligt at gøre den fænomenologiske fremgangsmåde fuldtud forudsigende (i det mindste med en rimelig grad af nøjagtighed). Dette hænger sammen med transportegenskabernes høje følsomhed, som diffusionskoefficienter til de volumetriske egenskaber i flydende tilstand.

I afhandlingens sidste kapitel udvikles en procedure til verificering af de eksperimentelle diffusionskoefficienter i multikomponentblandinger. Proceduren er baseret på anvendelse af Onsager reciprokke relationer, som introducerer de fænomenologiske koefficienters symmetri i multikomponentblandingerne. De fire eksperimentelt målte Fick diffusionskoefficienter, som normalt omtales, når diffusionen i ternære blandinger måles, kan

reduceres til Onsager fænomenologiske koefficienter ved hjælp af de termodynamiske transformationer. Verificering af de eksperimentelt målte diffusionskoefficienter gør det muligt at evaluere både kvaliteten af den eksperimentelle information og anvendeligheden af de termodynamiske modeller til modellering af diffusionskoefficienter.

Table of Contents

Preface i

Summary in English iii

Resumé v

Table of Contents ix

1. Introduction 1-1

2. Diffusion Mass Transfer in Liquids 2-1

    2.1 Fick Equation 2-1

        2.1.1 Binary Diffusion 2-1

        2.1.2 Multicomponent Diffusion 2-2

    2.2 Thermodynamics of Irreversible Processes 2-6

        2.2.1 Multicomponent Diffusion 2-6

    2.3 Maxwell-Stefan Equations 2-9

        2.3.1 Binary Diffusion 2-9

        2.3.2 Multicomponent Diffusion 2-12

    2.4 Connection Between Different Formalisms 2-14

        2.4.1 Binary Diffusion Coefficients 2-14

        2.4.2 Multicomponent Diffusion Coefficients 2-15

    2.5 Summary 2-17

3. Diffusion Experiments 3-1

    3.1 Diaphragm Cell 3-2

    3.2 The Taylor Dispersion Method 3-5

    3.3 Interferometry 3-10

    3.4 Other Methods 3-12

    3.5 Multicomponent Mixtures 3-16

    3.6 Summary 3-19

4. Diffusion Coefficients in Binary Mixtures: an Overview 4-1

    4.1 Phenomenological Approaches 4-1

        4.1.1 An Approach Based on the Diffusion Coefficients at Infinite Dilution 4-1

        4.1.2 The Free Volume Methods 4-10

        4.1.3 The UNIDIF and the GC-UNIDIF 4-13

    4.2 Molecular Dynamics Simulations 4-15

    4.3 Summary 4-17

5. Diffusion Coefficients in Binary Mixtures: Fluctuation Theory 5-1

    5.1 Theoretical Background 5-1

        5.1.1 Fluctuation Theory for Diffusion Coefficients 5-1

5.1.2 Modeling the Thermodynamic Factor 5-3
5.2 The Diffusion Coefficients 5-6
5.2.1 Exponential Form of the Expression for Penetration Lengths 5-6
5.2.2 Quadratic Form of the Expression for Penetration Lengths 5-15
5.3 Predicting Diffusion Coefficients 5-23
5.3.1 Sensitivity of the Model 5-38
5.4 Summary 5-39
6. Molecular Dynamics Simulations of Penetration Lengths 6-1
6.1 Theoretical Background 6-1
6.1.1 The Velocity Autocorrelation Approach 6-2
6.1.2 The Probability Approach 6-3
6.2 Details of Computations 6-4
6.2.1 Phenomenological Approach 6-4
6.2.2 The Molecular Dynamics Approach 6-5
6.3 Preliminary Test of the Model 6-6
6.3.1 Velocity Autocorrelation Approach 6-6
6.3.2 Probability Approach 6-6
6.4 Results 6-8
6.5 Summary 6-13
7. Diffusion Coefficients in Ternary Mixtures 7-1
7.1 Analyzing Ternary Diffusion Coefficients 7-1
7.1.1 Theoretical Background 7-2
7.1.2 Details of Computations 7-3
7.1.3 Results and Discussion 7-5
7.1.4 Discussion 7-10
7.2 Overview of Existing Models for Diffusion Coefficients in Multicomponent Mixtures 7-11
7.2.1 Reduction of the Number of Independent Coefficients 7-11
7.2.2 Interpolation Schemes 7-13
7.2.3 Free Volume and Activation Energy Models 7-16
7.2.4 The FT Approach 7-18
7.3 Summary 7-19
8. Conclusions and Future Work 8-1
Nomenclature 9-1
References 10-1
Appendix A-1
A.1 Residual Internal Energy A-1

A.2 Derivatives of Residual Internal Energy A-2
A.3 Verifying the Approach to Estimation of the Thermodynamic Matrix A-3
A.4 Computational Background A-5
A.5 Influence of the Thermodynamic Model A-7

1. Introduction

It is well known that molecules in liquids, solids and gases participate in chaotic random Brownian motion, which is induced by their thermal energy. The rate of Brownian motion depends upon the temperature, the structure of a substance and molecular interactions. In an equilibrium state the molecules of different components are evenly distributed in space. Correspondingly, there is no preferred direction of Brownian motion, and it becomes "invisible".

When the concentrations are not evenly distributed over the volume, the system is in non-equilibrium, but it tends to the equilibrium state. The presence of concentration gradients induces molecular motion, which is referred to as *diffusion*. Diffusion tends to evenly distribute the concentrations and may be considered as a natural mechanism of homogenization of a substance, or as a process of mixing. The diffusion fluxes arise in response to the concentration gradients and usually transport the molecules from the regions of high to regions of low concentrations.

Diffusion is commonly present in a variety of natural and environmental processes, as well as in many industrial processes related to chemical, petroleum and other industries. Typical examples of such processes are the processes of distillation, absorption, extraction, in chemical engineering, the process of geological-scale formation of the hydrocarbon distributions in petroleum reservoirs, and many more. Diffusion mass transfer is normally rather slow, and therefore it often becomes a limiting factor for the overall rate of a process.

The rate of the diffusion mass transfer depends upon values of *diffusion coefficients*. In turn, these coefficients depend upon the thermodynamic conditions (temperature, pressure, composition of the mixtures). Proper modeling of the diffusion mass transfer requires knowledge of the diffusion coefficients. Since a majority of the processes involve the mixtures consisting of many different components, knowledge of the multicomponent diffusion coefficients, rather than binary diffusion coefficients, is required.

Mass transfer in the n-component mixture is generally described by $n \cdot (n\text{-}1)/2$ independent diffusion coefficients (each component diffuses in each other). As a result multicomponent diffusion coefficients are very difficult to measure.

The kinetic theory of gases provides expressions, which may successfully be applied to estimation of the diffusion coefficients in ideal gas mixtures. However, for the liquids the situation is less satisfactory.

On one hand, the locations of molecules in liquids are not structured, like in solids. On the other, molecular interactions in liquids are strong and collective, while in ideal gas mixtures only binary molecular interactions may normally be considered. This creates a

number of difficulties for modeling the liquid state. Up to now, there has been no rigorous theory capable of predicting the diffusion coefficients in the liquid state.

Various existing models for diffusion coefficients in liquids are empirical or semi-empirical and have limited predictive capabilities. The recent growth and development of molecular simulation methods opens wide possibilities to study behavior the liquids on micro-level. However, due to extensive computation times, conventional molecular dynamics simulations meet difficulties when applied to estimations of the diffusion coefficients. The question of estimation of diffusion coefficients in multicomponent liquid mixtures remains open.

The current research aims at developing particular models for diffusion coefficients on the basis of the recently developed *fluctuation theory* for the transport properties. The approach, described in this thesis, may be considered as a more theoretically grounded alternative to existing methods for prediction of the diffusion coefficients. It is shown to have a strong potential.

Chapter 2 of the current thesis introduces the reader to the theory of diffusion mass transfer. Different approaches to describing of diffusion transfer are presented, discussed and related to each other. Chapter 3 analyzes the existing experimental methods for determination of the diffusion coefficients both in binary and ternary liquid mixtures, and introduces the collected database of experimental data. Chapter 4 describes the existing models for estimation of the diffusion coefficients in binary mixtures. Chapter 5 presents the newly developed approach, based on the fluctuation theory for diffusion coefficients. The approach is thoroughly tested on description and prediction of the diffusion coefficients in binary mixtures. Chapter 6 presents the extension of the approach, described in chapter 5. This extension is based on the combination of the molecular dynamics simulations and the fluctuation theory. Comparison of the constituting parameters in the expressions for the diffusion coefficients, obtained from the molecular dynamics simulations and from the experimental data, is presented. Chapter 7 discusses existing methods for estimation of the diffusion coefficients in ternary and multicomponent mixtures. A procedure for analysis of experimental values of the diffusion coefficients in ternary mixtures is developed and tested on the existing experimental data. Possible extensions to multicomponent mixtures of the approaches for evaluation of the diffusion coefficients in binaries, presented in Chapters 5 and 6, are discussed. Finally, Chapter 8 presents the conclusions from the Thesis and introduces some ideas, regarding future research in this area.

2. Diffusion Mass Transfer in Liquids

2.1. Fick Equation

The first studies of diffusion mass transfer were carried out by the two scientists: Thomas Graham and Adolf Fick. During the period of 1828-1833 Thomas Graham [58] conducted a large work on diffusion. He was the first to observe experimentally the process of diffusion in gases and, later, diffusion in liquids. His main conclusion was that diffusion fluxes were proportional to concentration gradients. Twenty years passed, until the German physiologist Adolf Fick proposed mathematical basics for the results of the Graham's experiments, which became the first theory of diffusion.

Back in 1855, Adolf Fick published his first work on mass transfer [48], where he showed the analogy between diffusion, heat conduction and electricity transfer. The phenomenological laws of heat transfer (Fourier's law) and electricity transfer (Ohm's law) were already developed at that time. The analogy between these transport phenomena, established by Fick, allowed formulation of the mathematical basics of the theory of diffusion based on other phenomenological laws.

2.1.1. Binary Diffusion

Fick's law of diffusion defines the connection between the concentration gradient and the diffusion flux, which is caused by the gradient. The modern form of the Fick's law for binary mixtures is the following:

$$\mathbf{J}_1 = -c_t D_{12} \nabla z_1 . \tag{2.1}$$

Here the gradient of molar fraction ∇z_1 of the diffusing component 1 is the driving force for the diffusion process; $\mathbf{J}_1$ is the molar diffusion flux of component 1; and c_t is overall molar density. The proportionality coefficient D_{12} is called the Fick diffusion coefficient, or diffusivity of component 1 in component 2. Diffusion mass transfer tends to distribute the concentration evenly. Thus, a component normally diffuses from high concentrated regions to regions of lower concentration, which is indicated by the "-" sign in the left-hand side of Eq. (2.1).

There is only one independent concentration gradient in binary mixtures. Also, due to the conservation of the total flux in the volume, there is only one independent diffusion flux. As a result the Fick diffusion coefficient in a binary mixture is symmetric:

$$D_{12} = D_{21} . \tag{2.2}$$

This symmetry essentially simplifies modeling of diffusion processes in the binary mixtures. Provided that the concentration gradient of one component is known, the only one value of diffusion coefficient is required to estimate the diffusion flux.

2.1.2. Multicomponent Diffusion

Symmetry of the Fick diffusion coefficients, together with the overall simplicity of the Fick's law in binary mixtures, creates a wide range of possibilities for experimental measurements of the binary diffusion coefficient. However, in industrial applications diffusion transfer mainly occurs in mixtures with more than two components, which significantly increases the number of unknown diffusion coefficients, as well as the number of independent diffusion fluxes and forces.

In a mixture of *n* components, *(n-1)* independent diffusion fluxes exist. The Fick law needs to be extended and generalized in order to take into account the interactions between fluxes and concentration gradients of different diffusing components [117]:

$$\mathbf{J}_i = -c_t \sum_{j=1}^{n-1} D_{ij} \nabla z_j \,,\ \left(i = 1,...,n-1\right). \tag{2.3}$$

The flux of diffusing component i now depends upon the concentration gradients of other components in the mixture.

The Fick description of multicomponent diffusion involves a matrix of $(n\text{-}1)^2$ diffusion coefficients, which generally is not symmetric:

$$D_{ij} \neq D_{ji}\,. \tag{2.4}$$

The matrix of diffusion coefficients consists of the *main* and the *cross* diffusivities. Main diffusivity D_{ii} connects the flux of a component with its own concentration gradient, while cross diffusivities D_{ij} connect the flux of the component with the concentration gradients of other components. The diffusion coefficients D_{ij} in multicomponent mixtures are not binary properties, but are affected by the molecules of the third-party species. The values of diffusion coefficients in multicomponent mixtures are the result of complex interactions between all the species. It is impossible to separate binary and multicomponent interactions. Hence the values of diffusivities D_{ij} in a multicomponent mixture are not equal to the D_{ij} in a binary mixture of the components *i* and *j*.

Reference frames

The nature of the diffusion flux comes from the fact that average velocities of the chemical species may differ from each other. The relative motion, caused by differences in the individual velocities of the components, is *diffusion*.

Therefore, the definition of the diffusion flux is based on the velocity difference between the individual velocities of components u_i and some reference average velocity $\overline{u}$:

$$\mathbf{J}_i = c_i\left(\mathbf{u}_i - \overline{\mathbf{u}}\right). \tag{2.5}$$

Different definitions of the diffusion fluxes may be introduced, depending upon the way of calculation of the reference velocity. These definitions are also referred to as *reference frames*:

- *The molar reference frame* is with regard to the average molar velocity:

$$\mathbf{J}_i = c_i\left(\mathbf{u}_i - \overline{\mathbf{u}}\right),\ \overline{\mathbf{u}} = \sum z_k \mathbf{u}_k\ ; \tag{2.6}$$

- *The mass reference frame* is based upon the mass average velocity expressed by means of mass fractions w_i:

$$\mathbf{J}_i^{\,m} = c_i\left(\mathbf{u}_i - \overline{\mathbf{u}}^m\right),\ \overline{\mathbf{u}}^m = \sum w_k \mathbf{u}_k\ ; \tag{2.7}$$

- *The volume reference frame* is based, correspondingly, on the volume average velocity and partial molar volumes of the species V_k:

$$\mathbf{J}_i^{\,V} = c_i\left(\mathbf{u}_i - \overline{\mathbf{u}}^V\right),\ \overline{\mathbf{u}}^V = \sum c_k \mathbf{u}_k V_k\ ; \tag{2.8}$$

- Other special definitions are possible, such as *the solvent-fixed reference frame*, also called *the Hittorf reference* system [64], where the reference velocity is defined as a velocity of a selected component n, called solvent:

$$\mathbf{J}_i^{\,H} = c_i\left(\mathbf{u}_i - \mathbf{u}_n\right). \tag{2.9}$$

The Fick diffusion coefficients are usually measured in the volume reference frame. However, the volume reference frame is rather inconvenient for theory. Therefore the experimentally measured values need to be transformed to a molar or mass reference frame.

The values of Fick diffusion coefficients generally are affected by the choice of reference frame. The binary diffusivities remain the same in different reference frames; however, this is not the case in multicomponent mixtures. Additional transformation equations are required to interconnect diffusion coefficients defined in different frames.

The transformation between the Fick diffusion matrices $\mathbf{D}$ and $\mathbf{D}^m$ in molar and mass frames, correspondingly, may be performed in the following way [108, 145]:

$$\mathbf{D} = \mathbf{g}\mathbf{D}^m\mathbf{G},\ \mathbf{D}^m = \mathbf{G}\mathbf{D}\mathbf{g}\,. \tag{2.10}$$

Here $\mathbf{g}$, $\mathbf{G}$ are the transformation matrices between mass and molar system reference frames, which are related as $\mathbf{g}=\mathbf{G}^{-1}$. These transformation matrices are defined as:

$$G_{ik} = M_i\delta_{ik} - \frac{M_i z_i (M_k - M_n)}{M},\ g_{ik} = \frac{1}{M_i}\delta_{ik} - z_i\left(\frac{1}{M_k} - \frac{1}{M_n}\right),$$
$$(M = \sum_{l=1}^{n} M_l z_l,\ i,k = 1,...,n-1). \tag{2.11}$$

The connection between molar and volume frames may be expressed in a similar way [157]:

$$\mathbf{D} = \mathbf{g}\mathbf{D}^V\mathbf{G}\,. \tag{2.12}$$

The two transformation matrices are:

$$g_{ik} = \delta_{ik} - z_i\left(1 - V_k/V_n\right), \qquad G_{ik} = \delta_{ik} - z_i\left(V_k - V_n\right)/V_t . \tag{2.13}$$

The mathematical form of the transformation equation (2.12) is the same as that of Eq. (2.11). However it requires the values of the partial molar volumes of the components, as well as the total volume of the mixture. This information should either be obtained from experiments and reference data tables, or from a thermodynamic model. The amount of reference data on partial molar volumes is limited and the majority of thermodynamic models are not well-suited for estimation of volumetric properties. This creates an essential problem for connecting diffusion coefficients defined in the volume frame with other reference frames.

Selection of the solvent

The multicomponent Fick law (2.3) expresses only *(n-1)* diffusion fluxes and driving forces in an *n*-component mixture. The flux of any component may be eliminated due to the relative character of the diffusion fluxes:

$$\sum_{i=1}^{n} \alpha_i^R \mathbf{J}_i = 0 . \tag{2.14}$$

Here α_i^R are the weighting factors, depending upon the choice of the reference frame. According to R. Miller et al. [108] the weighting factors are defined in the following way:

- the volume-fixed reference frame:

$$\mathbf{J}_i^V = -\sum_{j=1}^{n-1} D_{ij}^V \nabla c_j \,,\ \sum_{i=1}^{n} \overline{V}_i \mathbf{J}_i^V = 0 ; \tag{2.15}$$

- the solvent-fixed reference frame (component *n* is solvent):

$$\mathbf{J}_i^H = -c_n M_n \sum_{j=1}^{n-1} D_{ij}^H \nabla m_j \,,\ \sum_{i=1}^{n} \delta_{in} \mathbf{J}_i^H = 0 ; \tag{2.16}$$

- the mass-fixed reference frame:

$$\mathbf{J}_i^m = -\rho \sum_{j=1}^{n-1} \frac{1}{M_j} D_{ij}^m \nabla w_j \,,\ \sum_{i=1}^{n} M_i \mathbf{J}_i^m = 0 ; \tag{2.17}$$

- the mole-fixed reference frame:

$$\mathbf{J}_i = -c_t \sum_{j=1}^{n-1} D_{ij} \nabla z_j \,,\ \sum_{i=1}^{n} \mathbf{J}_i = 0 . \tag{2.18}$$

The choice of the solvent will naturally influence the diffusion coefficients defined in the solvent-fixed reference frame. However, it may also influence the diffusion coefficients defined in other, not solvent-dependent reference frames. In some cases the change of solvent results in changing the sign of the multicomponent diffusivities.

Transformation of the matrix of diffusivities caused by change of the solvent in four component mixtures may be performed in the following way [108]:

$$\mathbf{D}_3^R = \mathbf{A}^R \mathbf{D}_4^R \mathbf{B}. \tag{2.19}$$

Here $\mathbf{D}_3^R$ and $\mathbf{D}_4^R$ are the matrices of Fick diffusivities defined in any reference frame R under condition that the 3rd and the 4th components are chosen as solvent, correspondingly. The transition matrix $\mathbf{A}^R$ depends on the choice of the reference frame and weighting factors in Eq. (2.14). The transformation matrix **B** is expressed in the terms of the partial molar volumes in the following way:

$$\mathbf{B} = \begin{pmatrix} 1 & 0 & 0 \\ 0 & 1 & 0 \\ b_1 & b_2 & b_3 \end{pmatrix}, \text{ where } b_i = -V_i / V_3, i \neq 3 \text{ and } b_3 = -V_4 / V_3. \tag{2.20}$$

The definition of the matrix $\mathbf{A}^R$ for different reference frames may be found in [108]. Generally this expression is the same for all reference frames, except for the solvent-fixed frame.

Transformation of the Fick diffusivities caused by choice of the solvent sometimes requires knowledge of the partial molar volumes of the components. Therefore, as was discussed above, solvent-solvent transformation in multicomponent mixtures may be imprecise for some mixtures.

Restrictions to the values of the diffusion coefficients

Generally, the diffusivities in multicomponent mixtures can be both positive and negative. However, normally, the main diffusivities are positive. The values of the cross diffusivities may be negative and/or may be higher than the main diffusivities.

Based on fundamentals of non-equilibrium thermodynamics and the second law of thermodynamics, it is possible to show that any given matrix of the Fick diffusion coefficients must obey several criteria [108]. The criteria for a ternary mixture are as follows (here diffusion coefficients are defined in the volume reference frame):

$$\begin{aligned} T_1 &= D_{11}^V + D_{22}^V \geq 0 \\ T_2 &= \det\left(\mathbf{D}^V\right) = \left(D_{11}D_{22} - D_{12}D_{21}\right) \geq 0. \\ T_3 &= disc\left(\mathbf{D}^V\right) = \left(T_1^2 - 4T_2\right) \geq 0 \end{aligned} \tag{2.21}$$

Miller et al. [108] indicated that these inequalities are not necessarily true for other choices of the reference frames. However, the cases where the validity of Eq. (2.21) is doubtful are rather rare and mainly related to an inappropriate selection of the solvent. In particular, Miller et al. have shown that Eq. (2.21) is not necessarily valid when some of the

components in the mixture have negative partial molar volumes. Moreover, Eq. (2.21) is not valid only when such a component is selected as a solvent.

2.2. Thermodynamics of Irreversible Processes

In this section the approach to diffusion deduced from the fundamentals of *thermodynamics of irreversible processes* (TIP) is discussed for the general case of a multicomponent mixture.

2.2.1. Multicomponent Diffusion

The starting point in thermodynamics of irreversible processes is the equation for the entropy balance in the system:

$$\rho \frac{\partial S}{\partial t} = -\nabla \mathbf{J}_s + \dot{S} . \tag{2.22}$$

Here, the term on the left-hand side is the entropy accumulation. The first term on the right-hand side is the net flow of the entropy, both due to convection and diffusion. The last term is the entropy production, which is the measure of irreversibility in the system.

It may be shown that the entropy production $\dot{S}$ may be expressed in terms of the generalized thermodynamic forces $\mathbf{X}_i$ and the corresponding fluxes $\dot{\mathbf{x}}_i$:

$$\dot{S} = \sum_{i=1}^{n-1} \dot{\mathbf{x}}_i \cdot \mathbf{X}_i . \tag{2.23}$$

As a first approximation for slow processes, TIP assumes linear relation between the thermodynamic forces and the corresponding fluxes [61]:

$$\dot{\mathbf{x}}_i = -\sum_{j=1}^{n-1} L_{ij} \mathbf{X}_j . \tag{2.24}$$

Here L_{ij} are the proportionality coefficients called the *Onsager phenomenological coefficients*. The linear law may be explained by a Taylor expansion of the fluxes by the forces, where all but first terms are neglected. This neglect can be validated when system is close to equilibrium. However, for systems far from equilibrium nonlinear relations between the forces and the fluxes may exist.

The physical interpretation of the Onsager coefficients depends upon the system of thermodynamic coordinates, i.e. the combination of fluxes and driving forces.

Onsager [116] has proven the symmetry of phenomenological coefficients in multicomponent mixtures:

$$L_{ij} = L_{ji} . \tag{2.25}$$

The last equation, also known as the *Onsager reciprocal relations*, was proven by means of statistical perturbation theory, under the condition of *microscopic reversibility*.

Microscopic reversibility means the time reversibility of the processes on a molecular level [116]. The Onsager reciprocal relations were also proven experimentally [80, 105, 106]. The relations were applied to verification of experimental data on multicomponent diffusion [99], as described in Chapter 7.

Due to the Onsager reciprocal relations, the number of independent phenomenological coefficients in a multicomponent mixture is smaller than in the Fick approach: $n\times(n-1)/2$ for an n-component mixture.

Different systems of thermodynamic coordinates

A major advantage of the TIP approach is that different sets of thermodynamic forces and fluxes may be applied, thus allowing inclusion of additional driving forces and advanced diffusion fluxes. Under the condition that the sum of the products of driving forces and fluxes is equal to the entropy production in the system, the matrix of phenomenological coefficients remains symmetric, due to the Onsager reciprocal relations. Thermodynamics of irreversible processes does not provide any knowledge about the values of the Onsager coefficients. Moreover, these values depend upon the choice of the system of coordinates.

An additional transformation equation is required for connection of the Onsager coefficients defined in two different systems of thermodynamic coordinates:

$$\mathbf{X}=\{\mathbf{X}_i\},\ \dot{\mathbf{x}}=\{\mathbf{J}_i^1\},\ \mathbf{Y}=\{\mathbf{Y}_i\},\ \dot{\mathbf{y}}=\{\mathbf{J}_i^2\}. \tag{2.26}$$

Here $\mathbf{X,x}$ and $\mathbf{Y,y}$ are the driving forces and fluxes in two different systems of coordinates, correspondingly.

The transformation rule between the two systems has the form of [142, 145]:

$$\mathbf{Y}=\mathbf{A}\mathbf{X},\ \dot{\mathbf{y}}=\left(\mathbf{A}^T\right)^{-1}\dot{\mathbf{x}},\ \mathbf{L}^{(Y)}=\mathbf{A}^T\mathbf{L}^{(X)}\mathbf{A}, \tag{2.27}$$

where $\mathbf{A}$ is the transformation matrix, and $\mathbf{L}^{(Y)},\mathbf{L}^{(X)}$ are phenomenological coefficients in the two systems of coordinates.

As an example, let us consider the transformation between the following two systems of coordinates:

$$\mathbf{J}_i=-\frac{1}{T}\sum_{k=1}^{n-1}L_{ik}^{(1)}\nabla(\mu_k-\mu_n)\quad(i=1,...,n-1). \tag{2.28}$$

And

$$\mathbf{I}_i=-\frac{1}{z_nT}\sum_{k=1}^{n-1}L_{ik}^{(2)}\nabla\mu_k\quad(i=1,...,n-1). \tag{2.29}$$

Here $\mathbf{J}_i$ are the diffusion molar fluxes, while $\mathbf{I}_i$ are the relative fluxes, defined as:

$$\mathbf{I}_i=z_n\mathbf{N}_i-z_i\mathbf{N}_n=z_n\mathbf{J}_i-z_i\mathbf{J}_n\ \ (i=1,...,n-1). \tag{2.30}$$

$\mathbf{N}_i$ is the absolute flux, defined as follows:

$$\mathbf{N}_i = c_t z_i \mathbf{u}_i \tag{2.31}$$

The relations between $L_{ik}^{(1)}$ and $L_{ik}^{(2)}$ are determined according to Eq. (2.27). The transition matrix $\mathbf{A}$ for such a transformation is defined in the following way [142, 145]:

$$A_{ik} = \frac{1}{z_n}(\delta_{ik} - z_k)\,. \tag{2.32}$$

Matrix $\mathbf{A}$ defined in Eq. (2.32) is used for the direct transition $L_{ik}^{(1)} \to L_{ik}^{(2)}$. For the inverse transition one should apply $\mathbf{A}^{-1}$ instead of $\mathbf{A}$:

$$A_{ik}^{-1} = z_n \delta_{ik} + z_k\,. \tag{2.33}$$

More examples of different systems of coordinates may be found in the literature [61, 64, 142, 145].

Reference frames and choice of the solvent

Apart from different systems of thermodynamic coordinates, different definitions of the diffusion fluxes within a given system of coordinates are also possible [Kir60]. However, a new definition of the diffusion flux will result in a corresponding change of the forces, provided that the product of fluxes and forces describes the entropy production in a system. Therefore it is arguable whether it is still the old system of thermodynamic coordinates or a new one.

As in the case of the Fick approach, the choice of a reference frame influences the values of the Onsager coefficients. It was shown in [108] that the following transformations are required to transfer the Onsager coefficients $\mathbf{L}$ from a reference frame *S* to a reference frame *R*:

$$\mathbf{L}^R = \mathbf{A}^{RS}\mathbf{L}^S\left(\mathbf{A}^{RS}\right)^T\,. \tag{2.34}$$

Here the transition matrix $\mathbf{A}^{RS}$ is defined as:

$$\mathbf{A}_{ij}^{RS} = \delta_{ij} + \frac{c_i}{\sum_{k=1}^{n} a_k^R c_k}\left[\frac{a_n^R a_j^S}{a_n^S} - a_j^R\right],\ \left(i, j = 1,...,n-1\right), \tag{2.35}$$

where a^R are the weighting factors, defined in Eq. (2.14).

The values of weighting factors for specific reference frames were presented in [108]. It was shown also in [108] that a proper transformation of the fluxes and forces, within a given system of thermodynamic coordinates caused by the change of the reference frame results in symmetry of the phenomenological coefficients.

The problem of solvent selection, described previously for the Fick approach, also exists in the TIP formalism. The solvent-solvent transition may also be considered as a

transformation of the system of thermodynamic coordinates, in the same manner as for the reference frame transformations. Since there are only $(n\text{-}1)$ independent diffusion fluxes in an n-component mixture, the diffusion flux of one of the components, called solvent, may be eliminated. Change of the solvent changes the values of the phenomenological coefficients and may change the expression for the forces.

Transformation of the Onsager coefficients caused by the solvent transition may be done in the way similar to the one described in the Fick section, Eq.(2.19):

$$\mathbf{L}_3^R = \mathbf{A}^R \mathbf{L}_4^R \left(\mathbf{A}^R\right)^{\mathbf{T}}. \tag{2.36}$$

Equation (2.36) involves only one matrix, which for the reference frames other than solvent-fixed, is expressed in the following way [108]:

$$\mathbf{A}^R = \begin{pmatrix} 1 & 0 & 0 \\ 0 & 1 & 0 \\ a_1 & a_2 & a_3 \end{pmatrix}, \; a_i = -\alpha_i^R / \alpha_4^R. \tag{2.37}$$

The matrix is expressed in terms of the weighting factors, defined in Eq. (2.14). For the solvent-fixed (Hittorf) reference frame, Miller [108] has shown that the transformation matrix is determined as follows:

$$\mathbf{A}^H = \begin{pmatrix} 1 & 0 & a_1 \\ 0 & 1 & a_2 \\ 0 & 0 & a_3 \end{pmatrix}, \; \begin{matrix} a_i = -c_i / c_3, (i \neq 3) \\ a_3 = -c_4 / c_3 \end{matrix} \tag{2.38}$$

It is seen that the solvent-solvent transformation may be performed on a fairly routine basis, except the case of transformation of the volume-fixed reference frame. The problem, discussed above of proper determination of the partial molar properties is relevant to this case.

2.3. Maxwell-Stefan Equations

2.3.1. Binary Diffusion

Back in 1859 (just 4 years after the work of Fick) Maxwell published two works on diffusion, based upon the kinetic theory of gases [97]. Eleven years later in 1871 Stefan extended the theory, which is now known as *the Maxwell-Stefan* (MS) theory for transport phenomena.

The general idea of the Maxwell-Stefan approach is to consider equilibrium between driving forces and friction forces. Friction occurs between the diffusing components. A driving force can be represented as a gradient of a potential, which is the measure for the deviation

from equilibrium. The driving forces for diffusion are similar to those that were defined in the framework of thermodynamics of irreversible processes.

Depending upon the conditions of the mass transfer, many possible sets of driving forces may exist. Examples of possible driving forces are:

- the gradient of the chemical potential of a species,
- the pressure gradient,
- the gradient of the electrical potential,
- external forces, such as gravity, centrifugal, etc.

The basic force is the *chemical driving force*, related to the variation of the concentration in an ideal mixture, and to the gradient of the corresponding chemical potential in a non-ideal mixture. However, the Maxwell-Stefan formalism allows straightforward inclusion of other effects into the driving force.

Driving Force

Let us consider the simplest case of isothermal diffusion within and across a bulk fluid phase. Considering the balance of forces acting on the control volume [87], it can be shown that the chemical driving force is the gradient of the chemical potential under constant temperature and pressure:

$$\mathbf{d}_i^{chem} = -\nabla_{T,P}\mu_i \,. \tag{2.39}$$

This gradient of the chemical potential can be expressed in the terms of the gradient of molar fraction and of the activity coefficient γ_i:

$$\nabla_{T,p}\mu_i = \frac{RT}{z_i}\sum_{j=1}^{n-1}\left(\delta_{ij} + z_i\frac{\partial \ln \gamma_i}{\partial z_j}\right)\nabla z_j \,. \tag{2.40}$$

For an ideal mixture the activity coefficient is equal to unity, which results in the following simplification of the expression for the driving force:

$$\nabla_{T,p}\mu_i = \frac{RT}{z_i}\nabla z_i \,. \tag{2.41}$$

The chemical driving force (2.39) participates in almost every diffusion process. Thus generally speaking, the application of the MS model for non-ideal mixtures requires a thermodynamic model for estimation of the chemical potential of the species.

In case of the presence of a pressure gradient, the chemical driving force is extended in the following way [87]:

$$\mathbf{d}_i^{chem} = -\frac{z_i}{RT}\nabla_T\mu_i = -\frac{z_i}{RT}\left(\nabla_{T,p}\mu + V_i\nabla P\right). \tag{2.42}$$

Equation (2.42) is also applicable to the description of mass transfer of species with large values of the partial molar volumes in the presence of relatively small pressure gradients.

Friction force

The driving force is compensated by the frictional force between diffusing particles of the species. It is postulated [87, 169] that the friction between the species i and j is proportional to their relative velocity and to their molar fractions in the mixture. In a binary mixture, the friction force is expressed as follows:

$$\mathbf{d}_1^{friction} = \xi_{12} z_2 \left(\mathbf{u}_1 - \mathbf{u}_2 \right). \tag{2.43}$$

Here ξ_{12} is the friction coefficient between the species 1 and 2.

The friction coefficient is closely related to the *Maxwell-Stefan* diffusion coefficient:

$$\xi_{12} = \frac{RT}{Đ_{12}}. \tag{2.44}$$

By equating the expression for the driving force and the friction force the Maxwell-Stefan (MS) equation for diffusion in a binary mixture is derived:

$$-\nabla_T \mu_1 = \frac{RT}{Đ_{12}} z_2 \left(\mathbf{u}_1 - \mathbf{u}_2 \right). \tag{2.45}$$

The proportionality coefficient $Đ_{12}$ introduced during derivation of the friction force is the Maxwell-Stefan diffusion coefficient, or the MS diffusivity of the component i with regard to the component j. As in the case of the Fick law, there exists only one independent MS diffusion coefficient in a binary mixture.

Eq. (2.45) is the simplest form of the MS equation. It can also be expressed in the terms of the absolute fluxes and the molar diffusion fluxes, introduced above, Eq. (2.6).

$$-\frac{z_1}{RT} \nabla_T \mu_1 = \frac{z_1 z_2 \left(\mathbf{u}_1 - \mathbf{u}_2 \right)}{Đ_{12}} = \frac{z_2 \mathbf{N}_1 - z_1 \mathbf{N}_2}{c_t Đ_{12}} = \frac{z_2 \mathbf{J}_1 - z_1 \mathbf{J}_2}{c_t Đ_{12}}. \tag{2.46}$$

The last term in Eq. (2.46) is irrespective of the reference velocity frame [87], which makes the MS diffusion coefficients independent of the definition of the diffusion fluxes.

Generalized driving force

The *generalized driving force* should be defined to take into account the influence of the external body forces, such as electrostatic potential gradients and centrifugal forces [87]. Compared to the chemical driving force, defined in Eq.(2.42), the generalized driving force is defined in the following way:

$$\mathbf{d}_i = -\frac{z_i}{RT} \left(\nabla_T \mu_i - \mathbf{\Psi}_i \right). \tag{2.47}$$

Here $\mathbf{\Psi}_i$ represents the external body force, acting per unit of mole of species i.

As example, for isothermal, isobaric transport in electrolyte systems an additional driving force, caused by the electrostatic potential gradient $\nabla\varphi$ must be considered:

$$\mathbf{\Psi}_i = -M_i \varsigma_i \Phi \nabla\phi . \tag{2.48}$$

Here ς_i is the ionic charge of species i and Φ is the Faraday constant.

Another example is rotation of a body with the angular velocity Ω. The centrifugal force per unit mass of each component i acting at radial distance r is equal to

$$\mathbf{\Psi}_i = M_i \Omega^2 r . \tag{2.49}$$

Based on these two examples, it can be seen that definition of the generalized driving force makes it possible to account for a variety of different conditions under which the mass transfer occurs. Detailed derivations of the driving forces for a large number of special applications are available in [87] and [169].

2.3.2. Multicomponent Diffusion

The approach described above with respect to binary mixtures can easily be extended to the general multicomponent case. This is done by balancing the forces acting on component i, by the friction forces between this component and each other species present in the mixture. The resulting equation is (for the case of isothermal, isobaric diffusion):

$$-\nabla_{T,P}\mu_i = RT\sum_{j\neq i}\frac{z_i z_j\left(\mathbf{u}_i - \mathbf{u}_j\right)}{\text{Đ}_{ij}}, \quad \left(i, j = 1,2,...,n\right). \tag{2.50}$$

Equation (2.50) may be expressed in the terms of the absolute fluxes or the diffusion fluxes:

$$-\frac{z_i}{RT}\nabla_{T,P}\mu_i = \sum_{j\neq i}\frac{z_j\mathbf{N}_i - z_i\mathbf{N}_j}{c_t\text{Đ}_{ij}} = \sum_{j\neq i}\frac{z_j\mathbf{J}_i - z_i\mathbf{J}_j}{c_t\text{Đ}_{ij}}, \ \left(i, j = 1,2,...,n\right). \tag{2.51}$$

An important property of the multicomponent MS diffusion coefficients is their symmetry [169]:

$$\text{Đ}_{ij} = \text{Đ}_{ji} . \tag{2.52}$$

There is only one independent MS diffusion coefficient for a pair of components. This significantly reduces the number of the independent diffusion coefficients for multicomponent mixtures: $n\times(n\text{-}1)/2$ for an n-component mixture, instead of $(n\text{-}1)^2$ coefficients for the Fick model.

Another important property of the MS multicomponent diffusion coefficients is valid for ideal gases. In such gases multicomponent Maxwell-Stefan diffusion coefficients are equal to the binary coefficients and are (almost) independent of the mixture composition. In liquids, the third-party influence on interaction between two species contributes to the values of the

diffusion coefficients. As a result, the MS diffusivities in a multicomponent mixture are no longer equal to the binary diffusion coefficients.

Units, reference frames and bootstrap relations

The Maxwell-Stefan equations presented here are defined in molar units. Other units will not change the general structure of the equations. However, the expressions for the driving forces and for the diffusion coefficients may be changed. It is possible to show [169] that for the mass, molar and volumetric representations the following relations are true:

- mass to molar transition:

$$\mathbf{d}_i = M_i \mathbf{d}_i^m,\ \mathcal{D}_{ij}^m = \mathcal{D}_{ij}\frac{M_i M_j}{M^2}; \tag{2.53}$$

- mass to volume transition:

$$\mathbf{d}_i^V = \rho_i \mathbf{d}_i^m,\ \mathcal{D}_{ij}^m = \mathcal{D}_{ij}^V\frac{\rho_i \rho_j}{\rho^2}; \tag{2.54}$$

- molar to volume transition:

$$\mathbf{d}_i = V_i \mathbf{d}_i^V,\ \mathcal{D}_{ij}^V = \mathcal{D}_{ij}\frac{V_i V_j}{V^2}. \tag{2.55}$$

In order to express the driving forces in different units, let us consider a system where the chemical driving force is present, together with some generalized driving force acting per mole of species i. Since the driving forces are usually potentials, we can consider how the potentials change with the change of the units.

- the generalized potential Π in molar units:

$$\Pi_i = RT\ln\left(\gamma_i z_i\right) + \mathbf{\Psi}_i; \tag{2.56}$$

- the generalized potential in mass units:

$$\Pi_i^m = \frac{RT}{M_i}\ln\left(\gamma_i^m w_i\right) + \frac{\mathbf{\Psi}_i}{M_i}; \tag{2.57}$$

- the generalized potential in volume units:

$$\Pi_i^V = \frac{RT}{V_i}\ln\left(\gamma_i^V \upsilon_i\right) + \frac{\mathbf{\Psi}_i}{V_i}. \tag{2.58}$$

Rigorously speaking the change of the units of the overall potential requires also changes of the activity coefficients. However this does not make a difference, due to the following equality:

$$\gamma_i z_i = \gamma_i^m w_i = \gamma_i^V \upsilon_i. \tag{2.59}$$

The Maxwell-Stefan equations do not provide all the information about the absolute velocities of the components and the motion of the mixture as a whole. Actually, this also is

true for Fick and TIP approaches, since they are also expressed in the terms of the relative diffusion fluxes. In order to obtain the absolute velocities, additional constraints or the so-called *bootstrap relations* [169] are required. The bootstrap relations may be considered as physical conditions, required to complete the system of diffusion equations, providing additional conservation laws for the system as a whole. They should be determined by specific considerations for each case.

Deduction of a bootstrap relation may sometimes be non-trivial. Some examples are given below [169].

In the absence of net molar flow, mole balance considerations result in the conservation of the sum of the absolute fluxes of all the components:

$$\sum_{i=1}^{n} \mathbf{N}_i = 0. \tag{2.60}$$

During absorption, condensation or filtration one of the components may not diffuse through the interface. In this case the bootstrap relation requires that the flux of this component is equal to zero:

$$\mathbf{N}_i = 0. \tag{2.61}$$

In some applications, the chemical reaction is accompanied by diffusion of the products and reagents to and from the place of reaction. It may be shown [169] that for such processes the bootstrap relation has the form

$$\sum_{i=1}^{n} \frac{\mathbf{N}_i}{\chi_i} = 0, \tag{2.62}$$

where χ_i are the stoichiometric coefficients for the species i in the chemical reaction.

Based on these examples, it can be seen that the deduction of a bootstrap relation may be non-trivial. More practical examples of the bootstrap relations with extensive explanations may be found in [169].

2.4. Connection Between Different Formalisms

The definitions of diffusion coefficients are different in all the three approaches described above. Experimentally measured diffusivities, as reported in the literature, are usually Fick diffusivities. For modeling purposes, the Maxwell-Stefan or the TIP approach may be more convenient. Therefore, transformations of the diffusion coefficients between the three approaches should be defined.

2.4.1. Binary Diffusion Coefficients

Connection between the Maxwell-Stefan and the Fick diffusivities

Let us consider ordinary mass transfer in a binary mixture under constant temperature and pressure, in the absence of external driving forces. For such a process the MS equation reduces to the following form:

$$-\frac{z_1}{RT}\left(\frac{\partial \mu_1}{\partial z_1}\right)_{T,P} \nabla z_1 = \frac{z_2 \mathbf{J}_1 - z_1 \mathbf{J}_2}{c_t \mathcal{D}_{12}}. \qquad (2.63)$$

Here the MS equation is expressed in terms of the molar diffusion fluxes. The total diffusion flux $\mathbf{J}_1+\mathbf{J}_2$ is equal to zero. Thus, the following transformation of Eq. (2.63) is possible:

$$\mathbf{J}_1 = -c_t \mathcal{D}_{12} \frac{z_1}{RT}\left(\frac{\partial \mu_1}{\partial z_1}\right)_{T,P} \nabla z_1. \qquad (2.64)$$

Comparison with the Fick equation (2.1) yields the relation between the MS and the Fick diffusion coefficients:

$$D_{12} = \mathcal{D}_{12}\Gamma, \qquad (2.65)$$

where Γ is a thermodynamic correction factor:

$$\Gamma = \frac{z_1}{RT}\left(\frac{\partial \mu_1}{\partial z_1}\right)_{T,P} = 1 + z_1\left(\frac{\partial \ln \gamma_1}{\partial z_1}\right)_{T,P}. \qquad (2.66)$$

The transformation of the MS binary diffusion coefficient to the Fick coefficient requires a thermodynamic model for estimation of the compositional derivative of the activity coefficient. Generally, any thermodynamic model, such as an equation of state or an activity coefficient model, may be applied for estimation of the thermodynamic factor in Eq. (2.66).

2.4.2. Multicomponent Diffusion Coefficients

Connection between Onsager and Fick coefficients

The Onsager phenomenological coefficients are defined as the proportionality coefficients between the thermodynamic forces and the corresponding fluxes. Different sets of fluxes and forces and, correspondingly, different definitions of the Onsager phenomenological coefficients are available. The connection between the phenomenological coefficients determined in different systems of thermodynamic coordinates was discussed above.

Let us consider the system of thermodynamic coordinates, described in Eq. (2.28)

In the left-hand side of Eq. (2.28), there are diffusion fluxes, as well as in the left-hand side of Eq. (2.3). Comparison of these two equations results in the following simple transformation equation:

$$\mathbf{D} = \frac{1}{c_t T}\mathbf{L}^{(1)}\mathbf{G}\,. \tag{2.67}$$

Here $\mathbf{G}$ is the transition matrix, expressed in terms of the compositional derivatives of the chemical potentials under constant temperature and pressure:

$$G_{ik} = \partial(\mu_i - \mu_n)/\partial z_k,\ \ (i,k = 1,...,n-1)\,. \tag{2.68}$$

Again, as for the binary case, this transformation requires implementation of a thermodynamic model for estimation of the chemical potentials.

Connection between Onsager and Maxwell-Stefan coefficients

The Maxwell-Stefan equation is expressed in terms of the differences of the diffusion fluxes. First, we express Onsager coefficients in the thermodynamic system of coordinates, which is close by its form to the MS equation [142, 145], Eq. (2.29).

It may be shown [142, 145] that transformation of the Onsager coefficients, defined in Eq. (2.29), to Maxwell-Stefan coefficients may be done in the following way:

$$\mathbf{L}^{(2)} = \mathbf{l}^{-1}, \tag{2.69}$$

$$l_{i,j\neq i} = -\frac{R}{nz_n^2 Đ_{ij}}, \tag{2.70}$$

$$l_{ii} = \frac{R}{nz_i z_n Đ_{in}} + \sum_{\substack{j=1\\ j\neq i}}^{n-1} \frac{Rz_j}{nz_i z_n^2 Đ_{ij}}\,. \tag{2.71}$$

Equations (2.70) and (2.71) defines the relation between the Maxwell-Stefan diffusion coefficients and matrix $\mathbf{l}$, which is inverse to the matrix of Onsager coefficients, Eq. (2.69).

Therefore, to calculate the Onsager coefficients from MS it is necessary first to estimate transition matrix $\mathbf{l}$ and then, to find an inverse matrix. For inverse transition the matrix of Onsager coefficients must be inverted. Then the MS diffusivities $Đ_{ij}$ are found from Eq. (2.70). Once cross-terms are determined, Eq. (2.71) makes it possible to determine $Đ_{in}$. Application of the symmetry condition, $Đ_{in} = Đ_{ni}$, finalizes the procedure of transition.

Connection between the Maxwell-Stefan and the Fick diffusivities

The direct connection between the Maxwell-Stefan and the Fick multicomponent diffusivities may be rather cumbersome. Moreover, the transformation from the Fick to the MS diffusivities appears to be more complicated than the inverse transformation [134].

Instead of the direct transformation between the MS and the Fick coefficients, an alternative way may be proposed [145]. The MS and the Fick coefficients may be connected with each other via the formalism of TIP. A possibility to choose different systems of

thermodynamic coordinates in the TIP approach and, therefore, to connect the Onsager coefficients both to the MS and the Fick diffusivities was discussed above. In combination with the way described to connect Onsager coefficients, expressed in different sets of fluxes and forces, this creates a possibility to use the TIP approach as a bridge between the MS and the Fick approaches.

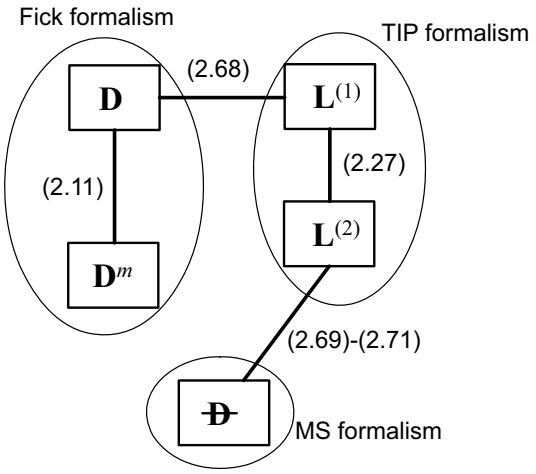

Figure 2.1: Scheme of transformations between different diffusion formalisms.

Figure 2.1 demonstrates the relations between different formalisms. It is easy to see that flexibility of the TIP formalism makes it possible to relate the Maxwell-Stefan and the Fick diffusion coefficients via the Onsager phenomenological coefficients.

2.5. Summary

The Fick approach

Fick's law looks very attractive due to its simplicity: clear dependence between the fluxes and the driving concentration gradients and unnecessity for a thermodynamic model for mass transfer calculations. In a binary mixture, the Fick law is even simpler: one diffusion flux, one concentration gradient and one diffusion coefficient. This is why the Fick law has become a standard for experimental measurements of the diffusion coefficients in binary mixtures. A majority of the measured binary diffusion coefficients are reported in terms of Fick diffusivities.

However, the simplicity of the Fick law is complicated by the non-trivial and often unpredictable behavior of the Fickian diffusion coefficients. Also, the Fick formalism in the form of equations (2.1) and (2.3) is only valid under constant temperature and pressure. It is

practically impossible to extend the Fick equation and to include other driving forces, rather than concentration gradients.

For multicomponent mixtures the situation becomes more complicated. The matrix of Fick diffusion coefficients is not symmetric, which results in $(n-1)^2$ independent diffusion coefficients for an *n*-multicomponent mixture. Moreover, these values are highly dependent upon the choice of the reference frame for the diffusion fluxes and the choice of the solvent. Thus, the values of the multicomponent Fick diffusion coefficients depend on pressure, temperature, concentration and even on the sequence of the components in the mixture. The Fick coefficients may be transformed from one reference frame to another. However, due to the fact that the experimentally measured values are usually expressed in the volume reference frame, this transformation requires knowledge of the partial molar volumes of the components, which sometimes are not available.

Thermodynamics of Irreversible Processes

The TIP formalism is derived from three basic postulates. The first postulate assumes that thermodynamic properties can be correctly defined in a differential volume of the system, which is not at equilibrium. The second postulate states that there exists a linear relation between the thermodynamic fluxes and the thermodynamic forces, provided that the sum of their mutual products is equal to the entropy production in the system. The proportionality coefficients in this linear dependence are called the Onsager phenomenological coefficients. The third postulate is about microscopic reversibility. On this basis it may be proven that the matrix of Onsager coefficients is symmetric (these are the so-called reciprocal relations). The first and second postulates introduce some limitations upon the area of applicability of the TIP approach. The developed approach is valid only for systems, which are not very far from equilibrium. However, this postulate is valid for almost any ordinary mass transfer process.

The form of equations derived via TIP is fairly simple and transparent. The possibility of introducing different driving forces is rather important, so that the formalism is not limited to any specific case of mass transfer. Due to the symmetry, there are only $n\times(n\text{-}1)/2$ independent phenomenological coefficients in an n-component mixture.

The Onsager coefficients exhibit complicated behavior and they may be extreme functions of the composition at dilute limits. Moreover, there also exists the problem of solvent-solvent transition, as for the Fick approach. The Onsager coefficients depend upon the choice of a solvent, as well as upon the choice of a reference frame for the diffusion flux. However, as it was stated above, it is arguable that the change of the reference frame and solvent results in a new system of thermodynamic coordinates.

The Maxwell-Stefan approach

To some extent, the Maxwell-Stefan approach is similar to the TIP approach. The MS approach is well grounded theoretically. It inherits some limitations from the TIP formalism: it is only applicable to systems close to equilibrium. However, strictly speaking, this limitation is common for all three approaches, including Fick's law. A system far from equilibrium, generally, cannot be described with any of the three approaches.

The Maxwell-Stefan approach allows for inclusion of different driving forces, however, based on a different principle than the TIP. As in the TIP, the Maxwell-Stefan diffusivities in multicomponent mixtures are symmetric.

The MS approach has a few major advantages compared to TIP. The Maxwell-Stefan diffusivities are independent both upon the choice of a reference frame and the choice of a solvent. Application of the MS approach to a specific case of mass transfer requires implementation of additional conditions, called the bootstrap relations. These relations define additional connections between the flows in a system. Their deduction may be nontrivial in some cases.

Selection of an approach

Each of the three discussed formalisms has a number of advantages and shortcomings. Any of them may be related to any other. The Maxwell-Stefan approach is becoming increasingly popular for modeling purposes, while the Fick approach remains standard in experimental measurements of the diffusion coefficients. The TIP serves as the rigorous theoretical ground for both Maxwell-Stefan and Fick approaches and may be considered as the bridge between them. The TIP approach is necessary in order to relate the descriptions of the diffusion processes on macro- and microlevels, and to connect the theory with the results of the non-equilibrium statistical thermodynamics and of molecular dynamic simulations.

In summary, it may be concluded, that, generally, the Fick approach is best-suited for experimental studies, the Maxwell-Stefan formalism is optimal for describing and modeling of practically important cases, and the TIP approach is a great instrument for developing the theoretical background for diffusion mass transfer.

3. Diffusion Experiments

The first diffusion experiments were performed by Graham back in the first half of the 19th century [58, 59]. Thomas Graham constructed two experimental apparata: one for the measuring diffusion coefficients in a gas state, and another for measuring diffusivities in a liquid. Graham's experiments may be considered as a beginning of research in the area of the diffusion mass transfer. In spite of the long time passed since the first diffusion experiments, no rigorous theory has been developed for diffusion coefficients in the liquid state. Up to now experimental studies and molecular dynamics simulations remain the major source of existing knowledge on diffusion coefficients.

There is a large variety of experimental methods for measuring diffusivities. An overview of existing experimental methods for measuring diffusion coefficients is presented in this chapter.

Generally, measurements of diffusion coefficients have proved to be a complicated task. This is mainly due to the large variety of phenomena which must be accounted and controlled during the measurements. However, neglecting of some of the factors results in simplification of the experimental method. As an example, diffusion coefficients may be measured on a fairly routine basis using a simple diaphragm cell, with an accuracy of 5-10 percent which is sometimes suitable for applications [32]. Thus, experimental measurements should be always considered as one of the options for estimation of diffusion coefficients in binary liquid mixtures. In multicomponent liquid mixtures the measurements are much more complicated. This is illustrated by the amount of experimental studies of multicomponent diffusivities reported in literature. To the best of our knowledge, there are only several experimental studies of diffusion in ternary mixtures (both in electrolyte and non-electrolyte systems [15, 32]). The quaternary diffusion coefficients in a non-electrolyte system have been measured only once [121].

The basic idea behind almost any experimental method is measuring the concentration profiles at the start and at the end of the experiment. Some methods require measurements of the concentrations during the experiment. All the experimental methods require a theoretical background for extraction of the diffusion coefficients based on the concentration profiles.

In general, all the existing methods can be classified by the nature of the diffusion process simulated in the experiment [32]:

- steady-state diffusion (the diaphragm cell method);
- unsteady-state diffusion in still media (the interferometer techniques, the capillary method, methods based on Raman spectroscopy);

- decay of a pulse (Taylor dispersion, nuclear magnetic resonance, dynamic light scattering).

Despite the large variety of existing experimental techniques, three of them have proved to be the most convenient and/or accurate, and have become today's standard for diffusion measurements: the diaphragm cell, Taylor dispersion methods, and holographic interferometry. The two first methods are simple, while the third one is very accurate. Other methods will also be briefly discussed.

3.1. Diaphragm Cell

The diaphragm cell is a very simple tool for measuring diffusion coefficients. Being first proposed by Barnes [16] it was later modified to its current form by Hammond and Stokes [67]. The setup does not involve any expensive or fragile parts and the accuracy of the method is usually between 2% and 5%. However, accurate measurements and rigorous analysis of the experimental results may provide diffusion coefficients with accuracy up to 0.5% [36, 54, 155].

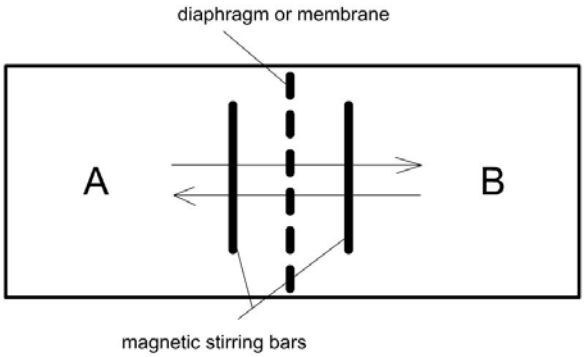

Figure 3.1: Scheme of diaphragm cell.

The idea behind the method is very simple. A diffusion cell consists of two compartments, each filled with solutions of different concentration (Figure 3.1). The compartments are separated by a very thin porous membrane or by a diaphragm. The solutions start to diffuse through the diaphragm or membrane. After some time (usually from three to six days) the compartments are emptied and concentrations of the solutions are measured.

The exact solution of the diffusion problem inside the diffusion cell (Figure 3.2) was originally proposed by Barnes [16]. However, later Robinson and Stokes [128] proposed a more practically convenient approximate solution of the problem.

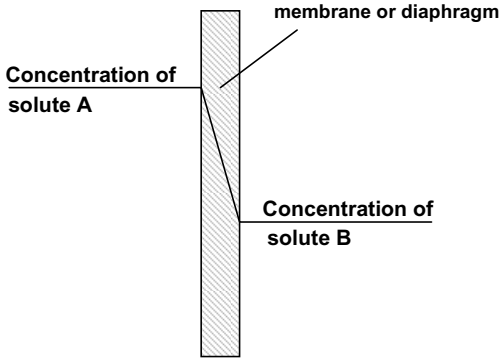

Figure 3.2: Typical concentration profile inside the diffusion cell.

Considering Figure 3.2, it is easy to see that the volume of the diaphragm is negligible compared to the volumes of the compartments. Since the fluid is well stirred it may be assumed that the concentrations will change slowly and be distributed rather uniformly in both compartments. At the same time the concentration profile inside the thin membrane varies rather quickly. Hence, the time of stabilization of the concentration profile inside the membrane is very small compared to the time change of the concentration inside the compartments. These considerations lie behind the main assumption of Robinson and Stokes [128] about quasi steady-state flux through the membrane.

Considering the steady state flux across the diaphragm and the balance equation, it may be shown [128] that the diffusion coefficient may be estimated as follows:

$$D = \frac{1}{\beta t} \ln\left(\frac{c^0_{1,lower} - c^0_{1,upper}}{c_{1,lower} - c_{1,upper}} \right). \tag{3.1}$$

Here β is a diaphragm-cell constant, t is the time and c_1 is the solute molar concentration.

It may be immediately seen that Eq. (3.1) does not involve the concentrations themselves, but the ratios of their differences. This imposes additional constraints on the accuracy of the concentration measurements. Even a reasonably good accuracy in measuring concentrations will result in a large error in diffusion coefficients, since the denominator in Eq. (3.1) tends to zero with a long time of the diffusion run.

The diaphragm-cell constant is the geometric factor of the cell. It is estimated in the following way:

$$\beta = \frac{S_D H}{l_D} \left(\frac{1}{V_{lower}} + \frac{1}{V_{upper}} \right), \tag{3.2}$$

where S_D is the diaphragm area, l_D is the effective thickness of the diaphragm and H is the fraction of the diaphragm available for diffusion.

A few important questions about validity of Eq. (3.1) arise. As was stated above, Eq. (3.1) was derived on the basis of the steady-state approximation of the flux, together with the mass balance equation. It may be shown [129] that Eq. (3.1) is only valid when the volume changes of mixing are negligible or absent. Therefore, additional analysis must be performed to estimate the validity of this condition for particular mixtures [129]. Substantiation for the assumption of steady-state flux through the diaphragm was given by Mills et al. [110]. It was shown that the steady-state approximation is valid under the condition that the volumes of the compartments are much larger than the volume of the diaphragm:

$$V_{diaphragm}\left(\frac{1}{V_{upper}}+\frac{1}{V_{lower}}\right)\ll 1. \qquad (3.3)$$

To further increase the accuracy of the method, the time for initial stabilization of the flow inside the diaphragm must be taken into account. It was shown in [39, 56] that the time of diffusion flux stabilization t_S may be approximately expressed as:

$$t_S = 1.2 l_D^2 / D. \qquad (3.4)$$

Here l_D is the effective length of a diffusion path in the diaphragm. Wedlake and Dullien [165] have shown that this time is generally around 2-3 hours. Hence, they proposed the experimental procedure in which the solutions in both compartments are first refilled via circulation to maintain the initial difference of concentrations. The beginning of the diffusion experimental run starts after a time of stabilization, Eq. (3.4).

The second important question is related to the overall time of the diffusion run. Robinson [129] has shown that the best accuracy is achieved when the total run time t_t is:

$$t_t = 1.2/\beta D. \qquad (3.5)$$

However, Robinson also indicated that the good accuracy is obtained over a broad range of times. Therefore, significant reduction of the overall measurement time results in rather slight increase of the measurement error.

It should be mentioned that almost all the values involved in Eq. (3.2), except the volumes of the compartments, are usually not well known. The diaphragm constant β generally must be found from calibration experiments. It is known that, under the same conditions, the diffusion coefficient in porous space differs from the coefficient in free space. The property which is used for recalculation of the diffusivities in macroporous and free space is *the porosity-tortuosity factor* [40]. A diffusion coefficient obtained in the experiments in the diaphragm cell is an effective value influenced by the porosity and the tortuosity of the membrane. It may be questioned whether the properly calibrated diaphragm cell may be

applied to measurements of diffusion coefficients in free space. Recently it was proven by Shapiro and Stenby [141] that the values of diffusion coefficients in macroporous media, such as a membrane, are rescaled in the same way, independently of the diffusing substances. This fact provides a rigorous theoretical background for estimation of the diaphragm constant from the calibration experiments.

In the later studies [23, 158] it was found that the construction of the diaphragm cell, known as the “Stokes diaphragm”, has one essential limitation. The Stokes diaphragm cell cannot be applied under varying temperatures and pressures. The two main effects, caused by increase of the temperature are expansion of the test liquid and evaporation, or even boiling. This requires re-design of the experimental setup. Calus and Tyn [23] developed a three-compartment diffusion cell. Construction of the cell involves an additional tube, which controls redistribution of the test liquids caused by the thermal expansion.

3.2. The Taylor Dispersion Method

The Taylor dispersion method is the second basic method for measuring the mutual diffusion coefficients in the fluid systems. It is rather simple. The accuracy of measured diffusivities is usually around 1-2%, with the best accuracies of 0.7% [101, 118, 131, 132, 134].

The experimental setup contains a thin tube filled by the flowing solvent (Figure 3.3). A sharp pulse of the solute is injected into the solvent in the experimental cell. The fact that the sharp concentration profile tends to relax into a set of the smooth profiles due to the *dispersion* is in the basis of the method (Figure 3.4). Dispersion is the result of the coupled action of convection and diffusion. By measuring the dispersed concentration profiles, it is possible to extract the value of the diffusion coefficient.

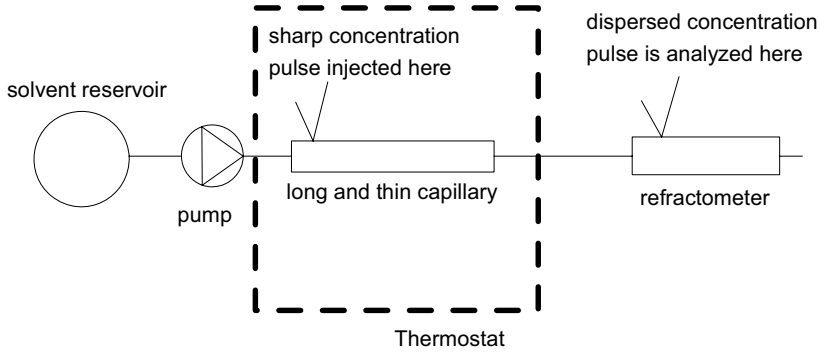

Figure 3.3: The Taylor dispersion method.

Despite a rather complex mathematical description of the process, the experimental setup can be built easily and is quite cheap, with the most expensive part being the differential refractometer for measuring the concentration profiles.

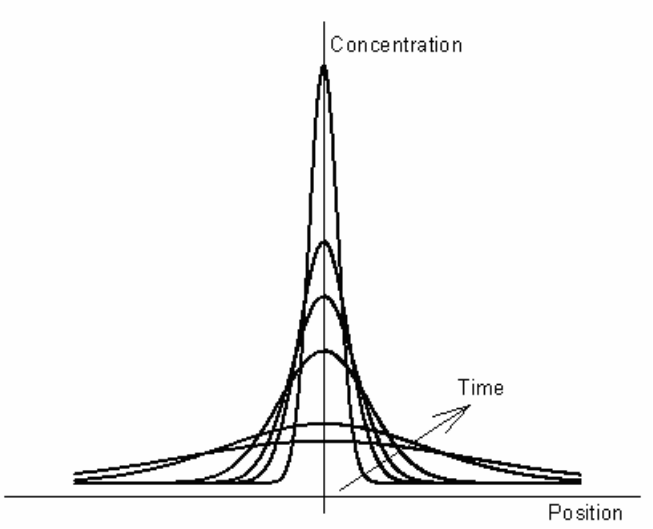

Figure 3.4: Relaxation of the concentration profile.

Before describing the mathematical basis of the process, let us first consider schematically the process of the concentration impulse flow in the capillary (Figure 3.5). The initial sharp pulse of the concentration tends to stretch due to convection. Then the simultaneous diffusion process starts. First the concentration profile tends to diffuse towards the walls; afterwards inverse diffusion tends to bring the solute from the walls towards the centre. Hence, the more sharp concentration profile at the outlet of the tube corresponds to a higher value of the diffusion coefficient. The explanation of this fact was given by Taylor [156].

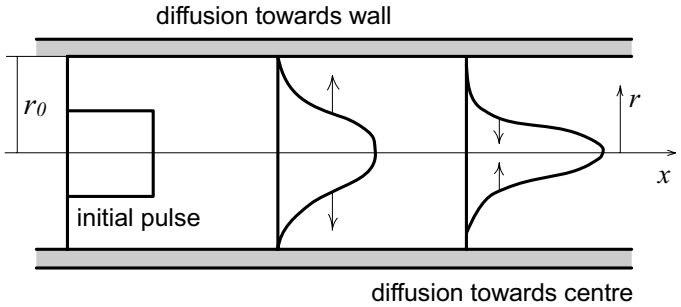

Figure 3.5: Schematic illustration of the flow in the tube.

The mathematical background of the method comes from the consideration of the differential equation relating the mechanisms of convection and diffusion:

$$\frac{\partial c}{\partial t} = D\left[\frac{\partial^2 c}{\partial x^2} + \frac{\partial^2 c}{\partial r^2} + \frac{1}{r}\frac{\partial c}{\partial r}\right] - U_0\left(1 - \frac{r^2}{r_0^2}\right)\frac{\partial c}{\partial x}. \quad (3.6)$$

Here c is the volume concentration of one of the components (solute), U_0 is the velocity of the flow at the centre of the tube, r is the radial coordinate and r_0 is the radius of the tube. The left hand-side of Eq. (3.6) is the accumulation term, the first term in the right hand-side is the expression for both axial and radial diffusion flux in cylindrical coordinates. The second term is the expression for the convective flux, based upon the parabolic velocity profile for laminar flow in the tube.

There is no exact analytical solution of Eq. (3.6). However, Taylor [156] introduced a few assumptions to simplify this equation. The first assumption is that the axial transport due to diffusion is small, compared to the axial convective transport. This results in the following simplification of Eq. (3.6):

$$\frac{\partial c}{\partial t} = D\left[\frac{\partial^2 c}{\partial r^2} + \frac{1}{r}\frac{\partial c}{\partial r}\right] - U_0\left(1 - \frac{r^2}{r_0^2}\right)\frac{\partial c}{\partial z}. \quad (3.7)$$

Before considering the next assumption let us first perform a transformation of the coordinates. We transform Eq. (3.7) to a moving reference frame, by introducing the new moving axial coordinate:

$$x' = x - 0.5U_0 t\,. \quad (3.8)$$

Taylor [156] has shown that such change of the coordinates allows to consider the process as quasi time independent. The assumptions, introduced at this point are that the radial concentration gradients induced by convection are immediately reduced by radial diffusion, within a small time step. This makes it possible to consider the balance between axial convection and radial diffusion as a quasi time independent process:

$$\frac{1}{2}U_0\left(1 - 2\frac{r^2}{r_0^2}\right)\frac{\partial c}{\partial x'} = D\left[\frac{\partial^2 c}{\partial r^2} + \frac{1}{r}\frac{\partial c}{\partial r}\right]. \quad (3.9)$$

Eq. (3.9) describes the variation of the radial concentration in a slice, moving with the mean velocity of the flow.

Solution of Eq. (3.9) provides the expression for the radial concentration profile in the slice:

$$c = c_{r=0} + \frac{r_0^2 U_0}{8D}\frac{\partial c}{\partial x'}\left[\frac{r^2}{R^2} - \frac{1}{2}\frac{r^4}{r_0^4}\right]. \quad (3.10)$$

Analysis of the mass balance over the slice, together with Eq. (3.10) results in the following expression for the molar flow of the solute out of the slice:

$$Q = -\pi r_0^2 E_D \frac{\partial c_{r=0}}{\partial x'}. \tag{3.11}$$

Here E_D is called the *dispersion* coefficient and is expressed in the following way:

$$E_D = \frac{\bar{U}^2 r_0^2}{48D}, \tag{3.12}$$

where $\bar{U} = 0.5U_0$ is the average velocity of the flow.

The last assumption, introduced by Taylor is that the radial diffusion is fast in comparison with convection. This assumption comes from the fact that the radial differences in concentration are small compared to axial differences and may be neglected. Therefore, the average concentration in the moving slice is equal to the concentration in the center of the tube:

$$Q = -\pi r_0^2 E_D \frac{\partial \bar{c}}{\partial x'}. \tag{3.13}$$

Considering the equation of continuity together with the equation for the flow out of the moving slice, Eq. (3.13), it may be shown that the dispersion of the entire concentration pulse of the solvent is described by the following differential equation:

$$\frac{\partial \bar{c}}{\partial t} = E_D \frac{\partial^2 \bar{c}}{\partial x'^2}. \tag{3.14}$$

The solution of Eq. (3.14), provided that the solute was injected in the form of a δ-pulse is as follows:

$$\bar{c} = \frac{n_M}{2\pi r_0^2 \sqrt{\pi E_D t}} \exp\left[-\frac{x'^2}{4E_D t}\right], \tag{3.15}$$

where n_M is the number of moles of solute in the injected δ-pulse.

Eq. (3.15) proves the previously discussed statement that a larger diffusion coefficient results in a sharper concentration distribution.

Eq. (3.15) may be used to extract the value of the diffusion coefficient from the known concentration of the solute at a given axial coordinate at a given moment of time. Usually, the measurements of the concentration are performed either at a fixed position at different moments of time, or at a fixed time at different positions [13]. Then the diffusion coefficient is extracted from the concentration profile or history as a fitting parameter in Eq. (3.15).

There is another way of extracting diffusion coefficients from the Taylor dispersion experiment. It is based on estimation of the statistical moments of the recorded concentration of the solute and does not require implementation of Eq. (3.15). The concentration of the solute is measured as a function of time at the end of the tube. Then the zero, first and second statistical moments are calculated. It was shown in [7, 12] that the diffusion coefficient may be determined from the second moment as:

$$D = \frac{R^2}{24\overline{t}\,\sigma_t^2}, \tag{3.16}$$

where σ_t is the variance, estimated in the following way:

$$\begin{aligned} \overline{c} &= \int_0^\infty c(t)\,dt, \\ \overline{t} &= (1/\overline{c})\int_0^\infty c(t)\,t dt, \\ \sigma_t^2 &= (1/\overline{c})\int_0^\infty c(t)\,(t-\overline{t})^2\,dt. \end{aligned} \tag{3.17}$$

Thus, measurement of the time variation of the concentration at a given position and further estimation of the second moment allows determination of the diffusion coefficient from Eq. (3.16). Melzer [101] has shown that accuracy of the mathematical approximation with application of Eqs. (3.16), (3.17) is better than 1%.

A different solution of Eq. (3.6) was given by Aris [12]. He included the axial diffusion into the considerations. As a result, the solution obtained by Aris does not provide the equation for the complete concentration profile. However, it provides an extended expression for the second moment of the concentration distribution:

$$\sigma_t^2 = \frac{2Dt}{\overline{U}^2} + \frac{r_0^2 t}{24D}. \tag{3.18}$$

Eq. (3.18) accounts for the effect of axial diffusion. Therefore, it must be applied, when axial diffusion cannot be neglected. It is easy to see from Eq. (3.18) that the axial diffusion may be neglected when the following condition is obeyed:

$$\frac{\overline{U}^2 r_0^2}{48D} \gg D. \tag{3.19}$$

As was shown by Alizadeh et al. [7], the effect of axial diffusion on the value of the variance is very small if the following relation is obeyed:

$$\frac{\overline{U}L}{D} = Pe > 700\frac{L}{r_0}, \tag{3.20}$$

where *L* is the total length of the tube, and Pe is Peclet number.

Other restrictions imposed by the assumptions, introduced during solution of Eq. (3.6) must be mentioned. The first restriction is that the flow of the solvent in the tube is laminar, that is the Reynolds number Re is

$$Re = \frac{2r_0\overline{U}}{\eta} \le 2000. \tag{3.21}$$

Here η is the kinematic viscosity of the solvent.

The restriction imposed by neglecting of the axial diffusion was already discussed above.

Another important assumption introduced by Taylor is that the radial variation of the concentration is lower than the axial variation. Taylor [156] and later Aris [12] have shown that this is true when

$$7.2\left(\frac{LD}{r_0^2\bar{U}}\right) \gg 1. \qquad (3.22)$$

The third important point is illustrated by Figure 3.5. Generally, due to obvious experimental problems, the injected pulse cannot be absolutely sharp. Baldauf and Knapp [14] have shown that the error related to the injection of the square pulse is small if the volume of the injected solute is much smaller than the volume of the capillary tube.

Additional and more detailed discussion of important questions about practical application of the Taylor dispersion technique may be found in [7, 101, 134].

3.3. Interferometry

The interferometry technique provides very high accuracy at large cost of both equipment and effort. The diffusion coefficients can be measured with accuracies down to 0.2% [130, 146].

Interferometry is based on measurements of the spatially varying gradient of the refraction index in a region where the diffusion takes place. Assuming that the indices of refraction of the two liquids are different and that the gradient of the refraction index is proportional to the gradient of the relative concentrations of either liquid, the mutual diffusion coefficient can be extracted from the temporary and spatial variation of the refractive index.

There is a variety of interferometer methods, which mainly differ in the optical construction of the experimental setup [68]. The first application of interferometry to measuring diffusion coefficients was described by Gouy [57]. A schematic description of the Gouy interferometer is presented in Figure 3.6.

As may be seen from Figure 3.6, the scheme of the experimental setup is rather simple. Monochromatic light is generated by a light source. Then the lens parallelizes the light. The light penetrates through the diffusion cell and generates the interference pattern on the photographic plate.

The diffusion cell used in interferometer measurements contains two compartments separated by one or two very thin slits [119]. The solutions, slightly different in concentration, are fed into the compartments and a steep concentration change is formed close to the slits [170]. Once such a concentration change is formed, the experiment starts and diffusion starts to weaken the concentration jump.

The light refraction index is different for the two inter-diffusing solutions. Therefore, when the light reaches the photographic plate, one can see the interference pattern of black horizontal lines (Figure 3.6). This pattern is related to the gradient of the refractive index, and, in turn, it is related to the gradient of the concentrations inside the diffusion cell. Hence, the analysis of the interference pattern together with solution of the diffusion mass transfer problem inside the diffusion cell may provide the value of the diffusion coefficient [107, 109, 119].

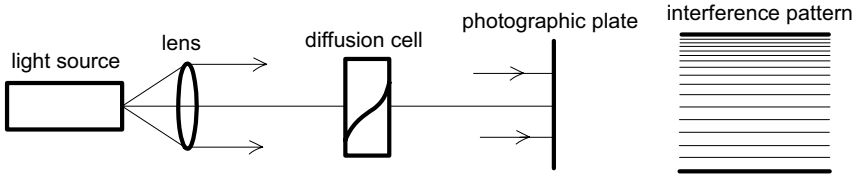

Figure 3.6: Schematic description of Gouy interferometer.

There are two other variations of the interferometer technique, which differ mainly in the arrangement of the additional lenses or mirrors. These are the Mach-Zehnder and the Rayleigh interferometers. These two interferometers are slightly more difficult to construct, but they provide interference patterns which are easier to analyze [68].

The construction of the Mach-Zehnder (MZ) interferometer is presented in Figure 3.7. In the Mach-Zehnder interferometer the light is split into the two beams, one passing through the diffusion cell and another (the reference beam) bypassing it. Then both beams are collected, and the interference pattern appears on the photographic plate due to the difference in phases between the beams [170].

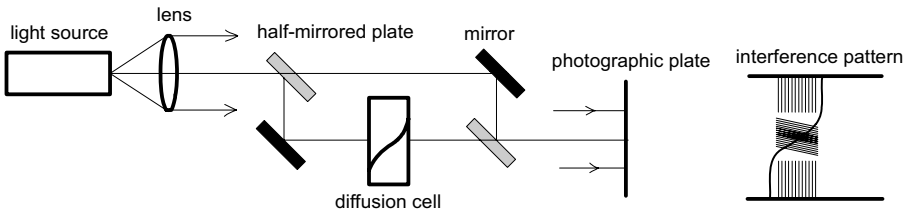

Figure 3.7: Schematic description of Mach-Zehnder interferometer.

A schematic picture of the interference pattern, produced by the MZ interferometer is presented in Figure 3.7. Examples of the interference patterns obtained in experiments may be found elsewhere [119, 170]. The vertical lines in the pattern indicate zones with no concentration gradients (regions of homogenous solution) (see Figure 3-7). As one approaches the zones with the concentration gradients, the fringes become curved or

horizontal. Wild [170] states that the number of horizontal lines depends upon the concentration difference between the solutions and must be constant during the experiment.

Construction of the Rayleigh interferometer is similar to that of the Mach-Zehnder interferometer, with cylindrical lenses instead of the mirrors [32, 68].

It was stated earlier that extraction of the diffusion coefficients from the time variation of the interference patterns requires solution of the diffusion problem inside the cell. Besides, a method for estimation of the concentration gradient from the interference patterns is required.

A theoretical description of the diffusion mass transfer in the diffusion cell comes from analysis of the Fick equation combined with the continuity equation [157]. Coupled with the method for extracting the concentration profiles from the interference patterns [107, 109, 119] solution of the diffusion problem provides a computational scheme for estimation of the diffusion coefficient as a fitting parameter from the sets of the interference fringes.

The interferometer technique has proved to be the main source of highly accurate experimental diffusion coefficients.

3.4. Other Methods

Three experimental methods discussed in details above are the most widely used (Table 3.1). Among 32 collected papers with experimental values of mutual diffusivities in liquid binary mixtures, 12 were based on application of the interferometry, 13 – diaphragm cells, 5 - Taylor dispersion and only 2 data sets were measured by other methods. This statistic does not pretend to be complete. However, it describes the general situation with experimental measurements of the diffusion coefficients in binary mixtures. Besides the three traditional methods, there are a few experimental techniques which are not directly applicable to measurement of the mutual diffusion coefficients. A new method is based on the application of Raman spectroscopy, which is rather promising, is not yet widely recognized.

Additionally, there is a bunch of methods, which do not measure the mutual diffusion coefficients, but the *tracer diffusion* and the *self-diffusion* coefficients, which have not been included into Table 3.1. Rigorous definitions of the *tracer* and the *self-* diffusion coefficients are given in the next chapter. The self-diffusion coefficient may be interpreted as the diffusion of a tagged (for example, radioactive) solute in an untagged, but otherwise chemically identical solvent. The tracer diffusion coefficient is generally the same as the self-diffusion coefficient, but with a solvent not necessarily being the same compound (moreover, the solvent may be a mixture of several components). The tracer diffusion coefficient reduces to the self-diffusion coefficient, when the solvent is pure and chemically identical to the solute. More precise definitions of the differences between the mutual, self- and tracer diffusion coefficients may be found in [4] and [32]. There is a set of experimental methods, where the

radioactively tagged components are applied to measurements of the tracer diffusion coefficients. These methods are not discussed here. However, the mutual diffusion coefficients may be related to the tracer diffusion coefficients by empirical relations, which will be considered in the next chapter.

Among the indirect methods, the most well-known one is the method of spin-echo nuclear magnetic resonance (NMR) [37, 65, 98]. This method involves rather complicated and expensive equipment. It has been found to be a very useful tool for study of diffusion. Due to its non-invasive nature, NMR is one of the few methods capable of measuring diffusion coefficients in porous media [127, 140]. With regard to measurement of diffusion coefficients in the free space, NMR has few advantages, the most important being the applicability to measurement of diffusivities in highly viscous fluids, where the traditional methods fail. The main disadvantages are the high price of equipment and relatively modest accuracy for binary mixtures (≥ 5%) [98, 37]. And the main disadvantage in our case is the impossibility of NMR to measure mutual diffusion coefficients. An extensive physical theory lies behind the NMR method [24, 65]. The NMR method may be described briefly as follows. The specimen is put into the coil, which is positioned inside an externally applied magnetic field, produced by the NMR technique. At equilibrium the nuclear magnetic moments of the species tend to be aligned parallel to the external field. Then short and intense bursts of radiofrequency energy are applied to the species in different directions. This results in the appearance of an induced voltage in the coil, which is the result of the free precession of the magnetization vectors of each nucleus of the species. The voltage appears only when the magnetization vectors of a given nucleus are in phase. Such an induced voltage is called “spin-echo”. Due to diffusion, the positions of the nuclei always change. It may be shown [65] that diffusion reduces the voltage induced in the coil. The rate of reduction of the voltage is related to the value of the diffusion coefficient.

The most widely used method for measuring the tracer diffusion coefficient is the so-called capillary method. The idea behind the method is discussed in [78]. A capillary is filled by the solution of known composition with one of the components being radioactively tagged. Then the capillary is immersed in a large volume of the same solution, but with untagged components. The setup stands for a few days (3-5) and then the capillary is removed, emptied, and counted. Afterwards the capillary is filled with the same tagged solution, which was injected in the beginning, emptied immediately and counted again. The ratio of these two counts, together with the solution of the corresponding diffusion problem, makes it possible to determine the diffusivity. The main source of error in the experiments is the convective transfer from the open end of the capillary. To remove convection, the open end may be covered by a porous glass membrane, which eliminates convection but allows diffusion. The diffusion problem must be changed to account for the presence of the

additional resistance imposed by the membrane. This resistance is constant of the membrane and must be determined from the calibration experiments. The overall estimated accuracy of the method is usually around 2-3% [78].

Raman spectroscopy is probably the most promising among the new methods for measurement of mutual diffusion coefficients. This is a method of chemical analysis that enables real-time characterization of compounds in a non-contact manner. A sample is illuminated by a laser beam and the scattered light is collected. The wavelengths and the intensities of the scattered light can be used to identify functional groups in the molecule. Raman spectroscopy has found wide application in the chemical, polymer, semiconductor, and pharmaceutical industries because of its high information content and the ability to avoid sample contamination. Raman spectroscopy is able to analyze with a very high speed, which makes it possible to track time change of the concentrations with a high temporal resolution and to apply it to measurements of the diffusion coefficients [15, 102]. The experimental setup used in this method may be rather complicated, involving a large number of optical components. However, the principle of the experiment is rather simple. A small diffusion cell is filled with the solution. Then a denser solution is injected from the bottom of the cell (to reduce the gravity effect) and diffusion starts. The focused beam of laser can be positioned at different heights of the cell and the dependence of the concentration on both coordinate and time may be measured.

Obviously, modeling the distribution of the mixture is required in order to extract diffusion coefficients from the measured concentration profile. This is done either by solving the diffusion equation with different boundary conditions or by considering a more detailed model, including the total mole balance, the component balance, the bootstrap relation, the diffusion equation and at some cases the equation of state [15].

The Raman spectroscopy method has a number of advantages and disadvantages. The main advantages are the possibility for fast measurements with small samples, the ability for extension to multicomponent measurements [15] and a high accuracy (down to 0.2% for a binary mixture [15]). The major disadvantage is the high sensitivity to external perturbations.

Table 3.1: Collection of experimental data of mutual diffusion coefficients in the binary liquid mixtures (mainly non-electrolyte systems)

Authors	Mixtures measured	Data points	Temp. range (K)	Method	Estimated accuracy, %	Reference
Harris K.R. et al.	3	25	298.15	Gouy interferometer	less than 1.0	[69]
Guarino G. et al.	2	24	278.15	Gouy interferometer	less than 0.5	[63]
Kulkarni M.V. et al.	1	13	298.15-308.15	Gouy interferometer	1.0	[90]
Rodwin L. et al.	1	13	298.15	Gouy interferometer	0.2	[130]
Shieh J.C. and Lyons P.A.	4	47	298.15-308.15	Gouy interferometer	0.2	[146]
Vitagliano V. et al.	1	28	298.15	Gouy interferometer	1.0	[163]
Anderson D.K. et al.	6	73	298.15-313.15	Mach-Zehnder interferometer	less than 1.0	[9]
Anderson D.K. and Babb A.L.	1	8	298.15	Mach-Zehnder interferometer	less than 1.0	[10]
Anderson D.K. and Babb A.L.	2	16	298.15	Mach-Zehnder interferometer	less than 1.0	[11]
Kelly C.M. et al.	1	12	298.15	Mach-Zehnder interferometer	1.5	[78]
Pertler M. et al.	2	18	298.15	Mach-Zehnder interferometer	0.6-0.9	[119]
Aminabhavi T.M. and Munk P.	2	22	293.15	Interferometry in analytical centrifuge	4.0	[8]
Lee Y.E. and Li S.F.Y.	1	18	303-13-313.13	Taylor dispersion	1.0	[91]
Melzer W.M. et al.	8	127	283.15-303.15	Taylor dispersion	0.7-8.6	[101]
Padrel de Oliviera C.M. et al.	4	40	283.15-298.15	Taylor dispersion	1.0	[118]
Rowley R.L. et al.	6	36	303.15	Taylor dispersion	2.0	[131]
Rowley R.L. et al.	6	36	303.15	Taylor dispersion	2.0	[132]
Sanni S.A. et al.	6	164	298.15-313.15	Three-compartment diaphragm cell	1.0-2.0	[136]
Sanni S.A. et al.	7	199	298.15-313.15	Three-compartment diaphragm cell	1.0-2.0	[137]
Tyn M.T. and Calus W.F.	3	193	298.15-358.15	Three-compartment diaphragm cell	2.6	[158]
Derlacki Z.J. et al.	1	17	278.15-298.15	Dullien diaphragm cell	0.5	[35]
Ghai R.K. and Dullien F.A.L.	2	NA[A]	298.15	Dullien diaphragm cell	0.5	[54]
Tasic A.Z. et al.	1	7	298.15	Dullien diaphragm cell	0.5	[156]
Wedlake G.D. and Dullien F.A.L.	3	32	298.15	Dullien diaphragm cell	1.0	[165]
Shroff G.H. and Shemilt L.W.	1	15	298.15	Modified Dullien diaphragm cell	less than 1.0	[147]
van Geet A.L. and Adamson A.W.	1	21	298.15-333.15	Stokes diaphragm cell	2.4	[53]
Ramakanth C. et al.	14	70	298.15	Stokes diaphragm cell	up to 8.0	[123]
Ramprasad G. et al.	8	50	301.15	Stokes diaphragm cell	up to 14.0	[124]
Bidlack D.L. and Anderson D.K.	1	8	298.15	Modified Stokes diaphragm cell	less than 1.0	[17]
Lo H.Y.	4	88	298.15	Modified Stokes diaphragm cell	less than 1.0	[95]
Sanchez V. and Cliffton M.	3	39	293.15	Limited-diffusion method	1.5	[135]
Bardow A. et al.	1	4	294.15	Raman Spectroscopy	less than 0.5	[15]

[A] experimental results have been approximated and coefficients of correlation are reported

3.5. Multicomponent Mixtures

Extension of the existing experimental methods to measurements of diffusion coefficients in multicomponent mixtures is discussed in this section. To the best of our knowledge, only Rai and Cullinan [121] measured diffusion coefficients in quaternary liquid mixtures of non-electrolytes, and there are only few sources describing measurements of the diffusion coefficients in ternary mixtures. Table 3.2 summarizes available measurements of diffusion coefficients in ternary liquid mixtures of both electrolytes and non-electrolytes. It may be seen that the number of mixtures and experimental data points is very small compared to the binary mixtures. The estimated accuracies for the ternary diffusivities are not much lower than the accuracies for the binary diffusion coefficients. However, the accuracies listed in Table 3.2 only concern the main term diffusivities. In ordinary ternary mixtures the absolute deviations for the measurements of main and cross diffusivities are rather close to each other: $(0.05\text{-}0.2)\cdot 10^{-9}$ m^2/s. However, the cross-terms in the diffusion matrix may be 4 to 5 times lower than the main terms, which results in very high average errors in the cross-term diffusivities (up to 50%). Moreover, there are cases where the cross-diffusivities are several orders of magnitude lower than the main diffusivities. Typically, these are diffusion coefficients in ideal mixtures, where cross interactions between the components are rather weak. In such cases the absolute error of the measurements may be higher than the value itself. Sometimes it is even difficult to evaluate the sign of a cross diffusivity. Checking the symmetry of the Onsager phenomenological coefficients may validate the experimental data, as described in Chapter 7.

Analyzing Table 3.2, it can be seen that majority of the papers were published in 1950 – 1960, after the development of thermodynamics of irreversible processes. In that time the measured ternary diffusion coefficients were mainly used for verification of the Onsager reciprocal relations [105, 106, 116, 117]. Afterwards, the interest in the measurements of the diffusivities in multicomponent mixtures decreased. Only in the middle of 1990s new measurements appeared (mainly for electrolyte solutions), a fact which may probably be explained by growing industrial demand.

Analysis of Table 3.2 provides also information about possible adaptation of experimental methods developed for measurements in binary mixtures to multicomponent systems. Generally, only two methods are applied to the ternaries, namely, different modifications of the diaphragm cell method and different types of the interferometry technique. Obviously, changes in both experimental procedure and data analysis are required to apply these methods to ternary mixtures. These changes are briefly discussed below.

The first important change is that the reference frame can no longer be neglected, as it was for binary mixtures, where the diffusion coefficients do not depend upon the choice of

the reference frame. Usually, all the experimentally measured values of the Fick diffusion coefficients are expressed in the volume-fixed reference frame.

The experimental procedure for both the diaphragm cell and the interferometer methods does not change essentially compared to the procedure for binary mixtures. The data analysis, however, is much more complicated.

The commonly used procedure for data analysis for the interferometer technique was developed by Fujita and Gosting [49]. They proposed the way for evaluating four ternary Fick diffusion coefficients (expressed in the volume-fixed reference frame) from a few measured quantities. The processing of data analysis generally requires solving a system of non-linear equations, to find values of the diffusion coefficients [31, 49]. In limiting cases of small cross-term diffusion coefficients, the procedure has to be further modified. Fujita and Gosting [49] proposed expressions for three cases (only D_{12} is close to zero, only D_{21} is close to zero, or both D_{12} and D_{21} are close to zero).

The procedure for experimental data analysis for the diaphragm cell technique and the ternary mixtures was proposed by Dunlop [42, 43, 44]. All the assumptions, which were introduced for derivation of Eq. (3.1), should be obeyed for the experiments with ternary mixtures. To estimate four ternary diffusion coefficients (in the volume-fixed reference frame), at least four measurements are required. In each of these measurements the following quantities must be obtained: initial concentration differences for components, the diaphragm cell constant and the concentration differences for the components at a given time. It is recommended, however, that more than four measurements are performed. The procedure for data analysis in the diaphragm cell method also requires specific considerations in the cases where the cross-term diffusivities are small [41, 42].

Initial concentration differences for both methods may be defined in two possible ways. The first is to have one initial concentration difference equal to zero and to vary another difference. This way is mainly used in the diaphragm cell method. Another way, consisting in setting both differences non-zero, is more advantageous in the interferometer techniques [31].

The final comments are due to the work of E.L. Cussler, Jr. and P.J. Dunlop [31]. They measured the diffusion coefficients in the same ternary system under the same conditions by both the diaphragm cell and the Gouy interferometer method. The diffusion coefficients measured by both methods agree with each other within the experimental error. However, the interferometer method is more accurate. The main sources of errors in the diaphragm method are in measuring the concentration differences and the diaphragm cell constant. In the interferometer technique the main error comes from the procedure of the graphical analysis of the interference patterns [31].

Table 3.2: Collection of experimental data for mutual diffusion coefficients in the ternary liquid mixtures (including electrolyte systems)

Authors	Mixtures measured	Data points	Temp. range (K)	Method	Estimated accuracy [A], %	Reference
Burchard J.K. and Toor H.L.	1	6	303.15	Stokes diaphragm cell	up to 5.0	[21]
Burchard J.K. and Toor H.L.	1	4	303.15	Stokes diaphragm cell	up to 5.0	[22]
Cullinan H.T. and Toor H.L.	1	9	298.15	Stokes diaphragm cell	2.0-6.0	[27]
Riede Th. and Schlunder E.-U.	1	7	323.15	Stokes diaphragm cell	2.0-3.0	[126]
Schmoll J. and Hertz H.G.	1	4	298.15	Stokes diaphragm cell	2.0-5.0	[139]
Shuck F.O. and Toor H.L.	1	4	303.15	Stokes diaphragm cell	up to 5.0	[148]
Mortimer R.G. and Hicks B.C.	1	5[B]	298.15-318.15	Rotating diaphragm cell	5.0	[114]
Cussler E.L., Jr. and Dunlop P.J.	1	1	298.15	Gouy interferometer/diaphragm cell	0.3/0.9	[31]
Cussler E.L., Jr., and Lightfoot E.N.	2	3	298.15-301.15	Gouy interferometer	up to 11.0	[30]
Dunlop P.J. and Gosting L.J.	1	6	298.15	Gouy interferometer	1.0-5.0	[42]
Dunlop P.J.	2	5	298.15	Gouy interferometer	1.0-5.0	[43]
Dunlop P.J.	1	1	298.15	Gouy interferometer	1.0-5.0	[44]
Fujita H. and Gosting L.J.	1	5	298.15	Gouy interferometer	1.0-7.0	[49]
Lo P.Y. and Myerson A.S.	1	20	298.15	Gouy interferometer	NA	[96]
Revzin A.	1	1	298.15	Gouy interferometer	0.6-1.0	[125]
Vergara A. et al.	1	8	298.15	Gouy interferometer	0.3-1.0	[160]
Wendt R.P.	1	4	298.15	Gouy interferometer	up to 12.0	[166]
Wu J. et al.	1	3	308.15	Gouy interferometer	1.0-3.0	[172]
Albright J.G. et al.	1	4	298.15	Rayleigh interferometer	0.2-1.0	[5]
Kett T.K. and Anderson D.K.	2	7	303.15	Mach-Zehnder interferometer	up to 6.0	[79]
Alimadadian A. and Colver C.P.	1	9	298.15	Custom-build Interferometer	4.69	[6]

[A] The presented values of accuracy are usually presented only for main diffusion coefficients, the accuracy of the cross diffusion coefficients is usually very low (up to 50%) and non-regular

[B] The temperature dependence of the ternary mutual diffusion coefficient was measured at the fixed composition

3.6. Summary

Experimental studies of the diffusion coefficients in binary mixtures are the main source of existing knowledge about diffusivities. Measurement of diffusion coefficients is a cumbersome task. There is a large variety of different experimental techniques. However, three methods are mainly applied to measuring the diffusivities in binary liquid mixtures.

The most widely used experimental method is the diaphragm cell method, providing accuracies as high as 0.5%, and accuracies of around 3-5% on average. Another basic method is the Taylor dispersion procedure. The average accuracy of this method is around 2%. It is more difficult to apply properly, compared to the diaphragm cell method; however, it is also less time consuming. The Taylor dispersion method requires a rather extensive mathematical background. However, it results in a simple procedure of the data analysis. The best accuracies achieved by the Taylor technique are around 0.7%. The interferometry methods are the most accurate. They use interferometry equipment for measuring concentration profiles. The price for high accuracy of the measurements is both the price of the equipment and the effort required. The processing of data requires good understanding of optical theory and involves extensive computations. However, an average accuracy of the interferometer methods is around 1%, which is better than for other methods. Interferometer methods are capable of producing results with an accuracy down to 0.2%, which is the best accuracy among the experimental methods for measuring binary diffusivities.

There are many other experimental techniques, besides the three widely used methods [32]. However, the majority of them may be considered as modifications of the basic techniques. There are also methods suitable for measuring self- or/and tracer diffusion coefficients, which are based on using of radioactively tagged chemicals and counting equipment. The NMR method is capable of measuring both self- and tracer diffusion coefficients. Moreover, the NMR method makes it possible to measure the diffusion coefficients in highly viscous fluids and in porous media.

Measurement of the diffusion coefficients in multicomponent mixtures is more complicated compared to the binary mixtures. The main complications are due to the data analysis, which needs to be changed dramatically. The analysis of the literature on experimental measurements of the ternary diffusion coefficients (Table 3.2) shows that only two experimental methods have been applied for such measurements, namely, the diaphragm cell method and interferometry. In both cases, no significant changes in the construction of the experimental setup are required. However, the procedure of data analysis needs to be significantly modified [42, 43, 44, 49]. The accuracy of determination of the main-term diffusion coefficients does not decrease significantly, compared to the accuracy for binary mixtures. However, the error in estimation of the cross diffusivities can sometimes be higher than the diffusivities themselves. This is due to sometimes low values of the cross-

terms, which both require more precise measurements and more accurate treatment of experimental data.

Generally, it can be concluded that experimental studies can provide accurate and reliable data for binary liquid mixtures and there are several experimental methods which are more convenient and accurate than others. For multicomponent mixtures, the measurements are more difficult, mainly due to problems with low values of the cross-term diffusivities.

4. Diffusion Coefficients in Binary Mixtures: an Overview

Approaches to estimation of diffusion coefficients in the binary mixtures are discussed in this chapter. The first section of the chapter is focused on an overview of existing phenomenological methods. The second section discusses the application of molecular dynamics simulations to estimation of diffusion coefficients.

4.1. Phenomenological Approaches

Apart from the dilute gas limit, where a rigorous physical theory of the diffusion coefficients has been proposed in the framework of the Boltzmann formalism [72], the available correlations for diffusion coefficients are built on empirical or semi-empirical grounds.

The most widely applied models are combinations of the mixing rules like those of Darken [34] or Vignes [161] and their modifications, with the dilute limit estimates of the diffusion coefficients based mostly on different modifications of the Einstein-Stokes formula [120]. This approach is capable of modeling monotonic variations of the diffusion coefficients with the molar fraction. Such a monotonous dependence is not observed even for some near-ideal mixtures (see the analysis of the experimental data below and in [169]). Another widely used approach to modeling employs the concepts of free volume and excess energy [38, 93, 168]. Other types of models have also been developed, for example, the group contribution model UNIDIF [74, 75].

4.1.1. An Approach Based on the Diffusion Coefficients at Infinite Dilution

Probably, the simplest and the most widely used approach to estimation of the mutual diffusion coefficients is based upon the concept of the diffusion coefficients at infinite dilution (see Figure 4.1). The starting point is estimation of the diffusion coefficients at infinitesimal concentrations. The values of diffusion coefficients in this limit may be estimated by means of *hydrodynamic* or *friction* models. The next step is application of a mixing rule for estimation of the concentration dependence of a mutual diffusion coefficient. Thus, the accuracy of this approach depends on both the accuracy of the model for dilute solution diffusivities and of the mixing rule for estimation of concentration dependence of the diffusion coefficients.

The model for dilute diffusion coefficients and the interpolation schemes for calculation of the concentration dependence are normally based on the semi-empirical considerations. There is a great variety for both of them. An overview of these modifications is presented here. Additional analysis of the existing models of such kind is available in [41, 92, 119, 134, 170].

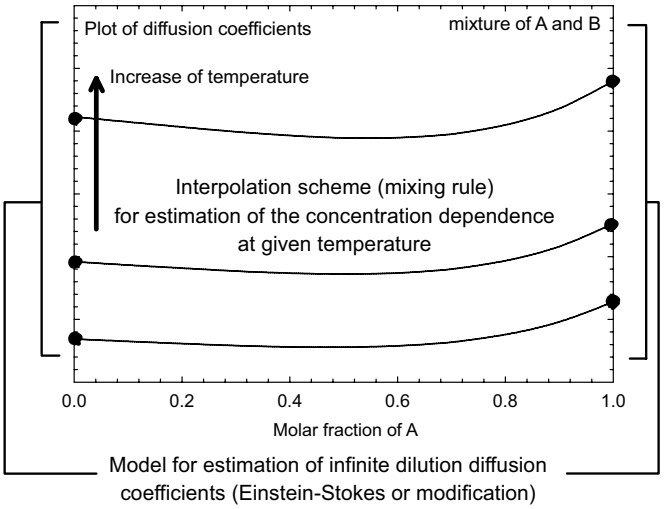

Figure 4.1: Estimation of diffusion coefficients based on the diffusion coefficients at dilute limits.

Estimation of the Diffusion Coefficients at the Dilute Solution Limit

Diffusion at the dilute solution limit may be described as independent motion of separate solute molecules between multiple molecules of a solvent. Einstein [46] described random walk of a single solute molecule in a continuous solvent, corresponding to the so-called Brownian motion (Figure 4.2). Complex influence of the solvent molecules on the solute particle may be represented as a combination of the viscous friction force and a random force produced by collisions with separate molecules. Einstein worked this out for the case where the solute molecules are large compared to the solvent molecules. Later simple modifications of the final expression were applied to the cases where the solute molecules are of the same size as, or even smaller than, the solvent molecules.

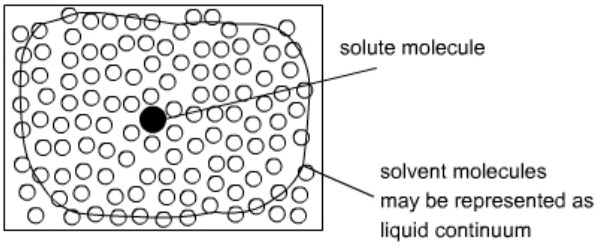

Figure 4.2: The Einstein approximation of the diffusion at dilute limit

More precisely, Einstein considered a mixture of the components i (solute) and j (solvent). A spherical particle of the solute with radius R_i moves in the solution under constant temperature and volume. The average effect of the solvent molecules on the solute

particle Is described by the friction force F_f. The problem becomes one-dimensional by projecting on axis *x*. Assume that the particles of the solute move by the distance δx. In equilibrium, variation of the Helmholtz energy must be equal to zero:

$$\delta U - T\delta S = 0, \tag{4.1}$$

where *U* is the internal energy and *S* is the entropy.

The expression for the change of the internal energy and entropy may be derived from considerations of the reference volume of the liquid, with the unity cross-section area and between two cross-planes – $x=0$ and $x=L$ under the assumption that solute molecules may be considered as an ideal gas:

$$\delta U = -\int_0^L F_f \nu_i \delta x dx; \delta S = \int_0^L R \frac{\nu_i}{N_A} \frac{\partial \delta x}{\partial x} dx = -\frac{R}{N_A} \int_0^L \frac{\partial \nu_i}{\partial x} \delta x dx. \tag{4.2}$$

Here R is the universal gas constant, N_A is the Avogadro number and ν_i is the number of the solute molecules per unit of volume of liquid.

Substitution of Eq. (4.2) into Eq. (4.1) results in the following condition of equilibrium:

$$-F_f \nu_i + \frac{RT}{N_A} \frac{\partial \nu_i}{\partial x} = 0 \text{ or } F_f \nu_i = \frac{\partial P}{\partial x}. \tag{4.3}$$

Eq. (4.3) has a clear physical interpretation: The gradient of the pressure is compensated by the friction force acting on all the solute molecules.

Let us now find the velocity of the solute particles. It can be determined by application of the Stokes equation for the average hydrodynamic friction force [150]:

$$F_f = 6\pi\eta_j R_i u_i, \tag{4.4}$$

here u_i is the velocity of the solute, η_j is the kinematic viscosity of the solvent. Expressing the flow of the particles per unit cross-sectional area per unit of time and taking into account the same flow of the particles due to the diffusion results in the following equation for conservation of the particles:

$$\frac{\nu_i F_f}{6\pi\eta_j R_i} - D_{ij} \frac{\partial \nu_i}{\partial x} = 0, \tag{4.5}$$

The first term in Eq. (4.5) is the flow of particles per unit of area and unit of time, obtained from Eq. (4.4). The second term in Eq. (4.5) is the diffusion flux. Here D_{ij} is the diffusion coefficient of the solute particles in the solution, or in our case the diffusion coefficient of the species i in the species j, under the condition that the solute concentration is small.

Comparison of Eq. (4.5) with Eq. (4.3) yields the following expression for the diffusion coefficient at the dilute limit:

$$D_{ij}^{i\to 0} = \text{Đ}_{ij}^{i\to 0} = \frac{kT}{6\pi\eta_j R_i}. \qquad (4.6)$$

Expression (4.6) is known as the Einstein-Stokes equation and is widely used for estimation of the diffusion coefficients at the dilute solution limit. Eq. (4.6) is valid both for the Fick and the Maxwell-Stefan diffusion coefficients at the dilute limit, since the thermodynamic correction factor, used for recalculation of the MS diffusivities into the Fick ones (see Chapter 2) is equal to unity at this limit.

Eq. (4.6) was later derived by Langevin in a completely different way [52]. Langevin considered the Newton equation of motion of a solute particle under the action of the two forces. The first force was the hydrodynamic friction force expressed by Eq. (4.4). Another force was described as a stochastic force, corresponding to the influence of the chaotic molecular motion on the solute particle. The equation of motion obtained by Langevin was

$$m_i \frac{d^2x}{dt^2} = -6\pi\eta_j R_i \frac{dx}{dt} + X. \qquad (4.7)$$

Here m_i is the mass of the solute particle and X is the stochastic force.

Eq. (4.7) is the *stochastic differential equation.* This work started a completely new area of mathematics, aimed in providing approaches to solution of such types of equations. A variety of rigorous methods for solving such equations was developed [52]. In the original Langevin considerations, the stochastic force was dropped by averaging, due to non-regularity of the force X, which made it possible to solve Eq. (4.7). The final expression for the diffusion coefficient obtained by Langevin, is identical to the expression derived by Einstein, Eq. (4.6). The key point in both approaches is the expression for the hydrodynamic force.

The Stokes equation (4.4) for the friction force can be substituted by some modifications. Three types of modifications are possible:

- modification of the pre-factor (six in original Einstein-Stokes equation (4.6));
- modification of the size factor (different approaches to estimation of the size of the solute molecules, or introduction of the ratios of the sizes of the solute and the solvent molecules);
- modification of the effective viscosity of the solvent.

Rutten [134] conducted an extensive analysis of different modifications of both the pre-factor and the size factor in Eq.(4.6). He has shown that the pre-factor depends upon the solvent and the solute. It varies from 2.0-3.0 for non-associating organic components to 6.0-7.0 for associating and polar organics. Also, he discussed four different approaches to estimation of the radius of the solute. While three of these approaches (the radius estimated from the molar volume, from the van der Waals volume [18] and from the critical volume) are

closely related to each other, the fourth approach is to use the radius of gyration [124]. The results obtained by Rutten indicate that there is no essential difference between the approaches to calculation of the radius of the solute molecules. However, application of the radius of gyration results in the worst performance of the model.

The inaccuracy of the original Einstein-Stokes equation is below 10% for simple non-associating components and may be as low as 20% for associating components [124, 134]. These accuracies are achieved by fitting the pre-factor to the experimental data, but keeping it constant for the data range. Application of the Einstein-Stokes equation with a pre-factor not suitable for describing given type of the mixture may result in higher errors [134]. The values of the pre-factor for different groups of non-polar liquids vary within 5% around the average value of 3.5 and for polar liquids within 8% around average value of 4.5. Therefore, the fixed value of the pre-factor may result in a 5-8% increase of the error.

Probably, the most widely known alternative to the Einstein-Stokes equation is the Wilke-Chang equation [171]. The best evidence of its popularity is the fact that the article of Wilke and Chang has the first rank in the list of "The 100 Most Cited Articles in AIChE Journal History" [3] with more than 1500 citations (the data on November, 2003). This fact also shows the popularity of this approach to estimation of diffusion coefficients. Wilke and Chang proposed the following empirical relation for estimation of the diffusion coefficients in the dilute solution limit [171]:

$$D_{ij}^{i\to 0} = \text{Đ}_{ij}^{i\to 0} = n\frac{T\sqrt{\psi M_j}}{\eta_j V_{b,i}^{0.6}}, \qquad (4.8)$$

Here n is a numerical coefficient (in the original paper [171] it is equal to $7.4\cdot10^{-8}$), ψ is the association coefficient and $V_{b,i}$ is the volume of the solute at its normal boiling point. The association coefficient is unity for non-associating components, between one and two for associating components and larger than two for highly associating components and water. Eq. (4.8) is similar in structure to the original Einstein-Stokes equation. However, the diffusion coefficients, predicted by Eq. (4.8), are related to the solute radius as

$$D_{ij}^{i\to 0} \sim R_i^{-1.8}.$$

According to Rutten [134], Reid et al. [124] and Wild [170], the performance of the Wilke-Chang equation may be worse than the performance of the Einstein-Stokes equation. Moreover, the Wilke-Chang model fails to predict diffusivities in mixtures of water and polar organics with the fixed value of the pre-factor equal to $7.4\cdot10^{-8}$ (the deviations are more than 150% [134]). If the pre-factor is adjusted to experimental data within the same class of components, the overall accuracy is around 15-20%. Probably, a better prediction by Eq. (4.8) may be achieved if it is applied within a more narrow class of components [134]. For example, if the diffusion coefficients of the alcohols must be predicted, the value of the

association parameter and the numeric pre-factor should be adjusted to the available experimental data for the near alcohols. However, this is true for all the empirical relations of the Einstein-Stokes type, and such a method cannot be considered as predictive.

A few equations should be mentioned as alternatives to the Einstein-Stokes equation. The equation proposed by King [81] provides a slightly better prediction than the Wilke-Chang equation; however it involves the ratio of the heats of evaporation of the solute and the solvent and is not suitable for aqueous solutions.

A modification of the Einstein-Stokes equation, proposed by Rutten [134], involves the ratio of the radii of the solute and the solvent:

$$D_{ij}^{i\to 0} = \text{Đ}_{ij}^{i\to 0} = \frac{kT}{n\pi\eta_j R_i}\left(\frac{R_j}{R_i}\right). \tag{4.9}$$

This simple modification results in a slightly better prediction, compared to the Einstein-Stokes equation. What is more important, the value of the numerical coefficient n becomes less sensitive to the change of the types of the components. For both associating and non-associating, as well as aqueous solutions, the value of *n* lies within the range 2-4, depending on the way for calculation of the solute and solvent radii.

Interpolation schemes

An interpolation scheme (mixing rule) is required to calculate the mutual diffusion coefficients in the concentrated solutions, starting from the dilute-solution diffusion coefficients (Figure 4.1).

There are two widely known mixing rules, namely the Darken [34] and the Vignes [161] rules. The expression which is nowadays known as the Darken mixing rule, was originally proposed by Adamson [1] for gases as a consequence of the gas kinetic theory and later extended to solids by Darken [161]:

$$\text{Đ}_{ij} = \frac{D_{ij}}{\Gamma} = \text{Đ}_{ij}^{i\to 0} z_j + \text{Đ}_{ij}^{j\to 0} z_i . \tag{4.10}$$

Here z is the mole fraction. Equation (4.10) is a simple linear mixing rule, connecting the two dilute diffusion coefficients by a straight line. Originally, both the Darken and the Vignes mixing rules were proposed for Fick diffusion coefficients, since the Maxwell-Stefan approach was not well known at that time. In the works of Darken and Vignes the “activity-corrected diffusion coefficient” is exactly the Maxwell-Stefan coefficient.

For the cases where there are large deviations from a linear dependence, Vignes proposed to apply a logarithmic dependence [161]:

$$\text{Đ}_{ij} = \frac{D_{ij}}{\Gamma} = \left(\text{Đ}_{ij}^{i\to 0}\right)^{z_j}\left(\text{Đ}_{ij}^{j\to 0}\right)^{z_i} . \tag{4.11}$$

Figure 4.3 illustrates the performance of the Vignes mixing rule for some selected mixtures. The Vignes rule can only represent monotonous behavior of the diffusivities.

The Vignes mixing rule is capable of describing diffusion coefficients in mixtures of non-polar components such as alkanes, where both the Fick and the Maxwell-Stefan diffusion coefficients behave monotonously, and their dependence on the molar fraction is concave. Such behavior is also sometimes observed in mixtures of polar compounds, and in this case the Vignes rule is also capable of describing the concentration dependence properly. Examples of such polar mixtures are the mixtures of acetone/chloroform [9, 98, 158], acetone/carbon tetrachloride [9] and different non-aqueous mixtures of acetic acids [101]. However, a majority of the binary mixtures with polar components, especially, of the aqueous solutions, demonstrates “non-ideal” behavior with maxima and minima in the concentration dependence of both the Fick and the Maxwell-Stefan diffusion coefficients.

As seen from Figure 4.3, the behavior of both Fick and MS diffusivities may be non-monotonous in strongly non-ideal mixtures. The activity correction factor for the mixtures presented in Figure 4.3 was calculated with the Soave-Redlich-Kwong (SRK) equation of state, and with an advanced modified Huron-Vidal mixing rule (MHV1) based on the UNIFAC activity coefficient model [103, 104]. As will be discussed later in more detail, this model has been found to be rather suitable for this type of computations.

A comprehensive study of the application of the Vignes and Darken rules can be found in [134]. A conclusion from the study is that the Vignes rule provides only slightly better prediction compared to the Darken rule. Deviations for the Vignes rule are around 5% for the ideal mixtures, 10% for the non-ideal, and around 20% for the polar and associating mixtures. Deviations for the Darken rule are just slightly higher for the ideal and non-ideal mixtures and similar for the associating mixtures. However, the difference between the Vignes and the Darken rules is not uniform. In some cases the Darken rule can be better than the Vignes rule and vice versa. The fact that the Vignes rule is no better than the Darken rule for highly non-ideal mixtures is well illustrated by Figure 4.3 (B and C).

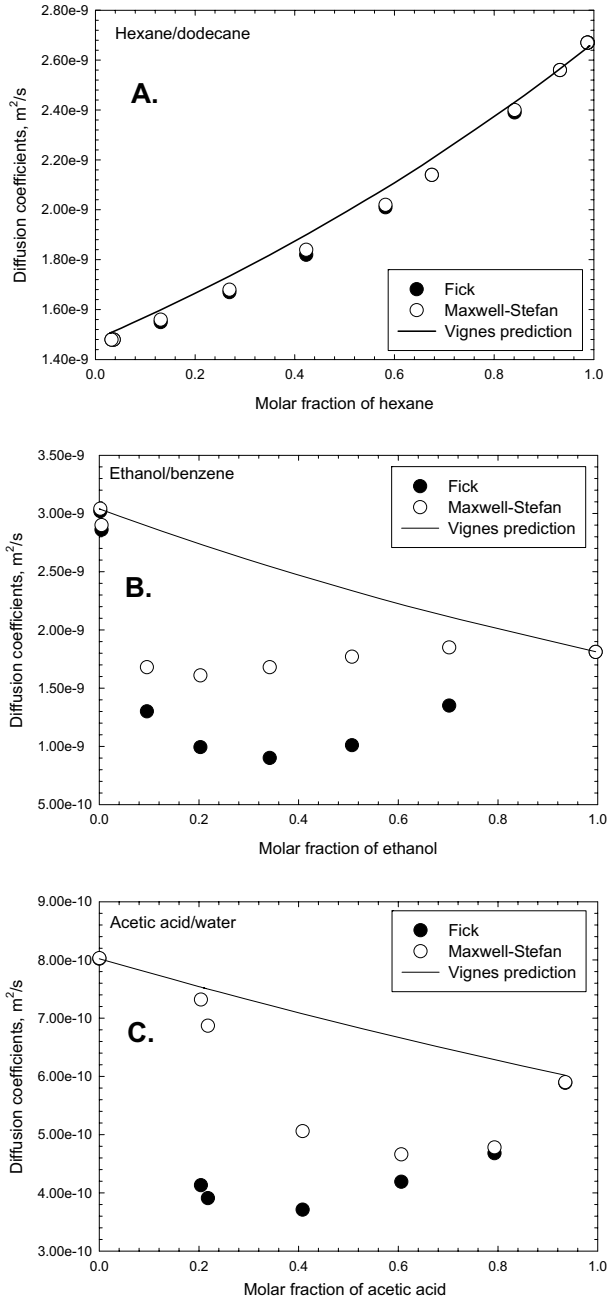

Figure 4.3: Typical performance of the Vignes rule for different binary mixtures. Experimental data: A - [146], B – [9] and C - [101].

Rutten [134] used the experimentally measured infinite dilution values of the diffusion coefficients in his comprehensive analysis of the interpolation schemes. The results, presented in Figure 4.3 are also obtained by using the experimental values of the infinite dilution diffusivities. Therefore, the discussed mixing rules provide interpolation, but not complete prediction. Such a prediction requires implementation of the models for limiting diffusivities, which results in significant increase of the error of predicted mutual diffusion coefficients (5-10% error of interpolation schemes + 10% error of limiting diffusivities for the simple ideal/non-ideal mixtures, and two times higher errors for the associating components).

There is a variety of methods attempting to improve the Vignes and the Darken scheme. Among the most widely used, there are three schemes based on the relations between the diffusion coefficient and the viscosity. The first method was introduced by Hartley and Crank [70]. It is analogous to the Darken rule:

$$\mathcal{D}_{ij} = \frac{D_{ij}}{\Gamma} = \frac{1}{\eta}\left[\left(\mathcal{D}_{ij}^{i\to 0}\right) z_j \eta_j + \left(\mathcal{D}_{ij}^{j\to 0}\right) z_i \eta_i\right]. \tag{4.12}$$

Here η_i is the kinematic viscosity of the pure component i and η is the viscosity of the mixture.

Leffler and Cullinan [92] proposed a Vignes-like expression with a viscosity correction:

$$\mathcal{D}_{ij} = \frac{D_{ij}}{\Gamma} = \frac{1}{\eta}\left(\mathcal{D}_{ij}^{i\to 0}\eta_j\right)^{z_j}\left(\mathcal{D}_{ij}^{j\to 0}\eta_i\right)^{z_i}. \tag{4.13}$$

Dullien and Asfour [41] proposed a different Vignes-like rule with viscosities:

$$\mathcal{D}_{ij} = \frac{D_{ij}}{\Gamma} = \eta\left(\frac{\mathcal{D}_{ij}^{i\to 0}}{\eta_j}\right)^{z_j}\left(\frac{\mathcal{D}_{ij}^{j\to 0}}{\eta_i}\right)^{z_i}. \tag{4.14}$$

The performance of the viscosity-corrected interpolation schemes may be better than the performance of the original schemes. However, if the viscosity or the logarithm of viscosity depends linearly on the concentration, the viscosity-corrected schemes tend to behave in a similar way as the original mixing rules. In some cases, the concentration dependence of the viscosity does not follow the concentration dependence of the diffusion coefficient (examples of such mixtures are benzene/toluene [136], heptane/hexadecane [17], benzene/heptane [136], water/ethanol [158], and some others [134]). In such cases the viscosity-corrected schemes provide worse prediction compared to the original schemes [134]. The Dullien scheme, Eq. (4.14), was tested only for ideal and slightly non-ideal mixtures [41]. Therefore, it is not recommended to apply Eq. (4.14) to prediction of the diffusion coefficients of the non-ideal mixtures.

Several interpolation schemes have been proposed for the friction coefficients, defined in Chapter 2 in derivations of Maxwell-Stefan equations for the mass transfer. The friction coefficients are related to the Maxwell-Stefan diffusivities as follows:

$$\xi_{ij} = \frac{RT}{\text{Đ}_{ij}}. \tag{4.15}$$

The interpolation schemes for the friction coefficients were considered and tested by Rutten [134]. These schemes assume linear or logarithmic dependencies for the friction coefficients. Since the Maxwell-Stefan diffusion coefficient is inversely proportional to the friction coefficient, the Darken-like interpolation scheme has the form of

$$\frac{1}{\text{Đ}_{ij}} = \frac{\eta}{\eta_j}\left(\frac{z_j}{\text{Đ}_{ij}^{i\to 0}}\right) + \frac{\eta}{\eta_i}\left(\frac{z_i}{\text{Đ}_{ij}^{j\to 0}}\right), \tag{4.16}$$

The Vignes-like logarithmic dependence is identical to that proposed by Leffler and Cullinan, Eq. (4.13). Extensive analysis, conducted by Rutten [134], demonstrates that Eq. (4.16) is not well-suited for ideal mixtures, where it provides a less accurate description than the original Vignes and Darken rules. However, for non-ideal non-associating mixtures it provides better accuracy.

Another method proposed by Rutten [134] is based on the variation of the Einstein-Stokes numerical constant in Eq. (4.6). Under assumption that the Einstein-Stokes constant varies linearly between the constants at dilute extremes, the following interpolation scheme may be derived:

$$\text{Đ}_{ij} = \frac{z_i\left(\text{Đ}_{ij}^{j\to 0}\eta_i R_j\right) + z_j\left(\text{Đ}_{ij}^{i\to 0}\eta_j R_i\right)}{\eta\left(z_i R_j + z_j R_i\right)}. \tag{4.17}$$

Here the molecular radii of both species are estimated either as the van der Waals radii [18, 19], or from the critical volume. Eq. (4.17) demonstrates rather good predictive capability both for ideal and non-ideal/non-associating mixtures [134].

A general conclusion regarding the interpolation schemes is that they are suitable for prediction of diffusion coefficients in concentrated solutions in ideal and non-ideal mixtures with accuracies around 10%. However, there is no suitable interpolation scheme for associating mixtures, where the discussed models exhibit deviations around 25% and higher. In many cases, even for relatively simple mixtures, the interpolation schemes do not reproduce the mixture behavior qualitatively. The choice of a thermodynamic model for estimation of the thermodynamic factor also plays an important role and may significantly influence the quality of prediction.

4.1.2. Free Volume Methods

The concept of free volume is based on empirical considerations, although it can be grounded in the framework of statistical mechanics [55, 72]. The free volume/activation energy theory operates in terms of self-diffusion coefficients. Although self-diffusion

coefficients can be related to mutual diffusion coefficients, the necessity for such an empirical relation may be considered as a major drawback of this approach.

The background of the free volume/activation energy methods lies in the Eyring theory of rate processes. Back in 1930 Eyring proposed the theory, to describe the rates of chemical reactions [55]. Eyring improved the well known Arrhenius expression [72] for the rate constant and proposed the following definition of the rate constant:

$$k_{rate} = \kappa\left(kT/h\right)\exp\left(-\Delta G^{a}/RT\right). \tag{4.18}$$

Here κ is the transmission coefficient, or the probability that a process actually takes place once a system is in the activated state; k_{rate} is the specific rate constant; ΔG^{a} is the activation Gibbs energy, and h is the Planck constant. Later it was realized that Eyring theory of rate processes can be applied to modeling of transport properties, since it may be assumed that in the condensed phase, in the course of the transport processes, the molecules pass through some sort of an activated state. The Eyring theory of rate processes postulates that the self-diffusion coefficient is directly proportional to the rate constant [72].

In later developments of the free volume/activation energy theory [72, 26] it was shown that the movement of molecules on the microlevel is possible under two conditions [113]. The first condition for a molecule to change its position is to have enough energy to escape from the force field of the neighboring molecules. The second condition is availability of free space to jump in. The second condition is considered in the free volume theory.

The free volume theory assumes that the volume of fluid consists of a volume occupied by molecules, and a part of the volume which is not occupied. The latter part is called *the free volume.* The free volume, in turn, may be divided into two parts. The first part is the interstitial volume, which includes small areas around the molecules, unavailable for mass transfer. The second part of the free volume is the volume of the “holes”, which are available for molecular motion. This volume is the key concept in all the free-volume theories. It is assumed that diffusive flows may only occur when the molecules can find holes large enough to jump into and, thus, to move to another position.

Cohen and Turnbull [26] related the self-diffusion coefficient to the free volume, using the Eyring theory of rate processes [72]. They showed that self-diffusion coefficients are proportional to the probability of finding a hole for a molecule to jump in:

$$D_{1\#,1} = D^{0}_{1\#,1}\exp\left(-\gamma\frac{V^{*}}{V^{f}}\right). \tag{4.19}$$

Here $D_{1\#,1}$ is the tracer diffusion coefficient of tracer 1 with regard to species 1, or in other words, the self-diffusion coefficient of species 1; V^{*} is the minimum (compressed) hole size into which a molecule can jump and V^{f} is the average free volume per molecule. The coefficient γ in the work of Cohen and Turnbull is a number between 0.5 and 1.

Wesselingh and Bollen [168] assumed that the coefficient γ is equal to 0.7 and proposed their own expression for the pre-factor in the formula of Cohen and Turnbull. For the cubic lattice model, it may be shown that the non-impeded self-diffusion coefficient is expressed as [168]:

$$\mathcal{D}_{1\#,1}^{0} \simeq \frac{1}{6}\sqrt{\frac{3kT}{\rho_1^* d_1}}. \tag{4.20}$$

Here ρ_1^* is the compressed density and d_1 is the molecular diameter of the first component. The self-diffusion coefficient correspondingly equals to:

$$\mathcal{D}_{1\#,1} = \mathcal{D}_{1\#,1}^{0} \exp\left(-0.7\frac{V^*}{V^f}\right) \tag{4.21}$$

The combined expression, relating both concepts of the free volume and the activation energy takes the following form [93]:

$$\begin{aligned} D_{1\#,1} &= D_{1\#,1}^{0}\frac{1}{N_A}\frac{V_f}{\gamma V} H \exp\left(-\alpha\frac{E_a}{kT}\right) \\ H &= \left(1+\gamma\frac{V^*}{V^f}\right)\exp\left(-\gamma\frac{V^*}{V^f}\right) \\ D_{1\#,1}^{0} &= \alpha\frac{V}{N_A\sigma^2}\left(\frac{kT}{\pi M}\right)^{1/2} \end{aligned} \quad . \tag{4.22}$$

Here α is numerical constant, γ is the numerical factor, responsible for accounting of overlapping, σ is the molecular diameter, E_a is the activation energy.

The practical application of Eq. (4.20) and Eq. (4.22) to modeling the diffusion coefficients requires an expression for the compressed and the free volumes, as well as for the activation energy. A common approach to estimation of the compressed volume is the empirical Guggenheim expression [168]:

$$\frac{V^*}{V_C} = \left[1+1.75\left(1-\frac{T}{T_C}\right)^{1/3}+0.75\left(1-\frac{T}{T_C}\right)\right]^{-1} . \tag{4.23}$$

Here V_C is the critical volume and T_C is the critical temperature. The free volume is correspondingly determined as a difference between the overall volume of the fluid and the compressed volume:

$$V^f = V - V^* . \tag{4.24}$$

Liu et al. [93] consider multiple expressions, relating the activation energy and the free volume with the thermodynamic properties from the ordinary thermodynamic models. For example, they show that the free volume and the activation energy entering Eq. (4.22) may

be determined from the compressibility factor, obtained by a simple cubic equation of state of the van der Waals type.

W. Fei and H.-J. Bart [47] have developed a model for estimation of the infinite dilution diffusion coefficients in the framework of the Eyring theory. They proposed to estimate the activation energy by a group contribution method. Such an approach demonstrates good prediction capabilities for binary mixtures. However it has not been tested yet on prediction of multicomponent diffusion coefficients at infinite dilution.

The free volume/activation energy formalism provides an adequate description of the self-diffusion coefficients [93, 168]. However, the predictive capabilities of the formalism need to be tested. Wesselingh and Bollen [168] observed that their model, Eq. (4.20), is capable of adequately predicting self-diffusion coefficients in simple liquids. Liu et al. [93] did not test their model.

The free volume/activation energy methods operate in the terms of the self-diffusion coefficients. Since the mutual diffusion coefficients are of main interest for practical applications, a relation between the self-diffusion coefficients and the mutual diffusivities is required. Wesselingh and Bollen [168] used the following geometric average mixing rules for the friction coefficients:

$$\xi_{ij} = \sqrt{\xi_{i\#,i}\xi_{j\#,j}} \ . \qquad (4.25)$$

Eq. (4.25) provides reasonable results [168]. A few other mixing rules are considered in [32, 145]. All these rules are built on an empirical basis. There is no mixing rule, which may be considered as a universal expression relating the self-diffusion coefficients and the mutual diffusivities.

The free volume approach shows good overall performance (including prediction) for polymer solutions [93, 145]. It is possible to extend it to multicomponent mixtures using simple mixing rules for free volume and activation energy [93, 168].

4.1.3. UNIDIF and GC-UNIDIF

The group contribution model *GC-UNDIF* for mutual diffusion coefficients was proposed by Hsu and Chen [75] on a basis of their first work, in which they developed the *UNIDIF* model [74]. The approach is an alternative to the methods described above. This is mainly due to extensive adjustment to the available experimental data, conducted by the authors of the method, and to the possibility of extending the approach to prediction of diffusion coefficients in multicomponent mixtures (although such a possibility was not investigated by the authors in detail).

Hsu and Chen define the rate of the motion for a mixture $k_{rate,m}$, according to the Eyring theory of the rate processes [55, 72]:

$$k_{rate,m} = \prod_{i=1}^{n} \left(\frac{kT}{2\pi M_i} \right)^{z_i/2} \exp\left(\frac{N_C}{2kT} \sum_{i=1}^{n} z_i q_i \sum_{j=1}^{n} E_{ji} \theta_{ji} \right). \quad (4.26)$$

Here N_C is the coordination number, q_i is the surface area of component i, E_{ji} is the potential energy of interaction between species j and species i, and θ_{ji} is the local composition parameter, related to the average fraction of the surface area of the components i and j. They also define a distance parameter for each component. This parameter is assumed to be proportional to the cubic root of the molar volume, or to the volume parameter in the UNIQUAC model for activity coefficients [74]. According to the Eyring theory [72], the mutual diffusion coefficient is defined in the following way:

$$D_{ij} = \lambda_{ij}^2 k_{a,ij}, \ \lambda_{ij} = \lambda_i^{z_j} \lambda_j^{z_i}. \quad (4.27)$$

Here λ_{ij} is the distance parameter of the mixture, found by the mixing rule from the individual distance parameters of the components.

The value of $k_{a,ij}$ is expressed as follows:

$$\ln k_{a,ij} = z_i \left(\frac{\partial \ln k_{a,m}}{\partial z_j} \right)_{T,P,\mathbf{z}} + z_j \left(\frac{\partial \ln k_{a,m}}{\partial z_i} \right)_{T,P,\mathbf{z}}. \quad (4.28)$$

Substitution of the expression for the rate of motion in the mixture, Eq. (4.26) into Eq. (4.28) and into Eq. (4.27) results in a rather cumbersome expression for the mutual diffusion coefficient, which may be interpreted as a sum of different contributions:

$$\ln D_{ij} = \ln D_{ij}^{REF} + \ln D_{ij}^{EX} + \ln D_{ij}^{RES}. \quad (4.29)$$

Here superscript "*REF*" denotes the diffusion coefficient at the reference state, "*EX*" denotes the excess diffusion coefficient, and "*RES*", correspondingly, the residual diffusion coefficient.

The reference diffusion coefficients are determined according to the Vignes rule, Eq. (4.11). Hence, the final expression may be considered as the Vignes expression with an additional thermodynamic correction factor, being the product of the excess and the residual diffusivities, Eq. (4.29).

Estimation of the thermodynamic factor requires, apart from the knowledge of the distance parameters, the two interaction parameters for a binary mixture, which are assumed to be characteristic properties of each specific pair of the diffusing components.

The authors [74] described a large set of mutual diffusion coefficients in binary mixtures, adjusting the two binary interaction parameters to the experimental data available. Increased accuracy of description is observed, compared to the Vignes and Darken mixing rules. The overall AAD (with the UNIQUAC activity coefficient model for estimation of the thermodynamic factor) is 5.6% for the Darken rule, 5.1% for the Vignes rule, and only 2.3%

for the UNIDIF model. However, this increase of the accuracy is expected, since the model has two additional adjustment parameters compared to the Vignes and the Darken rules.

The diffusion coefficient at the reference state is calculated using experimental values of the infinite dilution diffusivities. Hence, the proposed approach inherits the weaknesses of the previously described approaches. The UNIDIF model requires the dilute diffusivities at each temperature. Their reliable values can only be obtained in the experiments, since there is no way to predict the diffusion coefficients in dilute solutions with a reasonable accuracy.

An important extension of the model, developed in [74] was proposed by the authors of the approach in [75]. They developed a group contribution model on the basis of the UNIDIF approach, called the GC-UNIDIF. The difference between the GC-UNIDIF and the original UNIDIF is in the estimation of the residual contribution (Eq.(4.29)). The GC-UNIDIF model also requires the values of the limiting diffusivities and the equilibrium distance parameters, as does the original UNIDIF model [74].

The GC-UNIDIF model also involves the binary interaction parameters, which should be obtained from experimental data. By adjustment of the GC-UNIDIF to a large database of experimental diffusion coefficients, it was shown that binary interaction parameters are properties of different chemical groups. This makes the GC-UNIDIF an almost completely predictive approach, keeping in mind that GC-UNIDIF requires the limiting values of the diffusion coefficients. In principle, GC-UNIDIF may be applied to modeling of the diffusion coefficients in multicomponent mixtures. However, the question of applicability of the UNIDIF approach to the multicomponent mixtures requires further investigation and has not been yet verified.

4.2. Molecular Dynamics Simulations

Molecular dynamics (MD) simulations play an important role in the modern chemical science. There are two possible approaches to estimation of the transport properties by the MD simulations. The first is based on developments of the modern statistical theory of irreversible processes, which made it possible to use equilibrium MD simulations for the estimation of the non-equilibrium properties. The key developments in this area are due to the works of Green [60], Kubo [88, 89], and Mori [112]. The second approach is called non-equilibrium molecular dynamics (NEMD). It focuses on the numerical modeling of relaxation of the system from the non-equilibrium to the equilibrium state. Equilibrium MD simulations are considered here.

Self-diffusion coefficients may simply be estimated via MD simulations. There are two different approaches, which are related to each other. The first approach is based on the Green-Kubo equation [60]:

$$D_{i\#,i} = \frac{1}{3}\int_{t_0}^{\infty} \left\langle \mathbf{u}_i\left(t_0\right)\mathbf{u}_i\left(t_0+t\right)\right\rangle dt\,. \tag{4.30}$$

The integral term in Eq. (4.30) is the velocity correlation function for component *i*. The concept of the correlation function is behind the estimation of the non-equilibrium transport properties by MD simulations. Different transport properties, such as viscosity, heat conductivity, etc; are related to the corresponding correlation functions by equations, similar to Eq. (4.30).

The Einstein expression for the self-diffusion coefficient is based on tracking the positions of the atoms, rather than their velocities:

$$D_{i\#,i} = \frac{1}{6}\lim_{t\to\infty}\frac{d}{dt}\left\langle \left|\mathbf{r}_i\left(t_0\right)-\mathbf{r}_i\left(t_0+t\right)\right|^2\right\rangle. \tag{4.31}$$

Both expressions are equally correct, and the choice of approach is mainly governed by the technical aspects of the MD simulations. Both approaches provide rather accurate and reliable values of the self-diffusion coefficients with reasonable time expenses [66, 71, 73, 138, 175].

However, computation of the mutual diffusion coefficients, which are of main interest in the current study, is not very straightforward and reliable. The problem is that a mutual diffusivity is a collective, not an individual property like self-diffusivity. Therefore, there is a need to evaluate auto- and cross-correlation functions, which is time-consuming. Moreover, apart from the purely dynamic values, the thermodynamic factor has to be computed as a part of the mutual diffusion coefficient in a non-ideal mixture [71, 73, 138]. Hence, computation of the mutual diffusivities is much more time consuming. Moreover, calculation of the mutual diffusion coefficients involves the estimation of the activity coefficient and its compositional derivatives, which may introduce additional uncertainties into the estimated mutual diffusion coefficient. Haile [66] also indicates that the computations required for estimation of the mutual diffusivities involve fluctuations, which at the end may produce rather bad statistical evaluation [138].

There are a few alternative approaches to evaluation of the mutual diffusion coefficients. The first approach is based on the empirical models relating the mutual diffusion coefficients to the self-diffusion coefficients of the components with the help of the mixing rules of the Darken or Vignes type. There is a variety of different mixing rules for specific cases [176]. A usual form of these rules is presence of a “mixing” term, involving self-diffusion coefficients, and of the thermodynamic factor. Combination of the self-diffusion coefficients, determined by the MD simulations, with an empirical model makes it possible to determine mutual diffusivities [176]. This approach is not advantageous compared to the previously considered approaches based on mixing rules. Zhou and Miller [176] applied it to

a simple binary mixture of Argon-Krypton, and observed that the mutual diffusivities obtained on the basis of the self-diffusion coefficients and the mutual diffusivities, obtained directly from the MD simulation, coincide within 5-10%. They also observed, that even for such a simple mixture, the quality of the mutual diffusivities obtained directly from the MD simulations, depends significantly upon fluctuations in the system and the time of the velocity autocorrelation.

Schaink et al. [138] have successfully estimated a large set of the transport properties for the mixture of benzene-cyclohexane using a six-center Lennard-Jones (LJ) potential. They have estimated two values of the mutual diffusion coefficients at approximately equal concentrations of benzene and cyclohexane at room temperature. The agreement between the estimated and the experimental mutual diffusion coefficients is rather good (around 5%). However, the authors assumed that the thermodynamic contribution to the mutual diffusion coefficients is equal to unity (the case of ideal liquid), which allowed them to estimate the mutual diffusion coefficients based only on the cross velocity correlation functions. Although such a good performance of the MD approach with regard to prediction of the mutual diffusion coefficients in this ideal mixture is very promising [138], the application of MD studies to non-ideal mixtures may be problematic and should be further investigated.

The authors of a recent article [175] developed a fully predictive approach to estimation of the infinite dilution diffusion coefficients based on MD simulations and have conducted an extensive comparison with available experimental data. The overall accuracy of prediction of the infinite dilution diffusion coefficients is around 17% [175] which is actually comparable to the prediction of the limiting diffusivities by empirical schemes of the Einstein-Stokes type. The authors also conducted extensive computations of the self-diffusion coefficients by MD simulations. The total AAD for the self-diffusion coefficients in 17 mixtures is around 18%. Further research in the area of conventional MD simulations is required to predict self-diffusion coefficients with reasonable accuracy. Nevertheless, the MD simulations may already be applied in the absence of the experimental data for rough estimates of the diffusion coefficients in liquids.

In summary, it may be concluded that it is difficult to combine small computation times of mutual diffusivities with a reasonably high accuracy using the present level of the computational facilities. Further research in this area is required [66, 77].

4.3. Summary

Phenomenological Approaches

Several methods for evaluation of diffusion coefficients were discussed above. Although almost all the methods discussed involve theoretical considerations, they are

mainly empirical or semi-empirical. Therefore, their predictive and extrapolation capabilities are limited, and these methods more describe than predict diffusion coefficients.

A scheme summarizing the discussed methods for estimation of diffusion coefficients is presented in Figure 4.4.

The approaches based on the estimation of infinite dilution diffusion coefficients and subsequent application of mixing rules have several sources of error. The main error comes from the methods for estimation of the infinite dilution diffusivities. The error of predicting the dilute diffusion coefficients lies within 3-18% for different types of the compounds [134]. The second source of error is due to the interpolation scheme. The third source comes from the applied thermodynamic model.

For mixtures with a monotonous concentration behavior of the diffusion coefficients, the Vignes and Darken mixing rules, as well as their modifications, are capable of predicting the concentration dependence of the diffusivities with an average accuracy of around 5%. As it was already mentioned, this is the accuracy of interpolation, and it does not take into account the error of estimation of limiting diffusivities. However, monotonous behavior is not always observed, even for mixtures which are close to ideal from the thermodynamic point of view (like the mixtures of benzene/heptane, benzene/cyclohexane, cyclohexane/toluene and others). Non-monotonous behavior of the diffusion coefficients, with strong minima and maxima in the concentration dependence, is typical for the mixtures of polar and associating components (see analysis in next chapter). This results in the interpolation schemes producing an error as high as 10-15% for non-ideal mixtures, and more than 20% for mixtures of associating components [134]. These errors are estimated, provided that the values of the dilute-solution diffusion coefficients are known precisely, that is, have been measured experimentally.

The UNIDIF model is an alternative to the approach based on the mixing rules. It is capable of a more accurate prediction of the concentration dependence of the diffusion coefficients. However, it also requires the values of the infinite dilution diffusion coefficients.

Another series of methods for prediction of the diffusion coefficients is based on the concepts of free volume and activation energy. The approaches based on the free volume/activation energy theories are under intense development nowadays. They are simple and are related to the thermodynamic models, such as the cubic EoS [93]. The free volume theory has already been successfully applied to polymer solutions in the works of J.S. Vrentas and L. Duda [38, 145]. The possibility of applying the free volume theory to all transport properties [93] makes this approach rather universal. However, all the variations of this approach operate in terms of self-diffusion coefficients. The self-diffusion coefficients may be related to the mutual diffusivities (Figure 4.4). However this cannot be done in a rigorous and accurate way. Thus, although the free volume methods allow for reasonably

accurate modeling of the self-diffusion coefficients, the accuracy of the estimation of the mutual diffusivities is lost during transformation of the self-diffusion to the mutual diffusion coefficients. Despite this drawback, the free volume concept is a useful and still growing alternative to the empirical interpolation schemes.

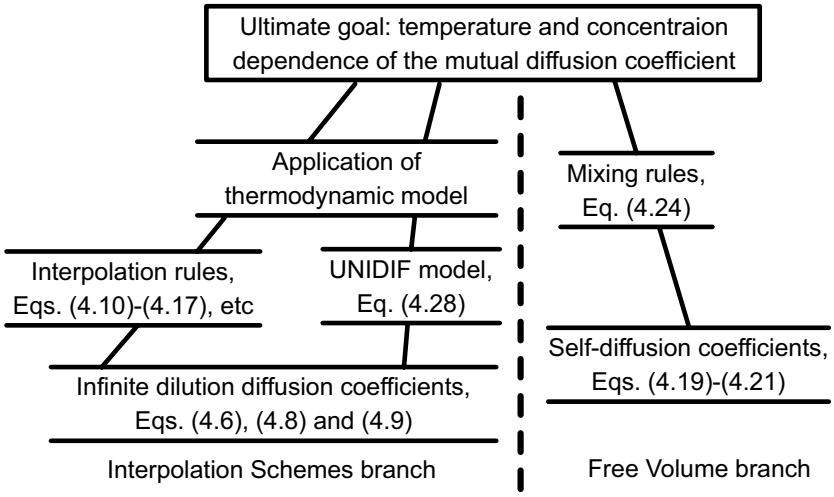

Figure 4.4: Approaches to the estimation of mutual diffusion coefficient.

Molecular Simulations

Molecular simulations provide an alternative approach to modeling the transport coefficients. Generally speaking, the molecular dynamics simulation should rather be considered as a numerical experiment, than as a model. Hence, there is a compromise between the computational expense and accuracy of the method. Statistical mechanics and non-equilibrium thermodynamics make it possible to determine the transport and the thermodynamic properties from information about motion and interaction of separate molecules.

MD simulations are widely applied for estimation of self-diffusion coefficients by the Green-Kubo or the Einstein formulas (Eqs. (4.30), (4.31)). However, as it was already discussed, the self-diffusion coefficients cannot be related to the mutual diffusion coefficients in a rigorous and universal way. Direct estimation of the mutual diffusion coefficients by MD simulations requires evaluation of the cross velocity correlation functions and of the thermodynamic factor. Strong influence of the fluctuations and, therefore, bad statistical estimation of the cross correlations makes it difficult to estimate the mutual diffusion coefficients with a good accuracy in a reasonable simulation time [66, 77].

Summarizing, it may be concluded that the present situation in the area of modeling mutual diffusion coefficients in the liquids requires further development. There is a necessity for a more rigorous theoretical framework, focusing on prediction of the diffusion coefficients, rather than their correlation.

5. Diffusion Coefficients in Binary Mixtures: Fluctuation Theory

The existing approaches to estimation of diffusion coefficients in binary mixtures were discussed in the previous chapter. The current chapter describes a newly developed approach, which is the key development of the present study.

5.1. Theoretical Background

5.1.1. Fluctuation Theory for Diffusion Coefficients

A rigorous theory for diffusion coefficients, based upon statistical mechanics and non-equilibrium thermodynamics, was developed in [143]. In [144] the theory was corrected and extended to the heat conductivities and thermodiffusion coefficients. The theory was tested in [143], and it was shown that it successfully explains the known facts and dependencies of the diffusion coefficients. The developed *fluctuation theory* (FT) for the diffusion coefficients contains no model assumptions. It may be considered not as a model for estimation of the diffusion coefficients, but rather as a rigorous theoretical framework for their modeling.

Explicit derivations of the FT will not be presented here, since it was not the objective of the current study. The basic idea behind this theory is to consider a classical system of two vessels, connected by a long and thin tube, the conductor. Fluctuations of the system around the equilibrium state are considered. These fluctuations are described by laws of linear non-equilibrium statistical thermodynamics, involving phenomenological coefficients. Considering the dynamics of the fluctuations, it may be shown that the matrix of phenomenological coefficients can be related to the covariance of the fluxes of the molecules leaving one of the vessels with the overall numbers of the molecules in the vessel. Such a covariance may be related to the probability of the molecule traveling through the conductor and not returning back. At this point a key concept of the fluctuation theory is introduced – the so-called *penetration length.* The penetration length is an average traveling distance, after which a molecule “forgets” its initial velocity [143]. In an *n*-component mixture there are *n* penetration lengths, one for each component. Knowledge of the penetration lengths makes it possible to estimate the Onsager coefficients. A more detailed discussion of the concept of penetration lengths is presented in the next chapter.

The fluctuation theory provides a rigorous approach, which reduces the problem of modeling a matrix of diffusion coefficients in a multicomponent mixture to a problem of modeling of the vector of penetration lengths. The essence of the present chapter is to provide the models for the penetration lengths and to apply them to practical calculations of the diffusion coefficients in the framework of the fluctuation theory.

The fluctuation theory operates in terms of the Onsager phenomenological coefficients. Here the diffusion-convective system of thermodynamic coordinates is used for definition of the binary phenomenological coefficient L_D [143]:

$$\mathbf{J}_1^m = L_D \nabla \left(\frac{\mu_2}{M_2 T} - \frac{\mu_1}{M_1 T} \right), \tag{5.1}$$

where $\mathbf{J}_1^m$ is the mass diffusion flux of the first component.

The fluctuation theory expresses the binary phenomenological coefficient L_D in terms of the *transfer matrix* $\mathbf{L}_{Tr}$, which is formed as a product of the three different factors affecting the diffusion rate: the *thermodynamic* $\mathbf{L}_T$,the *kinetic* $\mathbf{L}_K$ and the *resistance* $\mathbf{L}_R$:

$$\mathbf{L}_{Tr} = \frac{1}{4} \mathbf{L}_K \mathbf{L}_R \mathbf{L}_T . \tag{5.2}$$

The 2x2 *kinetic matrix* accounts for the rates of molecular motion and is determined as a diagonal matrix of the average molecular velocities C_i of different components:

$$\mathbf{L}_{K,ij} = \delta_{ij} C_j , \; C_j = \left(\frac{8RT}{\pi M_j} \right)^{1/2} \; (i, j = 1,2), \tag{5.3}$$

The 3x2 *thermodynamic matrix* is expressed in terms of the matrix $\mathbf{F}$ of the second order derivatives of the entropy S with regard to its natural variables: molar densities of the components N_i and internal energy U:

$$F_{ij} = \frac{\partial^2 S}{\partial N_i \partial N_j}, \; F_{i,n+1} = F_{n+1,i} = \frac{\partial^2 S}{\partial N_i \partial U}, \; F_{n+1,n+1} = \frac{\partial^2 S}{\partial U^2} \; , (i, j = 1,2). \tag{5.4}$$

Now, the thermodynamic matrix is determined as

$$L_{T,ij} = -f_{ij} \; (i = 1,...,3; j = 1,2), \tag{5.5}$$

where $\mathbf{f}$ is inverse to $\mathbf{F}$: $\mathbf{f}=\mathbf{F}^{-1}$.

The final contribution to the diffusion rate is the 2x3 *resistance matrix,* accounting for resistance to molecular motion by other molecules. It is expressed in terms of the penetration lengths Z_i [143]:

$$L_{R,ij} = \delta_{ij} Z_i (\mathbf{N}, U) - N_i \frac{\partial Z_i (\mathbf{N}, U)}{\partial N_i}, \; L_{R,i,n+1} = -N_i \frac{\partial Z_i (\mathbf{N}, U)}{\partial U} \; , \; (i = 1,...,2). \tag{5.6}$$

The penetration lengths may be estimated either by molecular dynamics simulations, or by fitting the diffusion coefficients to the available experimental data. Since the dependence of the diffusion coefficients on the penetration lengths is nontrivial, prior to fitting they should be expressed by simple dependencies with as few adjustment parameters as possible.

Estimation of the three factors affecting the diffusion rate makes it possible to evaluate the transfer matrix $\mathbf{L}_{Tr}$ (Eq. (5.2)), which is connected with the matrix of the phenomenological diffusion coefficients in the following way:

$$\mathbf{L}_D = \mathbf{G}\bar{\mathbf{L}}_{Tr}\mathbf{G}^{\mathrm{T}},\ \bar{\mathbf{L}}_{Tr} = \frac{1}{2}\left(\mathbf{L}_{Tr} + \mathbf{L}_{Tr}^{\mathrm{T}}\right), \tag{5.7}$$

where $\mathbf{G}$ is the *coordinate matrix* depending upon the choice of system of thermodynamic fluxes and forces, in which the matrix of phenomenological diffusion coefficients $\mathbf{L}_D$ is expressed. For a binary mixture, matrix $\mathbf{L}_D$ is reduced to a single coefficient defined in Eq. (5.1), and the coordinate matrix has the following form:

$$\mathbf{G} = \left[(1-w_1)M_1 \quad -w_1M_2\right]. \tag{5.8}$$

Here w_1 is the mass fraction of the first component in the mixture.

The expression connecting the Onsager phenomenological coefficient to the Fick diffusion coefficient is also required. The Fick law in binary mixture defines the relation between the mass diffusion flux and the gradient of mass fraction:

$$\mathbf{J}_1^m = \rho D \nabla w_1. \tag{5.9}$$

Comparison of the Fick law and Eq. (5.1) results in the following expression connecting the Onsager phenomenological coefficient and the Fick diffusion coefficient:

$$D = L_D \frac{M_{mix}}{M_1 M_2 T}\left(\frac{1}{z_1 M_2}\frac{\partial \ln \mu_2}{\partial N_2} + \frac{1}{z_2 M_1}\frac{\partial \ln \mu_1}{\partial N_1}\right). \tag{5.10}$$

The right hand-side of Eq. (5.10) is the so-called thermodynamic factor.

As it was stated above, the FT is not a model but a theoretical framework for modeling diffusion coefficients. Different expressions for the penetration lengths entering the resistance matrix defined in Eq.(5.6) result in different specific models for estimation of the diffusion coefficients. Practical application of the FT also requires a thermodynamic model for estimation of the thermodynamic matrix, Eq.(5.4) and the thermodynamic factor, Eq. (5.10).

5.1.2. Modeling the Thermodynamic Factor

Eq. (5.4) indicates that estimation of the diffusion coefficients within the FT approach requires estimation of the second order derivatives of the specific entropy with regard to molar densities and specific internal energy. Although these values are expressed in terms of the proper thermodynamic variables, their practical evaluation from a thermodynamic model may be problematic. The problem is that a common cubic or similar equation of state is given in the form of $P(T,V,N_i)$. Moreover, most of the available thermodynamic simulators operate in terms of fugacity coefficients $\phi(T,P,N_i)$. Direct expression of the dependence $S(U,V,N_i)$ starting from these dependencies is a cumbersome task. A relatively simple way to calculate the matrix **F** was developed in [100] and is presented in this subsection.

It follows from the second law of thermodynamics that

$$dS = \frac{1}{T}dU + \frac{P}{T}dV - \sum\frac{\mu_i}{T}dN_i. \tag{5.11}$$

According to this equation,

$$\left.\frac{\partial S}{\partial N_i}\right|_{U,V,\mathbf{N}} = -\frac{\mu_i}{T},\ \left.\frac{\partial S}{\partial U}\right|_{U,V,\mathbf{N}} = \frac{1}{T}. \tag{5.12}$$

In the formulae above the designation $|_{U,V,\mathbf{N}}$ does not mean "under constant $U,V,\mathbf{N}$", but rather "in the system of variables $U,V,\mathbf{N}$". A similar system of designations for other derivatives is kept throughout this thesis.

The matrix $\mathbf{F}$ may be expressed in the terms of the derivatives defined in Eq. (5.12):

$$\begin{aligned}
F_{ij} &= -\left.\frac{\partial\left(\mu^j/T\right)}{\partial N_i}\right|_{U,V,\mathbf{N}} = -\frac{1}{T}\left.\frac{\partial\mu^j}{\partial N_i}\right|_{U,V,\mathbf{N}} + \frac{\mu^j}{T^2}\left.\frac{\partial T}{\partial N_i}\right|_{U,V,\mathbf{N}}, \left(i,j=1,...,n\right);\\
F_{i,n+1} &= F_{n+1,i} = \left.\frac{\partial\left(1/T\right)}{\partial N_i}\right|_{U,V,\mathbf{N}} = -\frac{1}{T^2}\left.\frac{\partial T}{\partial N_i}\right|_{U,V,\mathbf{N}}, \left(i=1,...,n\right);\\
F_{n+1,n+1} &= \left.\frac{\partial\left(1/T\right)}{\partial U}\right|_{U,V,\mathbf{N}} = -\frac{1}{T^2}\left.\frac{\partial T}{\partial U}\right|_{U,V,\mathbf{N}}.
\end{aligned} \tag{5.13}$$

Changing from the set of variables U,V,N_i to T,V,N_i may be carried out with the help of the following relations:

$$\begin{aligned}
\left.\frac{\partial\mu^j}{\partial N_i}\right|_{U,V,\mathbf{N}} &= \left.\frac{\partial\mu^j}{\partial N_i}\right|_{T,P,\mathbf{N}} + \left.\frac{\partial\mu^j}{\partial T}\right|_{T,P,\mathbf{N}}\left.\frac{\partial T}{\partial N_i}\right|_{U,V,\mathbf{N}} + \left.\frac{\partial\mu^j}{\partial P}\right|_{T,P,\mathbf{N}}\left.\frac{\partial P}{\partial N_i}\right|_{U,V,\mathbf{N}},\\
\left.\frac{\partial P}{\partial N_i}\right|_{U,V,\mathbf{N}} &= \left.\frac{\partial P}{\partial N_i}\right|_{T,V,\mathbf{N}} + \left.\frac{\partial P}{\partial T}\right|_{T,V,\mathbf{N}}\left.\frac{\partial T}{\partial N_i}\right|_{U,V,\mathbf{N}},\\
\left.\frac{\partial T}{\partial N_i}\right|_{U,V,\mathbf{N}} &= -\frac{\partial U/\partial N_i|_{T,V,\mathbf{N}}}{\partial U/\partial T|_{T,V,\mathbf{N}}},\\
\left.\frac{\partial T}{\partial U}\right|_{U,V,\mathbf{N}} &= \frac{1}{\partial U/\partial T|_{T,V,\mathbf{N}}}.
\end{aligned} \tag{5.14}$$

Estimation of the derivatives defined in these equations requires a functional expression of the chemical potential and specific internal energy in the terms of either $T,P,\boldsymbol{N}$ or $T,V,\boldsymbol{N}$.

The internal energy consists of two parts, an ideal and a residual term[104]:

$$U = U^{id} + U^{r}. \tag{5.15}$$

The ideal part of the internal energy of an ideal liquid is [111]:

$$U^{id} = \sum N_i h_0^i\left(T\right) - NRT. \tag{5.16}$$

Here, standard enthalpies are equal to

$$h_0^k\left(T\right) = H^0 + \Delta h_f^k\left(298.2K\right) + \int_{298.2}^{T} C_p^k\left(T\right)dT. \tag{5.17}$$

It is possible to show that both constants in the last expression can be neglected when the second derivatives of the internal energy are calculated.

The residual internal energy and the chemical potentials are expressed in terms of the fugacity coefficients and the compressibility (see Appendix A.1 for derivation) [104]:

$$U^r\left(T,P,\mathbf{N}\right) = -P + NRT - RT^2\sum N_i \frac{\partial \ln \phi_i\left(T,P,\mathbf{N}\right)}{\partial T}, \tag{5.18}$$

$$\begin{aligned} &\mu^k = RT\ln\phi^k + RT\ln\left(\frac{N_k}{N}\frac{P}{P_0}\right) + h_0^k\left(T\right) - Ts_0^k\left(T\right), \\ &s_0^k\left(T\right) = S^0 + \Delta_f^k s\left(298.2K\right) + \int_{298.2}^{T}\frac{C_p^k\left(T\right)}{T}dT. \end{aligned} \tag{5.19}$$

Again, the constants in the last two expressions disappear when the derivatives are taken.

The residual internal energy, defined in Eq.(5.18), is expressed in coordinates $T,P,\mathbf{N}$, while the derivatives of the internal energy in Eq. (5.14) are expressed in coordinates $T,V,\mathbf{N}$. The solution to this difficulty is proposed in Appendix A.2. Also, the calculations demonstrate that the first two terms in Eq. (5.18) for residual internal energy do not affect the value of the thermodynamic matrix (this may be proved by considering the derivatives of the residual contribution of internal energy) and for this purpose the expression for the residual internal energy can be reduced to the sum of temperature derivatives of the fugacity coefficients.

The computations described above require knowledge of specific heat capacities. The specific heat capacity is a well-studied property, at least for the majority of simple liquids. There are extensive databases, including both experimental results and approximation models (e.g. the DIPPR Database [2] or the Korean Thermophysical Properties Data Bank [85]). They contain information on specific heat capacities and other caloric properties, including the ideal state enthalpies/entropies in Eq. (5.19). The ideal state enthalpies/entropies in Eq. (5.19) are not required for estimation of diffusion coefficients. However they are necessary for modeling of other transport properties by means of fluctuation theory, such as heat conductivity [144].

For practical computations in the framework of the developed approach, a computer code, developed as a part of the thermodynamic software SPECS [76], was applied. This code was developed in the Center for Phase Equilibria and Separation Processes, IVC-SEP, Technical University of Denmark. The core of SPECS is a module computing the volume, fugacity coefficients and their derivatives in the coordinates $T,P,\mathbf{N}$. The values of the pressure derivatives in coordinates $T,V,\mathbf{N}$ in Eq. (5.14) are also implicitly estimated in the SPECS computational libraries, and may be extracted from the code. Application of the SPECS code

provided an extensive, fast and robust computational background, capable of delivering required thermodynamic properties in the framework of different thermodynamic models.

The proposed method for computation of the thermodynamic matrix is not the only possible approach to estimation of the thermodynamic factor in terms of the properties produced by the equations of state. Few other methods were developed and tested during this study, however they appeared to be less convenient or/and accurate and generally, much more complex than the method presented here.

Verification of the proposed approach to modeling thermodynamic matrix is discussed in Appendix A.3.

5.2. The Diffusion Coefficients

5.2.1. Exponential Form of the Expression for Penetration Lengths

Proper selection of the expression for penetration lengths is a key point of the developed approach. The expression for penetration lengths should obey several basic principles. First, these lengths should be simple monotonous functions of the thermodynamic parameters, so that complex behavior of the diffusion coefficients may be attributed to the thermodynamic peculiarities of the mixture and to the structure of the model. Second, the penetration lengths should contain a limited number of adjustable parameters (preferably constants), which can be correlated on the basis of a limited set of experimental data. Third, it should be possible to substantiate the expressions for the penetration lengths based on physical considerations (although the complete proof may not be available). Finally, it is desirable that particular sets of parameters used for the penetration lengths in specific mixtures should lead to well-known rules for the diffusion coefficients, such as the Darken or the Vignes mixing rules [34, 161].

The first expression for the penetration lengths, which was proposed and applied in the current study, is the exponential expression [100]:

$$Z_i = \sqrt{\frac{M_i}{M_{mix}}} A_i \exp\left(-B_1 N_1 - B_2 N_2\right),\ M_{mix}^{-1} = \sum M_i^{-1},\left(i = 1,2\right). \tag{5.20}$$

The exponential factor with the two penetration volumes B_i is kept the same for both components in a binary mixture, while the penetration amplitude A_i is different for each component. Hence, there are four adjustable parameters for a binary mixture.

The dependence (5.20) is simple and monotonic. There are other specific physical reasons for selecting the penetration lengths in the exponential form. Such a form is characteristic of different probabilistic events depending on Markov processes, like the random walk of an individual molecule in a mixture. The number of interactions which a

molecule experiences during its random walk is proportional to the individual molar densities. The higher the densities are, the larger the number of interactions is, and the faster the molecule "forgets" its initial velocity. Therefore, the expression under the exponent should be a decreasing function of the molar densities.

The exponential expression for penetration lengths can also be explained from the point of view of the free volume theory. The exponential expression (5.20) is the product of a pre-factor Z^0, multiplied by the probability to find the 'hole' to jump in to [26, 168]:

$$Z_i = Z_i^0 \exp\left(-\frac{z_1 B_1 + z_2 B_2}{V}\right). \tag{5.21}$$

The proposed expression for the penetration lengths is independent of the temperature. It is assumed that, although the molecules move faster at a higher temperature, the spatial correlations of their velocities remain the same. This assumption is reasonable, at least when a mixture is far from the critical point. The results reported below indicate that the assumption of independence of Z_i of the temperature leads to excellent correlation with experimental data for diffusion coefficients at different temperatures.

Let us assume that a given binary mixture may be described as an ideal gas mixture. This assumption is taken only as an (oversimplified) example, since it does not work for liquid mixtures. In this case the thermodynamic matrix $\mathbf{L}_T$ becomes diagonal, and the expression for the diffusion coefficient assumes the following explicit form [143]:

$$D = \frac{1}{4} C_1 \left(Z_1 - N_1 Z_{11} + N_2 Z_{12}\right) + \frac{1}{4} C_2 \left(Z_2 - N_2 Z_{22} + N_1 Z_{21}\right), \; Z_{ij} = \frac{\partial Z_i}{\partial N_j}. \tag{5.22}$$

Substituting Eq. (5.20) into Eq. (5.22) results in the following expression:

$$\begin{aligned} &D = \frac{1}{4} C_{mix} \exp(-B_1 N_1 - B_2 N_2)\left[A_1 + A_2 + (A_1 - A_2)(B_1 N_1 - B_2 N_2)\right], \\ &C_{mix} = \left(8RT/\pi M_{mix}\right)^{1/2}. \end{aligned} \tag{5.23}$$

In particular, if A_1=A_2, the expression for D is reduced to a simple exponential dependence. In another form, this dependence may be reformulated as a mixing rule expressing the diffusion coefficient in terms of the two dilute solution limits:

$$D = D\left(N_1 \to 1\right)^{N_1} D\left(N_2 \to 1\right)^{N_2}. \tag{5.24}$$

The last equation may be called *the modified Vignes rule*, to be compared with the standard Vignes rule [161]:

$$D = D\left(z_1 \to 1\right)^{z_1} D\left(z_2 \to 1\right)^{z_2}. \tag{5.25}$$

This example demonstrates that under certain simplifications the exponential expression (5.20) applied within the FT approach may be reduced to a rather simple and well-known empirical "mixing rule" for the diffusion coefficients.

Our computations show that the original and the modified Vignes rules give very close results in simple cases where the original Vignes rule provides a good correlation (see Figure 5.1 for such a comparison). Moreover, our approach may be slightly better when the multi-temperature dependence is fitted, since we use the same three parameters $A_1=A_2$, B_1, B_2 for all temperatures, while the dilute solution coefficients in the original Vignes rule need re-fitting at each temperature (four coefficients were adjusted for obtaining results, presented in Figure 5.1), or application of the correlations like that of Einstein-Stockes, which are not very precise.

The binary mixtures do not all obey the Vignes or the modified Vignes rules, even if they are very close to ideal mixtures. An example is the nearly ideal mixtures containing benzene, whose diffusion coefficient exhibits a clear minimum (Figure 5.2). This minimum cannot be reproduced by Eq. (5.25) or any other monotonous dependence. Moreover, it cannot be reproduced by the FT model with the exponential expression with equal amplitudes. However, as we will show below, the general dependence (5.20) may successfully be applied to this complex case.

The first practical application of the developed FT approach was in describing the experimental data on diffusion in binary mixtures of non-polar components. The computations were carried out using the FTCode (Appendix A.2), with the Soave-Redlich-Kwong (SRK) equation of state (EoS) [104] applied to estimate the thermodynamic matrix and with the exponential expression for penetration lengths, Eq. (5.20).

The experimental data was described by adjusting four values of the penetration coefficients. The results of the correlation, as well as the values of the penetration coefficients are presented in Table 5.1. The absolute average deviation is usually within 2% and is always within 3%, except for one mixture analyzed below.

The mixtures considered may approximately be classified as “Vignes-like” (obeying the modified Vignes rule (5.24)) and other mixtures. The “Vignes-like” mixtures are characterized by the fact that thermodynamically they are close to ideality and that A_1 is approximately equal to A_2. All the normal alkane mixtures may be considered as “Vignes-like”. The deviations from this rule increase for the mixtures containing heavy hydrocarbons. If, additionally to $A_1 \approx A_2$, the approximate equality $B_1 \approx B_2$ is obeyed, then the dependence of the diffusion coefficient on composition becomes almost linear, “Darken-like” (although this cannot directly be proven on the basis of Eqs. (5.22) or (5.23).

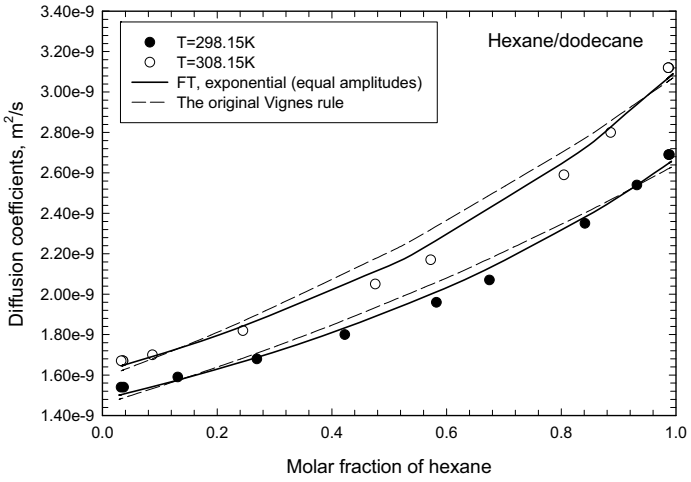

Figure 5.1: Deviations of the experimental data [146] from the dependencies for diffusion coefficients calculated by the original Vignes rule and the FT model with an exponential expression for penetration lengths and the assumption that amplitudes are equal (3 parameters). Average absolute deviation is 2.76% for FT model with exponential expression and equal amplitudes and 3.02% for the original Vignes rule.

One of the best-correlated mixtures is the mixture of cyclohexane-carbon tetrachloride, presented in Figure 5.2a. This “Darken-like” mixture is well documented (78 experimental points) and may be correlated with an average deviation of less than one percent. The thermodynamic part of the model can in this case predict the slopes of the straight lines approximating the values of the diffusion coefficients at three different temperatures. Generally, for all the eight studied mixtures, where the data at several temperatures was available, it turned out to be possible to correlate the data for different temperatures with the same sets of temperature independent parameters.

The worst predicted mixture is also well documented: this is the mixture of benzene and n-heptane (75 experimental points; a deviation of 6.82%). For this mixture, four different sources of experimental data are available. These data, together with the best fitted curves, are presented in Figure 5.2b. This figure clearly indicates that the data from different sources largely disagree, which is probably the reason for the relatively large deviations. If the data from the two sources is used for correlation ([136,137] with the 33 experimental points), and data from other sources is excluded, the deviation is reduced to 2.22%. The corresponding plots are shown in Figure 5.2c (and in a separate row in Table 5.1).

Table 5.1: Summary of the comparison of the diffusion model with exponential expression for penetration lengths with experimental data.

System (component 1 + component 2)	Data points	Temp. range (K)	Parameters for the penetration length				AAD (%)	References
			$A_1 \cdot 10^6$,(m)	$A_2 \cdot 10^6$,(m)	$\nu_1 \cdot 10^3$, (m^3mol^{-1})	$\nu_2 \cdot 10^3$, (m^3mol^{-1})		
Normal alkanes								
n-Hexane + n-dodecane	23	298.15-308.15	0.1731	0.2230	1.1472	2.0284	2.2743	[146]
n-Octane + n-dodecane	21	298.15-333.15	2.2403	3.1304	1.9051	2.6192	3.0962	[53]
n-Heptane + n-decane	21	298.15	4.7298	6.8252	2.0601	2.9121	1.4020	[95]
n-Heptane + n-dodecane	20	298.15	7.9022	7.5038	2.0971	3.7565	1.1639	[95]
n-Heptane + n-hexadecane	8	298.25	2.2663	6.2287	1.8279	4.4071	1.7569	[17]
n-Hexane + n-heptane	10	283.15-298.15	0.3677	0.4265	1.3577	1.5544	1.2798	[118]
n-Heptane + n-tetradecane	23	298.15	3.4834	7.5931	2.1117	4.3714	1.3853	[95]
n-Dodecane + n-hexadecane	9	298.15	3.7050	8.3001	3.3903	4.6840	0.3324	[146]
n-Octane + n-tetradecane	24	298.15	0.2534	0.3475	1.8406	3.4633	1.9682	[95]
Non-polar + non-polar								
Cyclohexane + carbon tetrachloride	78	298.15-328.15	2.2485	3.4601	1.4244	1.2519	0.8512	[90,136,137]
n-Hexane + *idem*	6	303.15	6.6693	5.4031	1.7153	1.3463	1.5392	[17,131,132]
n-Heptane + *idem*	6	303.15	2.5708	1.7504	1.8064	1.2506	0.5779	[131,132]
n-Octane + *idem*	6	303.15	6.7371	4.0902	1.8883	1.2470	2.1004	[131,132]
3-Methylpentane + *idem*	6	303.15	4.2923	3.3914	1.4193	1.1631	0.9363	[131,132]
2,3-Dimethylpentane + *idem*	6	303.15	0.8833	5.0610	1.6719	1.0159	3.0717	[131,132]
2,2,4-Trimethylpentane + *idem*	6	303.15	4.6925	2.8139	1.8233	1.1825	0.7820	[131,132]
Benzene + n-hexane	11	298.15	1.3246	6.5551	1.1597	1.6080	0.7071	[69]
Benzene + n-heptane	75	298.15-358.15	0.6996	1.6116	1.1110	1.6468	6.8214	[23,69,136,137]
Benzene + n-heptane	33	298.15-328.15	1.2412	3.0568	1.1825	1.7322	2.2194	[136,137]
Benzene + cyclohexane	56	298.15-333.15	5.1121	2.5207	1.1471	1.4617	1.6103	[98,130,136,137]
Toluene + cyclohexane	65	298.15-328.15	13.230	12.159	1.5752	1.5965	1.2638	[136,137]
Toluene + benzene	22	298.15-313.15	38.008	42.572	1.7633	1.3935	0.6444	[136,137]
						Overall AAD	1.7175%	

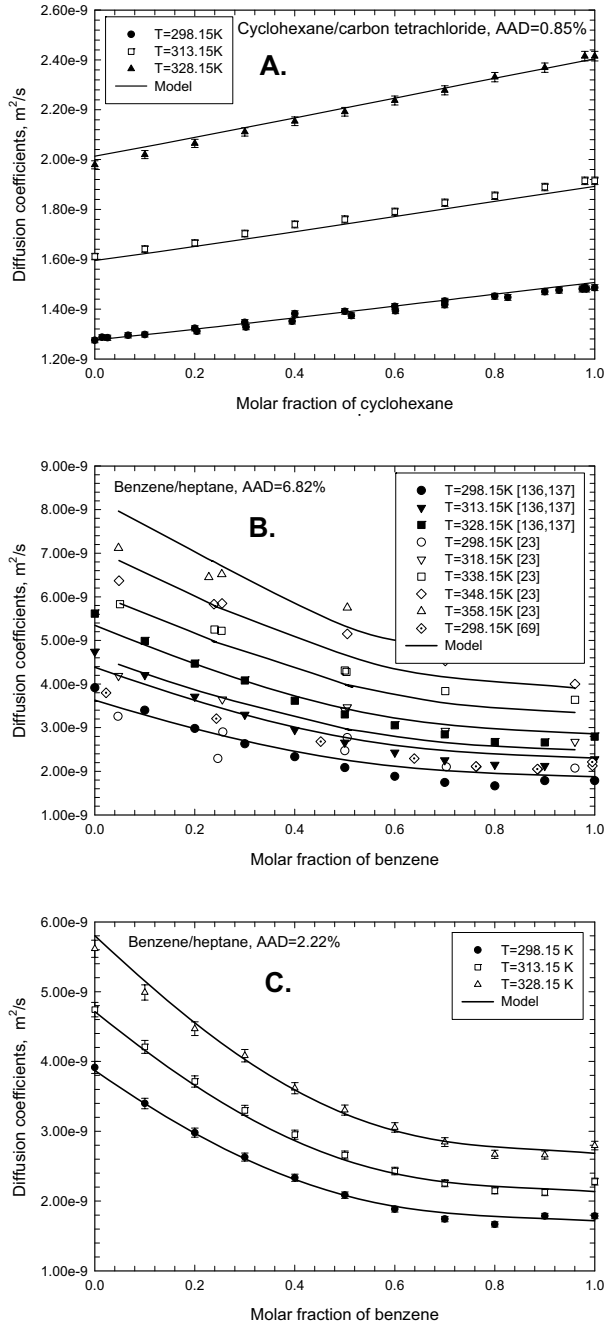

Figure 5.2: Comparison of the diffusion model with experimental data. Figure A: data from [90,136,137] with 0.80% error bars; figure B: data from [23, 69,136,137]; figure C: [136,137] – 2.20%.

The formula for diffusion coefficients is much more sensitive to the penetration volumes than to the penetration amplitudes, since the penetration volumes stay under the exponent and are multiplied by the molar densities, being of the order of a few thousand. This can be observed by comparison of the two lines of Table 5.1, describing the mixture of benzene/n-heptane based on the full and on the reduced number of the data. If only the multi-temperature data sets are considered, one can observe a regular behavior of the penetration volumes and penetration amplitudes as functions of the individual component properties.

Also, the behavior of the penetration parameters for the mixtures where data for only one temperature are available is less regular than for mixtures, where the temperature dependence is available. This question will be discussed further.

Another example of good correlation of the diffusion coefficient for a well-documented nearly ideal mixture exhibiting a minimum of diffusion coefficients is shown in Figure 5.3a. It was possible to correlate the available 56 experimental points for the mixture of benzene-cyclohexane at three different temperatures within 1.26% average absolute deviation. Data from different sources agrees well for this mixture.

The mixture of octane-dodecane, despite its thermodynamic ideality, is correlated with a modest accuracy of around 3.0%. Analysis of Figure 5.3b shows that slopes of the concentration dependencies vary essentially with temperature. The model does not adequately describe the diffusion coefficients at 313.15K.

The thermodynamically nearly ideal mixture of benzene/toluene is described with very high accuracy of 0.64% (Figure 5.3c). The mixture is “Darken-like”.

Generally, it may be concluded from presented results that the model has shown a good performance in correlation of the experimental data on diffusion coefficients for binary non-polar mixtures. Only four constant parameters are required to correlate the data within 3% or a higher accuracy in a wide temperature range.

There are few factors, which make it difficult (at least with a reasonable accuracy) to apply the exponential dependence for the penetration lengths for prediction purposes. The deficiencies of the exponential expression can be demonstrated by analysis of the penetration coefficients listed in Table 5.1. First, the penetration coefficients are clearly not individual properties of the components. The penetration volumes and the amplitude of a selected component depend upon the mixture where diffusion is studied. Moreover, the exponential dependence implies high sensitivity of the penetration lengths upon the penetration parameters (mainly the penetration volumes).

Results of the investigation of the sensitivity of the description of the diffusion coefficients upon the change of the penetration parameters are presented in Table 5.2. Example 1 shows the AAD of description of the experimental values of diffusion coefficients obtained by the optimization procedure. In the following examples the values of the

penetration amplitudes and penetration volumes are changed, and values of the diffusion coefficients, based on the changed values of penetration parameters, are estimated.

Table 5.2: Sensitivity of the quality of description to the change of the penetration parameters. The studied mixture is benzene/cyclohexane [98,130,136,137] (56 data points, 3 isotherms).

Example	$\delta A_{Benzene}$,%	$\delta A_{Cyclohexane}$,%	$\delta B_{Benzene}$,%	$\delta B_{Cyclohexane}$,%	AAD,%
1	-	-	-	-	1.6103
2	-	0.5*	-	-	1.6868
3	0.5	-	-	-	1.6382
4	0.5	0.5	-	-	1.7299
5	-	-	-	0.5	4.3437
6	-	-	0.5	-	3.0834
7	-	-	0.5	0.5	6.5699
8	-	-	1.0	1.0	12.673
9	1.0	1.0	1.0	1.0	11.790
10**	1.0	1.0	1.0	1.0	15.573

*Note: the equation for estimation of new values of penetration parameter $X_{new} = X_{original} - X_{original} \cdot \delta X$

**Note: in examples 9 and 10 the directions of the change are different

Table 5.2 demonstrates that variation of the penetration amplitudes does not significantly change the values of the diffusion coefficients and therefore does not significantly affect the quality of description. In the same time, the error in the estimation of the penetration volumes results in the significant increase of the modeling error. In example 9, the effect of variation of the penetration volumes is partially compensated by variation of the penetration amplitudes, compared to example 8. This compensation is due to the fact that the direction of variation for the penetration volumes was the same as the direction for penetration amplitudes. In example 10 the directions of variation are different, which results in an increase of the error. It may be seen that 1% error in the penetration volumes results in a significant increase of the error (12%, compared to the original AAD of 1.6%)

Strong dependence of the diffusion coefficients upon the penetration volumes is in a good agreement with the facts observed in applications of the free volume theory. Wesselingh and Bollen [168] have shown that the concentration dependence of the self-diffusion coefficient is strongly affected by the ratio of the free volume and the minimum compressible volume. They mentioned that this sensitivity is also observed in the application of the free-volume theory to viscosity modeling.

Both high sensitivity of the diffusion coefficients to the penetration volumes and the fact that these values are not individual require another expression for the penetration lengths, to improve the prediction capabilities of the model.

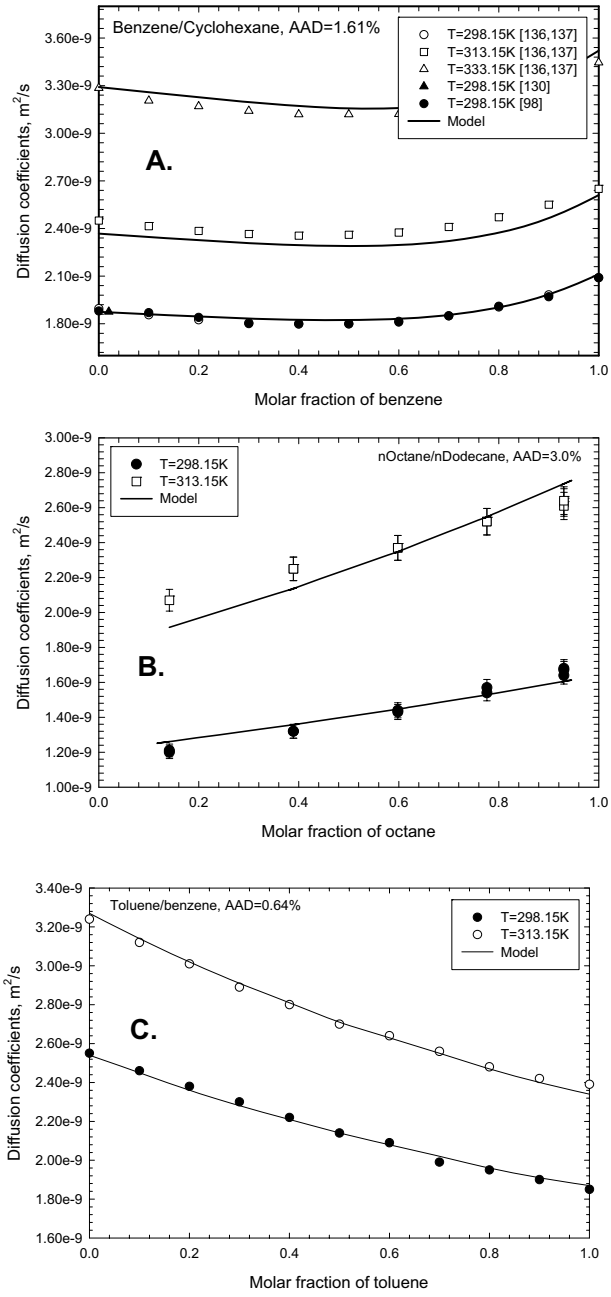

Figure 5.3: Comparison of the diffusion model with experimental data.

Figure A: data from [98,130,136,137] with 1.25% error bars; figure B: data from [53] with 3.0 error bars; figure C: data from [136].

5.2.2. Quadratic Form of the Expression for Penetration Lengths

To reduce the problem of sensitivity, the following quadratic dependence for the penetration lengths in binary mixtures was proposed:

$$Z_i = \sqrt{\frac{M_i}{M_{mix}}} A\left(1 - B_1 N_1 - B_2 N_2 - B_{12}\frac{N_1 N_2}{N}\right). \qquad (5.26)$$

Eq. (5.26) contains one common penetration amplitude A for the mixture, two penetration volumes B_i, and one interaction parameter B_{12} accounting for the mixing effect, which gives four independent parameters for a binary mixture.

In the cases of a relatively simple behavior of the binary diffusion coefficients, the term $B_{12}N_1N_2/N$ may be omitted, and Eq. (5.26) is reduced to even simpler linear dependence:

$$Z_i = \sqrt{\frac{M_i}{M_{mix}}} A\left(1 - B_1 N_1 - B_2 N_2\right). \qquad (5.27)$$

Eq. (5.27) involves only three parameters for a binary mixture. Application of Eq. (5.27) cannot provide a proper description of the very non-ideal and non-monotonous behavior of diffusion coefficients, however it is capable of describing the maxima and the minima with only slightly reduced quality of description, compared to the quadratic mixing rule (Figure 5.4). The tests demonstrated that the linear expression fails to properly describe mixtures of associating compounds, although the quadratic rule is capable of describing them with good accuracy (see further discussion).

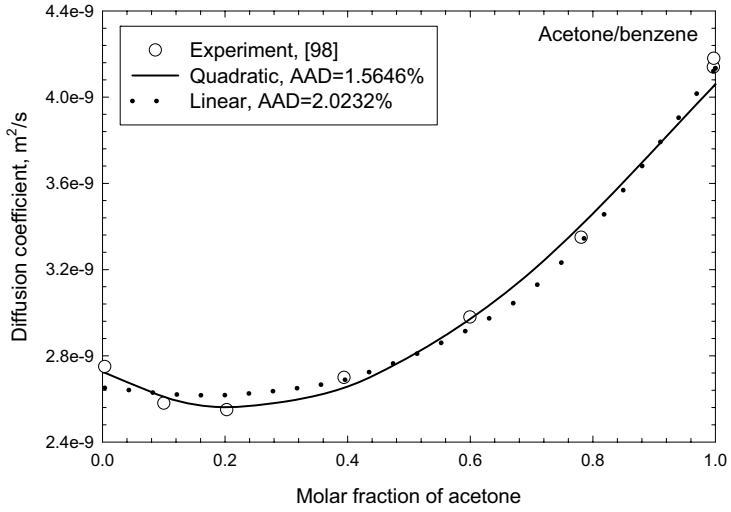

Figure 5.4: Description of the diffusion coefficients in the mixture acetone/benzene [98] by quadratic and linear mixing rules.

Let us now discuss in detail the physical meaning of the quadratic expression for the penetration lengths. This expression may be written as:

$$Z_i = Z_i^0 \zeta,$$
$$Z_i^0 = \sqrt{\frac{M_i}{M_{mix}}} A, \zeta = \frac{V - z_1 B_1 - z_2 B_2 - z_1 z_2 B_{12}}{V} = 1 - \frac{z_1 B_1 + z_2 B_2 + z_1 z_2 B_{12}}{V}. \quad (5.28)$$

The value of the penetration amplitude Z^0 is comparable with the size of a molecule. Probably, it may be described similarly to that proposed in [168] for non-impeded self-diffusion coefficients in a cubic lattice.

Let us now assume that the penetration volumes have the physical meaning of a sort of irreducible volume (the minimum volume that the liquid molecules can take). Then the expression V-z_1B_1-z_2B_2 represents a part of the volume open for molecular motion. This assumption will be confirmed by the fact that the penetration volumes are very close to the b-parameters from the cubic EoS, which have the physical meaning of the irreducible volume. The term $z_1z_2B_{12}$ may be interpreted as a correction caused by non-ideality of molecular packing, especially, in strongly interacting polar mixtures. Thus, the value of ζ has the physical meaning of the fraction of the volume available for molecular motion. It can also be shown that ζ may be related to the probability to find a hole larger than the size of a molecule.

In their expression for self-diffusion coefficient, Cohen and Turnbull [26] applied an exponential probability distribution for the free volume, which results in the exponential expression for the probability for molecule to find a hole large enough to jump in. The exponential distribution means that, generally, the chance to find a large hole decreases with increasing size of the hole. In the same manner Eq. (5.28) may be deduced based on the assumption that the free volume is evenly distributed among the pores:

$$p(V_h) dV_h = \frac{1}{V_f} dV_h. \quad (5.29)$$

Here V_h is the volume of the hole of a given size, V_f is the overall free volume in the mixture and p is the probability to find a hole with a volume between V_h and V_h+dV_h. The probability to find a hole, which is larger than the minimum irreducible size of the particle V^* can be estimated as:

$$\zeta \equiv P = \int_{V^*}^{V_f} p(V_h) dV_h = \frac{1}{V_f}\left[V_f - V^*\right] = 1 - \frac{V^*}{V_f}. \quad (5.30)$$

In the previous subsection the developed model was applied to description of the diffusion coefficients in binary mixtures of non-polar components. The next step is to apply the new quadratic expression for penetration lengths, Eq.(5.26), for description of the diffusion coefficients in binary mixtures of polar components. Application of the quadratic

expression to the description of the mixtures of non-polar components will also be conducted.

A thermodynamic model for polar mixtures should be able to reflect strongly non-ideal behavior. As a basis, we have selected the Soave-Redlich-Kwong (SRK) equation of state (EoS), due to its simplicity, as well as availability of its implementation in the efficient and robust simulation code. Since we are interested in prediction, but not correlation, of thermodynamic properties, all the calculations were carried out with zero interaction parameters for the EoS. The common way of applying the SRK EoS with classical linear-quadratic mixing rules is not well suited for description of the mixtures of polar components. However, performance of the SRK EoS can be essentially improved by application of the advanced mixing rules based on activity coefficient models. The most widely used mixing rules of such type are the Huron-Vidal mixing rule and a variety of its modifications (Modified Huron-Vidal – MHV1 rule [103]). Several activity coefficient models are available for application with the MHV1 mixing rules. The most common are the UNIFAC and the UNIQUAC models and their modifications. The cubic equations of state with different modifications of the Huron-Vidal mixing rule and different activity coefficient models were tested for description of the diffusion coefficients in binary mixtures of polar components. For comparison, the SRK EoS with the classical mixing rules and zero interaction parameters was also applied.

Fourteen references containing experimental measurements of the Fick diffusion coefficients were used. From these works, a database of diffusion coefficients for 28 binary mixtures containing polar components was formed.

The set of experimental diffusion coefficients was described by adjusting the values of the penetration parameters. The quality of description and the adjusted values of the parameters are summarized in Table 5.3. It is demonstrated that the choice of a thermodynamic model influences mainly the values of the penetration parameters, while the quality of description is generally the same.

Modeling of the diffusion coefficients in the mixtures of polar components appeared to be a more complex problem than modeling of the diffusion coefficients of non-polar mixtures described above. The diffusion coefficients in polar mixtures exhibit highly non-ideal behavior, and they do not obey common linear or logarithmic “mixing rules” [169].

A typical example of a mixture with highly non-ideal behavior is the mixture of ethanol-benzene [9], where the diffusion coefficient exhibits a minimum at a molar fraction of ethanol around 0.4. Figure 5.5a demonstrates that the model describes the compositional dependence of the diffusion coefficient reasonably. However, the behavior around the minimum of the dependence and the infinite dilution coefficients are not well described, which results in an average quality of description, with the AAD equal to 12.98%. This is one

of the worst results; the quality of description of most of the mixtures with quadratic dependence is significantly better, with an average deviation of 4.0-4.5%, depending on the model.

The mixture of acetone-chloroform [158], despite of its thermodynamic non-ideality exhibits monotonous behavior of the diffusion coefficient (Figure 5.5b). Still, this is not ideal behavior, since the dependence of the diffusion coefficient on molar fraction is convex, while the classical “mixing rules” predict a linear or concave dependence. The measured diffusion coefficients are described with high accuracy (AAD=1.428%). However, the model predicts a slight maximum of the diffusion coefficient when the mixture is close to pure acetone, which is not confirmed by experimental results.

The mixture of the associating components ethanol–water [158] exhibits strong non-ideal behavior, both in terms of thermodynamic properties and of the diffusion coefficients. There is a pronounced minimum in the molar fraction dependence of the diffusion coefficient, Figure 5.5c, which is well described by the model. There are slight deviations between the model and the experimental data in the dilute water limit at higher temperatures, which results in an overall performance with the AAD=5.73%.

Another mixture of associating components, methanol-water [91], demonstrates behavior similar to the mixture of the ethanol-water. The minima in the concentration dependence are properly reproduced by the model (Figure 5.6a). Despite the non-ideal behavior, the overall AAD is 3.944%

Experimental data were also available for the mixtures containing acetic acid [101]. Description of the diffusion coefficients for such mixtures is rather good, except for the mixture of acetic acid-water (Table 5.3), which exhibits strong association. This mixture is problematic for the majority of ordinary thermodynamic models, which do not account for association interactions. The behavior of the diffusion coefficients is also non-trivial (Figure 5.6b). There are deep and wide minima in the molar fraction dependence and the diffusion coefficients at infinite dilution are very high compared to the values of diffusion coefficients for middle molar fractions. The description of the diffusion coefficients by our model is relatively poor (the AAD is equal to 10.795%), however, it is qualitatively correct.

Another mixture containing acetic acid, but exhibiting a weaker association, is the mixture with n-butyl acetate [101]. The good performance of the model for this mixture is illustrated in Figure 5.6c and the overall AAD is 2.390%.

Table 5.3a: Parameters and deviations for binary mixtures of polar components, with the SRK EoS (classical mixing rule)

System (component 1 + component 2)	Data points	Temp. range (K)	Parameters for the penetration length				AAD (%)	References
			$A \cdot 10^{11}$, (m)	$B_1 \cdot 10^4$, (m^3/mole)	$B_2 \cdot 10^4$, (m^3/mole)	$B_{12} \cdot 10^8$, (m^3/mole)		
Non-polar + polar								
Acetone + benzene	33	298.15	-7926.	0.9460	0.9827	-0.0016	1.5793	[27,98]
Acetone + carbon tetrachloride	12	298.15-298.30	467.57	0.9381	1.0467	0.0077	2.3564	[9,27]
Acetone + cumene	12	283.15-303.15	28.114	0.8407	1.4842	0.1717	6.4736	[101]
Acetone + cyclohexane	11	298.15	8.1542	0.5165	0.8938	0.7447	4.1953	[155]
Acetic acid + carbon tetrachloride	9	298.15	-233.01	0.8436	1.0570	-0.0227	1.4970	[11]
Methyl ethyl ketone + *idem*	7	298.15	3.9851	0.1522	0.6099	0.6373	2.3399	[11]
Isobutyric acid + cumene	12	298.15-303.15	26.936	1.2522	1.5231	0.0211	2.0163	[101]
Methanol + benzene	8	313.15	-1462.	0.5465	1.0007	0.0071	14.853	[9]
Benzene + ethanol	17	298.30-313.13	20.642	0.8908	0.6233	0.1835	14.654	[9]
Methanol + carbon tetrachloride	12	293.15	-344.91	0.5355	1.0473	0.0040	6.3710	[135]
n-Propanol + carbon tetrachloride	12	293.15	572.98	0.8554	1.0433	-0.0074	2.2037	[135]
n-Butanol + carbon tetrachloride	12	293.15	232.53	1.0368	1.0416	-0.0114	1.4112	[135]
n-Propanol + toluene	15	298.15	-3561.	0.8610	1.2078	0.0019	6.4323	[135]
Polar + polar								
Diethyl ether + chloroform	8	298.15	44.218	1.0484	0.8068	-0.0428	0.9264	[10]
Acetone + chloroform	48	298.15-328.15	33.701	0.8469	0.7926	-0.0465	1.3503	[158]
Acetone + 1,2 dichlorobenzene	13	283.15-303.15	27.302	0.8339	1.3326	0.1155	2.8855	[101]
Chloroform + acetic acid	28	298.15	35.914	0.8071	0.8055	-0.0202	0.6789	[163]
Acetic acid + 5-methyl-2-hexanone	19	283.15-303.15	22.940	0.8037	1.5588	0.0222	2.3377	[101]
Acetic acid + methyl isobutyl ketone	20	283.15-303.15	21.637	0.8008	1.3335	0.0136	2.1193	[101]
Acetic acid + n-butyl acetate	18	283.15-303.15	25.355	0.8041	1.4293	0.0128	2.4613	[101]
Acetic acid + water	19	283.15-303.15	10.590	0.7989	0.2233	0.0272	13.446	[101]
Isobutyric acid + water	12	283.15-303.15	3.0886	1.2246	0.2030	0.1580	11.862	[101]
Methyl isopropyl ketone + water	8	293.15-298.15	-167.82	1.2315	0.2385	-0.0034	0.5811	[119]
Methanol + water	18	278.15-313.13	16.748	0.5028	0.2256	0.0153	5.6591	[91]
Ethanol + water	70	313.15-358.15	12.916	0.6651	0.2173	0.0441	6.7820	[158]
n-Butanol + water	37	298.15	7.2645	0.9984	0.2193	0.0819	2.1730	[119]
Dimethylformamide + water	12	278.15	-20.214	1.2231	0.2398	0.0066	3.8367	[63]
n-Methylpyrrolidone + water	12	278.15	-10.617	1.2249	0.2415	0.0065	4.5422	[63]
						Total AAD	4.5723%	

Table 5.3b: Parameters and deviations for binary mixtures of polar components, with the SRK EoS (MHV1 mixing rule with UNIFAC)

System (component 1 + component 2)	Data points	Temp. range (K)	Parameters for the penetration length				AAD (%)	References
			$A \cdot 10^{11}$, (m)	$B_1 \cdot 10^4$, (m^3/mole)	$B_2 \cdot 10^4$, (m^3/mole)	$B_{12} \cdot 10^8$, (m^3/mole)		
Nonpolar + polar								
Acetone + benzene	33	298.15	194.42	0.9274	0.9698	0.0220	1.5646	[27,98]
Acetone + carbon tetrachloride	12	298.15-298.30	223.04	0.9293	1.0427	0.0447	4.4666	[9,27]
Acetone + cumene	12	283.15-303.15	27.312	0.8381	1.4805	0.1996	6.4100	[101]
Acetone + cyclohexane	11	298.15	-74.222	0.9919	1.1998	-0.0151	3.6489	[155]
Acetic acid + carbon tetrachloride	9	298.15	42.462	0.8121	1.0143	0.0518	1.5466	[11]
Methyl ethyl ketone + *idem*	7	298.15	-230.79	1.1211	1.0582	0.0121	1.3630	[11]
Isobutyric acid + cumene	12	298.15-303.15	25.978	1.2497	1.5208	0.0459	2.5009	[101]
Methanol + benzene	8	313.15	-185.87	0.5522	1.0152	0.0135	10.928	[9]
Benzene + ethanol	17	298.30-313.13	21.123	0.8964	0.6246	0.2024	12.979	[9]
Methanol + carbon tetrachloride	12	293.15	-49.856	0.5512	1.0632	-0.0069	4.0928	[135]
n-Propanol + carbon tetrachloride	12	293.15	-36.508	0.8782	1.0687	0.0020	1.2711	[135]
n-Butanol + carbon tetrachloride	12	293.15	-24.642	1.0777	1.0757	0.0018	0.9604	[135]
n-Propanol + toluene	15	298.15	-169.27	0.8670	1.2208	0.0086	5.4280	[135]
Polar + polar								
Diethyl ether + chloroform	8	298.15	10.185	0.6103	0.6615	-0.1720	1.3084	[10]
Acetone + chloroform	48	298.15-328.15	34.336	0.8489	0.7939	-0.0686	1.4284	[158]
Acetone + 1,2 dichlorobenzene	13	283.15-303.15	26.451	0.8312	1.3303	0.1315	3.1831	[101]
Chloroform + acetic acid	28	298.15	-10.857	0.9951	0.9485	0.0311	0.6521	[163]
Acetic acid + 5-methyl-2-hexanone	19	283.15-303.15	22.940	0.8039	1.5588	0.0222	2.3377	[101]
Acetic acid + methyl isobutyl ketone	20	283.15-303.15	21.858	0.8012	1.3343	-0.0070	1.9928	[101]
Acetic acid + n-butyl acetate	18	283.15-303.15	25.189	0.8038	1.4292	0.0044	2.3898	[101]
Acetic acid + water	19	283.15-303.15	12.953	0.8051	0.2262	0.0155	10.795	[101]
Isobutyric acid + water	12	283.15-303.15	3.2553	1.2272	0.2056	0.1271	11.672	[101]
Methyl isopropyl ketone + water	8	293.15-298.15	-310.90	1.2251	0.2381	-0.0100	0.4353	[119]
Methanol + water	18	278.15-313.13	19.460	0.5076	0.2278	0.0098	3.9435	[91]
Ethanol + water	70	313.15-358.15	13.604	0.6668	0.2196	0.0345	5.7287	[158]
n-Butanol + water	37	298.15	10.995	1.0144	0.2260	0.0460	2.6469	[119]
n,n-Dimethylformamide + water	12	278.15	233.35	1.1768	0.2349	-0.0002	0.4503	[63]
n-Methylpyrrolidone + water	12	278.15	-44.382	1.1948	0.2368	0.0032	5.0873	[63]
						Total AAD	3.9718%	

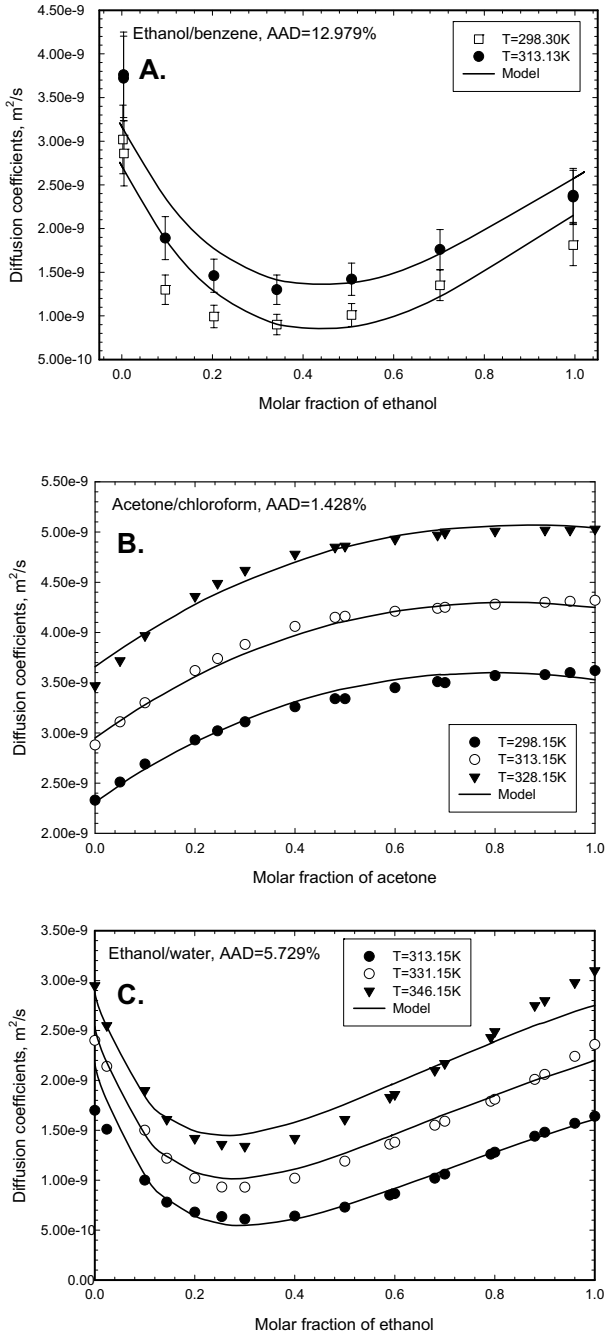

Figure 5.5: Comparison of the diffusion model with experimental data.

Figure A: data from [9] with 13% error bars; figure B: data from [158]; figure C: data from [158]

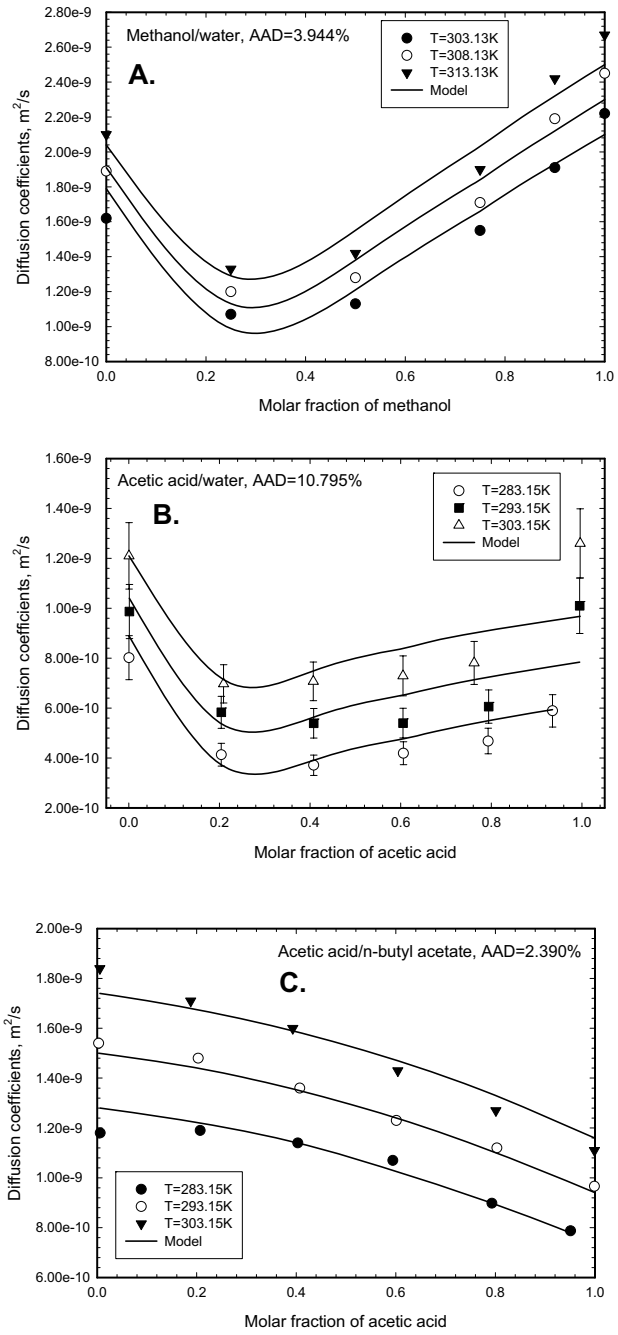

Figure 5.6: Comparison of the diffusion model with experimental data. Figure A: data from [91]; figure B: data from [101] with 11% error bars; figure C: data from [101].

Based on the results presented in Table 5.3, it may be concluded that the proposed model is able to describe adequately all the types of the concentration and temperature behavior of the diffusion coefficients in polar and associating mixtures. By adjusting only four constant penetration parameters, the overall quality of the description for the whole database of the mixtures of polar components was around 4.0% for the SRK+MHV1/UNIFAC model and around 4.6% for the SRK model with ordinary quadratic mixing rules.

Moreover, the preliminary analysis of the Table 5.3 indicates that the penetration volumes demonstrate individual behavior, since the values of the penetration volumes for the selected components are similar in different mixtures. This makes it possible to investigate the prediction capabilities of the quadratic expression for penetration lengths.

5.3. Predicting Diffusion Coefficients

This subsection aims at establishing a semi-empirical relation of the penetration coefficients with other properties of the components. On the basis of the comparison of model with quadratic dependence for penetration lengths Eq. (5.26) with experimental data described above, a large set of penetration parameters was formed using experimental information. This made it possible to carry out analysis of the parameters in expression (5.26) for the penetration lengths and to establish correlations, which would allow prediction of the diffusion coefficients in multicomponent mixtures.

For the analysis, only the parameters of the mixtures where experimental data at different temperatures is available were used. Fitted parameters for other mixtures behave in a less regular way. This may be explained by the fact that fitting the parameters to experimental data obtained for the only temperature may result in “over-performance” of the optimization procedure. Figure 5.7 illustrates an example of such a case. Optimization of the penetration parameters for the mixture of acetone/cyclohexane [155] is considered. The points on the plot (Figure 5.7) denote steps of the optimization procedure. Each step corresponds to the specific set of the penetration parameters and to the specific deviations of calculated diffusion coefficients from the experimental values. At the first stage of optimization (not shown in Figure 5.7) the penetration amplitude is being optimized. The second stage adjusts the description of the compositional behavior of the diffusion coefficients by rapid optimization of the penetration volumes and the interaction parameter at almost fixed value of the amplitude (Figure 5.7). At the end of the second stage the optimization procedure converges to physically reasonable values of penetration parameters. However, in the cases where the diffusion coefficients are available at only one temperature, a further very small increase of the accuracy of description may be achieved (the third stage). It can be seen from Figure 5.7 that during the last stage an insignificant increase of the accuracy of description is achieved (standard deviation 0.1103 instead of 0.1307) but the

penetration amplitude and the fraction of free volume become negative. At the end of stage 3 the set of parameters converges to a global minimum, corresponding to non-physical values of the penetration parameters. In the case where the diffusion coefficients are available at different temperatures, physically reasonable values of penetration parameters correspond to the global optimization minimum. Otherwise, there is no guarantee that the optimized values of the penetration parameters are physically reasonable.

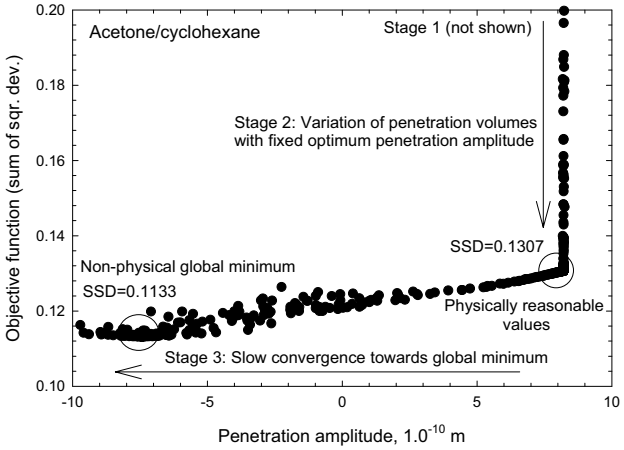

Figure 5.7: Illustration of optimization procedure, resulting in the global minimum, corresponding to non-physical values of the penetration parameters.

Another comment regarding the optimization procedure is that the optimization surface is very complex. To guarantee that the system converges on the global minimum, several consecutive optimization cycles are implemented in the FTCode (Appendix A.2). The first optimization cycle uses an initial guess for the penetration parameters and performs optimization in order to reduce the deviation of the calculated diffusivities from the experimental values. Once the tolerance condition is satisfied, the optimized penetration parameters from the first optimization cycle are used as the initial estimate for the next optimization cycle. There are a total of three optimization cycles. The calculations demonstrate that the systems, where both temperature and concentration dependencies are available, converge to the global minima already in the first optimization cycle. For the mixtures with no temperature dependence, there are many cases where the minimum found in the second cycle is different from the minimum found in the first cycle. However, for all the considered mixtures, the third cycle repeats the minimum found in the second cycle. This may be considered as substantiation of the fact that all the reported results correspond to the global optimization minimum. However, still not all of them correspond to the minima with physically reasonable values of the penetration parameters. Hence a database of 22

mixtures of both polar and non-polar components for which the diffusion coefficients were measured at different temperatures was formed for further analysis.

The quadratic expression for the penetration lengths, Eq.(5.26), was applied to correlate diffusion coefficients for selected mixtures. Three different thermodynamic models were used for estimation of the thermodynamic matrix, namely the Soave-Redlich-Kwong and the Peng-Robinson EoS with classical mixing rules, and the SRK EoS with the MHV1-UNIFAC mixing rules. The results of modeling the diffusion coefficients, as well as the values of the obtained penetration parameters, are presented in Table 5.4.

Table 5.4 demonstrates that the SRK and the PR EoS with classical mixing rules can also be applied to evaluation of the diffusion coefficients. The absolute average deviations for all the three models are around 4.0%. Superiority of the SRK+MHV1/UNIFAC model is not significant. The performance of the SRK+MHV1/UNIFAC model is better than the performance of the SRK and PR EoS mainly for mixtures of polar components. However, at the same time, the SRK+MHV1/UNIFAC EoS demonstrates less accurate description of the mixtures of alkanes, compared to the SRK EoS with ordinary quadratic mixing rules. However, the values of the penetration parameters depend upon the selected thermodynamic model. As it will be shown later, the more advanced thermodynamic model provides more explainable values of penetration parameters.

Analysis of Table 5.4 shows that the penetration volumes B_i exhibit individual behavior, that is, the same compounds have very close values of the penetration volumes in different mixtures. Average values of the penetration volumes for individual compounds and deviations from them are presented in Table 5.5. The deviations from average values are generally within 2%, which proves that the penetration volumes are individual properties. The volumes obtained by application of the classical SRK EoS exhibit slightly higher deviations from the average than the volumes obtained by application of the PR EoS and of the SRK EoS with the MHV1-UNIFAC mixing rule (Table 5.5).

Table 5.4a: Parameters and deviations for all available mixtures with temperature dependence of the diffusion coefficients, with the SRK EoS (classical mixing rule).

System (component 1 + component 2)	Data points	Temp. range (K)	Parameters for the penetration length				AAD (%)	References
			$A \cdot 10^{11}$, (m)	$B_1 \cdot 10^4$, (m^3/mole)	$B_2 \cdot 10^4$, (m^3/mole)	$B_{12} \cdot 10^8$, (m^3/mole)		
Normal alkanes								
n-Hexane + n-dodecane	23	298.15-308.15	28.828	1.1507	2.0763	0.0135	1.2298	[146]
n-Octane + n-dodecane	21	298.15-333.15	31.867	1.4915	2.1042	0.0001	1.2644	[53]
n-Hexane + n-heptane	10	283.15-298.15	36.754	1.3068	1.5194	-0.0237	0.8472	[118]
Non-polar + non-polar								
Cyclohexane + carbon tetrachloride	78	298.15-328.15	25.462	1.0871	0.9897	0.0014	1.3741	[90,136,137]
Benzene + n-heptane	33	298.15-328.15	31.941	0.9218	1.4617	0.2578	3.4039	[136,137]
Benzene + cyclohexane	56	298.15-333.15	31.586	0.9165	1.0978	0.0296	0.4811	[98,130,136,137]
Toluene + cyclohexane	65	298.15-328.15	32.999	1.1075	1.1153	0.0224	2.6909	[136,137]
Toluene + benzene	22	298.15-313.15	36.953	1.1190	0.9322	0.0180	1.2342	[136,137]
Non-polar + polar								
Acetone + carbon tetrachloride	12	298.15-298.30	467.57	0.9381	1.0467	0.0077	2.3564	[9,27]
Acetone + cumene	12	283.15-303.15	28.114	0.8407	1.4842	0.1717	6.4736	[101]
Isobutyric acid + cumene	12	298.15-303.15	26.936	1.2522	1.5231	0.0211	2.0163	[101]
Benzene + ethanol	17	298.30-313.13	20.642	0.8908	0.6233	0.1835	14.654	[9]
Polar + polar								
Acetone + chloroform	48	298.15-328.15	33.701	0.8469	0.7926	-0.0465	1.3503	[158]
Acetone + 1,2 dichlorobenzene	13	283.15-303.15	27.302	0.8339	1.3326	0.1155	2.8855	[101]
Acetic acid + 5-methyl-2-hexanone	19	283.15-303.15	22.940	0.8037	1.5588	0.0222	2.3377	[101]
Acetic acid + methyl isobutyl ketone	20	283.15-303.15	21.637	0.8008	1.3335	0.0136	2.1193	[101]
Acetic acid + n-butyl acetate	18	283.15-303.15	25.355	0.8041	1.4293	0.0128	2.4613	[101]
Acetic acid + water	19	283.15-303.15	10.590	0.7989	0.2233	0.0272	13.446	[101]
Isobutyric acid + water	12	283.15-303.15	3.0886	1.2246	0.2030	0.1580	11.862	[101]
Methyl isopropyl ketone + water	8	293.15-298.15	-167.82	1.2315	0.2385	-0.0034	0.5811	[119]
Methanol + water	18	278.15-313.13	16.748	0.5028	0.2256	0.0153	5.6591	[91]
Ethanol + water	70	313.15-358.15	12.916	0.6651	0.2173	0.0441	6.7820	[158]
						Total AAD	3.9777%	

Table 5.4b: Parameters and deviations for all available mixtures with temperature dependence of the diffusion coefficients, with the PR EoS (classical mixing rule).

System (component 1 + component 2)	Data points	Temp. range (K)	Parameters for the penetration length				AAD (%)	References
			$A \cdot 10^{11}$, (m)	$B_1 \cdot 10^4$, (m^3/mole)	$B_2 \cdot 10^4$, (m^3/mole)	$B_{12} \cdot 10^8$, (m^3/mole)		
Normal alkanes								
n-Hexane + n-dodecane	23	298.15-308.15	35.885	1.1849	2.4390	-0.0064	1.4874	[146]
n-Octane + n-dodecane	21	298.15-333.15	40.867	1.6016	2.4680	-0.0084	1.7674	[53]
n-Hexane + n-heptane	10	283.15-298.15	38.687	1.1659	1.3563	-0.0178	0.8479	[118]
Non-polar + non-polar								
Cyclohexane + carbon tetrachloride	78	298.15-328.15	26.712	0.9683	0.8810	0.0011	1.3695	[90,136,137]
Benzene + n-heptane	33	298.15-328.15	33.535	0.8210	1.3072	0.1942	3.4019	[136,137]
Benzene + cyclohexane	56	298.15-333.15	33.148	0.8164	0.9774	0.0222	0.4929	[98,130,136,137]
Toluene + cyclohexane	65	298.15-328.15	34.710	0.9887	0.9923	0.0168	2.7047	[136,137]
Toluene + benzene	22	298.15-313.15	38.957	0.9986	0.8300	0.0135	1.2435	[136,137]
Non-polar + polar								
Acetone + carbon tetrachloride	12	298.15-298.30	493.36	0.8322	0.9292	0.0057	2.3606	[9,27]
Acetone + cumene	12	283.15-303.15	29.716	0.7504	1.3272	0.1286	6.4979	[101]
Isobutyric acid + cumene	12	298.15-303.15	28.678	1.1198	1.3603	0.0161	2.0171	[101]
Benzene + ethanol	17	298.30-313.13	27.193	0.7952	0.5580	0.1374	14.678	[9]
Polar + polar								
Acetone + chloroform	48	298.15-328.15	35.207	0.7547	0.7053	-0.0350	1.3513	[158]
Acetone + 1,2 dichlorobenzene	13	283.15-303.15	28.946	0.7450	1.1907	0.0860	2.8497	[101]
Acetic acid + 5-methyl-2-hexanone	19	283.15-303.15	24.381	0.7172	1.3928	0.0171	2.3339	[101]
Acetic acid + methyl isobutyl ketone	20	283.15-303.15	22.964	0.7147	1.1919	0.0105	2.1139	[101]
Acetic acid + n-butyl acetate	18	283.15-303.15	26.928	0.7175	1.2764	0.0100	2.4544	[101]
Acetic acid + water	19	283.15-303.15	11.120	0.7129	0.1995	0.0208	13.581	[101]
Isobutyric acid + water	12	283.15-303.15	3.2561	1.0962	0.1823	0.1197	11.916	[101]
Methyl isopropyl ketone + water	8	293.15-298.15	-169.38	1.0938	0.2124	-0.0025	0.5826	[119]
Methanol + water	18	278.15-313.13	17.610	0.4482	0.2014	0.0116	5.6852	[91]
Ethanol + water	70	313.15-358.15	13.551	0.5930	0.1943	0.0334	6.8179	[158]
						Total AAD	4.0252%	

Table 5.4c: Parameters and deviations for all available mixtures with temperature dependence of the diffusion coefficients, with the SRK EoS (MHV1-UNIFAC mixing rule).

System (component 1 + component 2)	Data points	Temp. range (K)	Parameters for the penetration length				AAD (%)	References
			$A \cdot 10^{11}$, (m)	$B_1 \cdot 10^4$, (m^3/mole)	$B_2 \cdot 10^4$, (m^3/mole)	$B_{12} \cdot 10^8$, (m^3/mole)		
Normal alkanes								
n-Hexane + n-dodecane	23	298.15-308.15	34.030	1.3291	2.7266	-0.0086	1.4589	[146]
n-Octane + n-dodecane	21	298.15-333.15	38.586	1.7952	2.7604	-0.0120	1.7225	[53]
n-Hexane + n-heptane	10	283.15-298.15	36.751	1.5194	1.3068	-0.0236	0.8469	[118]
Non-polar + non-polar								
Cyclohexane + carbon tetrachloride	78	298.15-328.15	25.432	1.0872	0.9896	0.0067	1.2896	[90,136,137]
Benzene + n-heptane	33	298.15-328.15	31.659	0.9211	1.4597	0.2651	3.4449	[136,137]
Benzene + cyclohexane	56	298.15-333.15	31.099	0.9152	1.0966	0.0418	0.5116	[98,130,136,137]
Toluene + cyclohexane	65	298.15-328.15	32.588	1.1058	1.1146	0.0348	2.6735	[136,137]
Toluene + benzene	22	298.15-313.15	36.983	1.1191	0.9323	0.0167	1.2341	[136,137]
Non-polar + polar								
Acetone + carbon tetrachloride	12	298.15-298.30	223.04	0.9293	1.0427	0.0447	4.4666	[9,27]
Acetone + cumene	12	283.15-303.15	27.312	0.8381	1.4805	0.1996	6.4100	[101]
Isobutyric acid + cumene	12	298.15-303.15	25.978	1.2497	1.5208	0.0459	2.5009	[101]
Benzene + ethanol	17	298.30-313.13	21.123	0.8964	0.6246	0.2024	12.979	[9]
Polar + polar								
Acetone + chloroform	48	298.15-328.15	34.336	0.8489	0.7939	-0.0686	1.4284	[158]
Acetone + 1,2 dichlorobenzene	13	283.15-303.15	26.451	0.8312	1.3303	0.1315	3.1831	[101]
Acetic acid + 5-methyl-2-hexanone	19	283.15-303.15	22.940	0.8039	1.5588	0.0222	2.3377	[101]
Acetic acid + methyl isobutyl ketone	20	283.15-303.15	21.858	0.8012	1.3343	-0.0070	1.9928	[101]
Acetic acid + n-butyl acetate	18	283.15-303.15	25.189	0.8038	1.4292	0.0044	2.3898	[101]
Acetic acid + water	19	283.15-303.15	12.953	0.8051	0.2262	0.0155	10.795	[101]
Isobutyric acid + water	12	283.15-303.15	3.2553	1.2272	0.2056	0.1271	11.672	[101]
Methyl isopropyl ketone + water	8	293.15-298.15	-310.90	1.2251	0.2381	-0.0100	0.4353	[119]
Methanol + water	18	278.15-313.13	19.460	0.5076	0.2278	0.0098	3.9435	[91]
Ethanol + water	70	313.15-358.15	13.604	0.6668	0.2196	0.0345	5.7287	[158]
						Total AAD	3.7929%	

Table 5.5a: Averaged individual penetration volumes and their correlation with the volume parameter, obtained by the SRK EoS (classical mixing rule).

Component name	Number of observations	Penetration volume, $\times 10^4$ m^3/mole	Error of averaging, %	SRK volume, $\times 10^4$ m^3/mole	SRK prediction, $\times 10^4$ m^3/mole	Deviations, %
nHexane	2	1.2288	6.35	1.2087	1.2936	-5.0152
nHeptane	2	1.4906	1.94	1.4201	1.5158	-1.6639
nOctane	1	1.4915	-	1.6452	1.7523	-14.883
nDodecane	2	2.0903	0.67	2.6043	2.7601	-24.268
Cyclohexane	3	1.1001	0.92	0.9790	1.0522	4.5444
Benzene	4	0.9153	1.34	0.8268	0.8922	2.5901
Toluene	2	1.1133	0.52	1.0382	1.1144	-0.1060
Carbon Tetrachloride	2	1.0182	2.80	0.8788	0.9470	7.5238
Acetone	4	0.8649	4.23	0.7787	0.8417	2.7525
Cumene	2	1.5037	1.29	1.4164	1.5119	-0.5442
Methanol	1	0.5028	-	0.4561	0.5027	0.0276
Ethanol	2	0.6442	3.24	0.6021	0.6562	-1.8240
Chloroform	1	0.7926	-	0.7061	0.7654	3.5479
1,2 dichlorobenzene	1	1.3326	-	1.2477	1.3346	-0.1504
5-methyl-2-hexanone	1	1.5588	-	1.4581	1.5557	0.2014
n-butyl acetate	1	1.4293	-	1.3283	1.4192	0.7095
Isobutyric acid	2	1.2384	1.11	1.1778	1.2612	-1.8044
Acetic Acid	4	0.8019	0.25	0.7370	0.7978	0.5048
Methyl isopropyl ketone	1	1.2315	-	1.0313	1.1072	10.093
Methyl isobutyl ketone	1	1.3335	-	1.2587	1.3461	-0.9395
Water	5	0.2207	3.81	0.2114	0.2455	-10.121
		AAD of averaging	**2.3733%**		**AAD of correlation**	**4.5115%**

Table 5.5b: Averaged individual penetration volumes and their correlation with the volume parameter, obtained by the PR EoS (classical mixing rule).

Component name	Number of observations	Penetration volume, $\times 10^4$ m^3/mole	Error of averaging, %	PR volume, $\times 10^4$ m^3/mole	PR prediction, $\times 10^4$ m^3/mole	Deviations, %
nHexane	2	1.1754	0.81	1.0859	1.2007	-2.1039
nHeptane	2	1.3318	1.84	1.2503	1.3840	-3.7772
nOctane	1	1.6016	-	1.4180	1.5711	1.9411
nDodecane	2	2.4535	0.59	2.0795	2.3092	6.2482
Cyclohexane	3	0.9793	0.88	0.9136	1.0084	-2.8796
Benzene	4	0.8157	1.25	0.7714	0.8497	-4.0040
Toluene	2	0.9937	0.50	0.9481	1.0468	-5.0813
Carbon Tetrachloride	2	0.9051	2.66	0.8258	0.9104	-0.5857
Acetone	4	0.7706	4.00	0.6981	0.7679	0.3479
Cumene	2	1.3438	1.23	1.2594	1.3942	-3.6207
Methanol	1	0.4482	-	0.3659	0.3973	12.808
Ethanol	2	0.5755	3.04	0.4659	0.5089	13.094
Chloroform	1	0.7053	-	0.6556	0.7205	-2.1105
1,2 dichlorobenzene	1	1.1907	-	1.1598	1.2830	-7.1958
5-methyl-2-hexanone	1	1.3928	-	1.2381	1.3704	1.6335
n-butyl acetate	1	1.2764	-	1.1363	1.2568	1.5557
Isobutyric acid	2	1.1080	1.06	0.9206	1.0161	9.0416
Acetic Acid	4	0.7156	0.25	0.6171	0.6776	5.6059
Methyl isopropyl ketone	1	1.0938	-	0.9078	1.0019	8.9944
Methyl isobutyl ketone	1	1.1919	-	1.0897	1.2048	-1.0723
Water	5	0.1972	3.61	0.1864	0.1970	0.0847
		AAD of averaging	**1.8112%**		**AAD of correlation**	**4.4659%**

Table 5.5c: Averaged individual penetration volumes and their correlation with the volume parameter, obtained by the SRK EoS (MHV1-UNIFAC mixing rule).

Component name	Number of observations	Penetration volume, $\times 10^4$ m^3/mole	Error of averaging, %	SRK volume, $\times 10^4$ m^3/mole	SRK prediction, $\times 10^4$ m^3/mole	Deviations, %
nHexane	2	1.3180	0.85	1.2087	1.3159	0.1522
nHeptane	2	1.4896	2.00	1.4201	1.5456	-3.6260
nOctane	1	1.7952	-	1.6452	1.7901	0.2850
nDodecane	2	2.7435	0.62	2.6043	2.8319	-3.1221
Cyclohexane	3	1.0995	0.92	0.9790	1.0664	3.0995
Benzene	4	0.9163	1.14	0.8268	0.9010	1.6953
Toluene	2	1.1125	0.60	1.0382	1.1307	-1.6138
Carbon Tetrachloride	2	1.0162	2.61	0.8788	0.9576	6.1184
Acetone	4	0.8619	3.91	0.7787	0.8488	1.5421
Cumene	2	1.5007	1.34	1.4164	1.5416	-2.6544
Methanol	1	0.5076	-	0.4561	0.4983	1.8742
Ethanol	2	0.6458	3.28	0.6021	0.6570	-1.7055
Chloroform	1	0.7939	-	0.7061	0.7699	3.1146
1,2 dichlorobenzene	1	1.3303	-	1.2477	1.3583	-2.0621
5-methyl-2-hexanone	1	1.5588	-	1.4581	1.5868	-1.7668
n-butyl acetate	1	1.4292	-	1.3283	1.4458	-1.1476
Isobutyric acid	2	1.2385	0.91	1.1778	1.2824	-3.4255
Acetic Acid	4	0.8035	0.14	0.7370	0.8034	0.0038
Methyl isopropyl ketone	1	1.2251	-	1.0313	1.1232	8.3177
Methyl isobutyl ketone	1	1.3343	-	1.2587	1.3702	-2.6229
Water	5	0.2233	3.83	0.2114	0.2324	-3.9243
		AAD of averaging	**1.8455%**		**AAD of correlation**	**2.5654%**

Further analysis of Table 5.5 makes it possible to establish a correlation between the individual penetration volumes and the *b*-parameters for the corresponding equation of state (Figure 5.8). The following standard dependencies for estimation of the *b*-parameters for the cubic equations of state were used [104]:

$$b = \Omega \frac{RT_c}{P_c},\ \Omega_{SRK} = \left(\sqrt[3]{2} - 1\right)/3,\ \Omega_{PR} = 0.08794 - 0.03452\omega + 0.00330\omega^2$$

where ω is the acentric factor, T_C, P_C are the critical temperature and pressure, correspondingly.

The following correlations between the penetration volumes and the *b*-parameters were obtained for the classical SRK and PR EoS, and the SRK EoS with the MHV1-UNIFAC mixing rule correspondingly:

$$B_{SRK} = 2.34 \cdot 10^{-6} + 1.0509 b_{SRK} - 0.2245 {b_{SRK}}^2,$$

$$B_{PR} = -1.10 \cdot 10^{-6} + 1.1158 b_{PR} - 0.0199 {b_{PR}}^2,$$

$$B_{MHV1} = 2.80 \cdot 10^{-7} + 1.0864 b_{SRK} - 0.2586 {b_{SRK}}^2. \qquad (5.31)$$

The obtained correlations are almost linear, with a very small quadratic term. The values of B_i are approximately equal to the values of b_i. Figure 5.8 demonstrates that, generally, higher deviations from the correlations above are observed for higher values of the *b*-parameters, which correspond to the components with a high molecular weight. The predicted values of B_{SRK}, B_{PR} and B_{MHV1} as well as the deviations of these values from the individual penetration volumes are listed in Table 5.5. The best correlations are observed for the SRK EoS with the MHV1-UNIFAC mixing rule (AAD=2.5%). Average deviations for other models are around 4.5% for both PR and SRK EoS. Superiority of the SRK+MHV1/UNIFAC model for prediction of the diffusion coefficients is in good agreement with the fact that this model is more advanced, compared to the classical cubic equations of state.

Correlation of the volumes B_1, B_2 with the individual component properties makes it possible to reduce the number of adjustment parameters in the expressions for diffusion coefficients. To verify this statement, the diffusion coefficients were refitted applying individual values of the B-parameters and adjusting the amplitude A and the interaction parameter B_{12} as the only fitting parameters. The SRK+MHV1/UNIFAC thermodynamic model was applied for this purpose, since, as demonstrated above, it provides better correlation of the penetration volumes and the diffusion coefficients compared to other thermodynamic models.

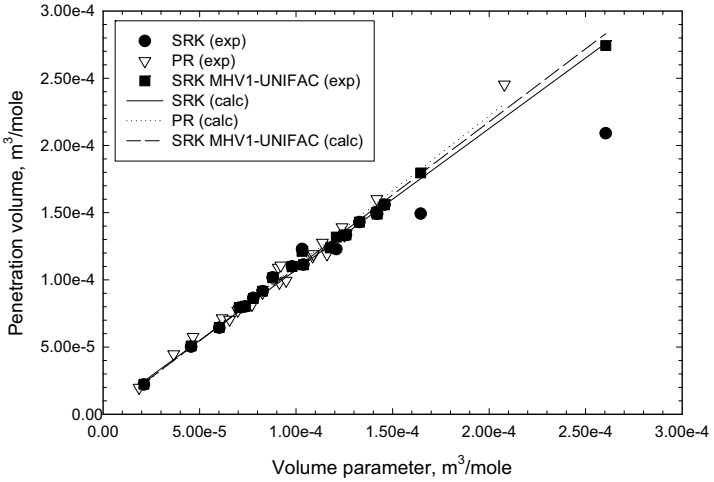

Figure 5.8: Correlation between penetration volumes and volume parameters of EoS.

The results of the new fitting are summarized in Table 5.6, for mixtures of both polar and non-polar components. For some components, average individual penetration volumes were not available, since no temperature dependencies of the diffusion coefficients were available for analysis. As expected, the description presented in Table 5.6 is less accurate in comparison with the previous results (Tables 5.1, 5.3 and 5.4). This is explained by additional deviations produced by the procedure of averaging the values of the penetration volumes. The average deviation in Table 5.6 is around 7% for the mixtures of non-polar and around 12% for the mixtures of polar components.

Another approximation to the values of diffusion coefficients was tested. It was obtained on the basis of the values of the individual volumes predicted by Eq.(5.31). Again, only two parameters, A and B_{12}, were fitted. The results are shown in Table 5.7. Due to the additional deviations produced by correlation (5.31), the description presented in Table 5.7 is even less accurate compared to the results presented in Table 5.6. The overall AAD is around 20%, with somewhat smaller deviations for the mixtures of non-polar components (17%). This is the price for the improved predictive capabilities of the model. Such performance is at some point similar to the performance of prediction of diffusion coefficients by models described in Chapter 4. Further research is required to increase prediction capabilities of the model.

Table 5.6a: Parameters and deviations of the concentration and temperature dependence of the diffusion coefficients for binary mixtures of non-polar components with the SRK EoS (MHV1-UNIFAC mixing rule), and averaged individual penetration volumes from Table 5.5c.

System (component 1 + component 2)	Data points	Temp. range (K)	Parameters for the penetration length		AAD (%)	References
			$A \cdot 10^{11}$, (m)	$B_{12} \cdot 10^{8}$, (m^3/mole)		
Normal alkanes						
n-Hexane + n-dodecane	23	298.15-308.15	35.156	0.0190	6.3162	[146]
n-Octane + n-dodecane	21	298.15-333.15	37.843	0.0386	2.7793	[53]
n-Heptane + n-decane	21	298.15	NA	NA	NA	[95]
n-Heptane + n-dodecane	20	298.15	30.516	0.0752	9.4517	[95]
n-Heptane + n-hexadecane	8	298.25	NA	NA	NA	[17]
n-Hexane + n-heptane	10	283.15-298.15	35.587	0.0000	7.8157	[118]
n-Heptane + n-tetradecane	23	298.15	NA	NA	NA	[95]
n-Dodecane + n-hexadecane	9	298.15	NA	NA	NA	[146]
n-Octane + n-tetradecane	24	298.15	NA	NA	NA	[95]
Non-polar + non-polar						
Cyclohexane + carbon tetrachloride	78	298.15-328.15	33.231	-0.0078	10.116	[90,136,137]
n-Hexane + carbon tetrachloride	6	303.15	48.703	0.0612	7.5686	[17,131,132]
n-Heptane + carbon tetrachloride	6	303.15	40.310	0.1098	12.187	[131,132]
n-Octane + carbon tetrachloride	6	303.15	52.235	0.0782	4.4975	[131,132]
3-Methylpentane + carbon tetrachloride	6	303.15	NA	NA	NA	[131,132]
2,3-Dimethylpentane + carbon tetrachloride	6	303.15	NA	NA	NA	[131,132]
2,2,4-Trimethylpentane + carbon tetrachloride	6	303.15	NA	NA	NA	[131,132]
Benzene + n-hexane	11	298.15	22.732	-0.4656	21.520	[69]
Benzene + n-heptane	33	298.15-328.15	34.611	0.2691	5.1874	[23,69,136,137]
Benzene + cyclohexane	56	298.15-333.15	31.816	0.0400	0.8732	[136,137]
Toluene + cyclohexane	65	298.15-328.15	31.542	0.0443	7.4499	[98,130,136,137]
Toluene + benzene	22	298.15-313.15	33.637	0.0223	2.5045	[136,137]
				Total AAD	7.5590%	

Table 5.6b: Parameters and deviations of the concentration and temperature dependence of the diffusion coefficients for binary mixtures of polar components with the SRK EoS (MHV1-UNIFAC mixing rule), and averaged individual penetration volumes from Table 5.5c.

System (component 1 + component 2)	Data points	Temp. range (K)	Parameters for the penetration length		AAD (%)	References
			$A \cdot 10^{11}$, (m)	$B_{12} \cdot 10^{8}$, (m^3/mole)		
Non-polar + polar						
Acetone + benzene	33	298.15	40.082	0.0643	4.8891	[27,98]
Acetone + carbon tetrachloride	12	298.15-298.30	46.993	0.0108	7.8311	[9,27]
Acetone + cumene	12	283.15-303.15	33.504	0.0153	7.6217	[101]
Acetone + cyclohexane	11	298.15	37.382	0.2233	11.630	[155]
Methyl ethyl ketone + carbon tetrachloride	7	298.15	NA	NA	NA	[11]
Acetic acid + carbon tetrachloride	9	298.15	42.923	0.6824	8.2935	[11]
Isobutyric acid + cumene	12	298.15-303.15	21.532	0.0568	3.6751	[101]
Methanol + benzene	8	313.15	34.373	0.1159	25.656	[9]
Benzene + ethanol	17	298.30-313.13	27.548	0.1577	14.882	[9]
Methanol + carbon tetrachloride	12	293.15	29.940	0.0558	31.848	[135]
n-Propanol + carbon tetrachloride	12	293.15	NA	NA	NA	[135]
n-Butanol + carbon tetrachloride	12	293.15	NA	NA	NA	[135]
n-Propanol + toluene	15	298.15	NA	NA	NA	[135]
Polar + polar						
Diethyl ether + chloroform	8	298.15	NA	NA	NA	[10]
Acetone + chloroform	48	298.15-328.15	36.866	-0.0649	2.9964	[158]
Acetone + 1,2 dichlorobenzene	13	283.15-303.15	32.609	0.1072	11.131	[101]
Chloroform + acetic acid	28	298.15	30.322	-0.0088	6.1034	[163]
Acetic acid + 5-methyl-2-hexanone	19	283.15-303.15	22.899	0.0223	2.3758	[101]
Acetic acid + methyl isobutyl ketone	20	283.15-303.15	22.296	-0.0026	2.6342	[101]
Acetic acid + n-butyl acetate	18	283.15-303.15	25.116	0.0047	2.3966	[101]
Acetic acid + water	19	283.15-303.15	12.054	0.0196	10.876	[101]
Isobutyric acid + water	12	283.15-303.15	66.611	0.0939	36.070	[101]
Methyl isopropyl ketone + water	8	293.15-298.15	310.57	0.0163	29.082	[119]
Methanol + water	18	278.15-313.13	18.585	0.0135	7.8368	[91]
Ethanol + water	70	313.15-358.15	12.092	0.0355	17.817	[158]
n-Butanol + water	37	298.15	NA	NA	NA	[119]
n,n-Dimethylformamide + water	12	278.15	NA	NA	NA	[63]
n-Methylpyrrolidone + water	12	278.15	NA	NA	NA	[63]
				Total AAD	12.282%	

Table 5.7a: Parameters and deviations of the concentration and temperature dependence of the diffusion coefficients for binary mixtures of non-polar components, with the SRK EoS (MHV1-UNIFAC mixing rule), and predicted penetration volumes from Table 5.5c.

System (component 1 + component 2)	Data points	Temp. range (K)	Parameters for the penetration length		AAD (%)	References
			$A \cdot 10^{11}$, (m)	$B_{12} \cdot 10^{8}$, (m^3/mole)		
Normal alkanes						
n-Hexane + n-dodecane	23	298.15-308.15	79.873	0.2800	35.105	[146]
n-Octane + n-dodecane	21	298.15-333.15	35.846	-0.6891	16.167	[53]
n-Heptane + n-decane	21	298.15	54.522	0.0496	13.374	[95]
n-Heptane + n-dodecane	20	298.15	68.330	0.0934	26.301	[95]
n-Heptane + n-hexadecane	8	298.25	NA*	NA	NA	[17]
n-Hexane + n-heptane	10	283.15-298.15	42.186	-0.0159	4.3075	[118]
n-Heptane + n-tetradecane	23	298.15	NA	NA	NA	[95]
n-Dodecane + n-hexadecane	9	298.15	NA	NA	NA	[146]
n-Octane + n-tetradecane	24	298.15	NA	NA	NA	[95]
Non-polar + non-polar						
Cyclohexane + carbon tetrachloride	78	298.15-328.15	20.049	0.0291	5.4272	[90,136,137]
n-Hexane + carbon tetrachloride	6	303.15	38.909	0.1528	16.869	[17,131,132]
n-Heptane + carbon tetrachloride	6	303.15	40.253	0.1776	19.193	[131,132]
n-Octane + carbon tetrachloride	6	303.15	45.054	0.2160	23.841	[131,132]
3-Methylpentane + carbon tetrachloride	6	303.15	35.298	0.1669	18.360	[131,132]
2,3-Dimethylpentane + carbon tetrachloride	6	303.15	37.460	0.2040	19.085	[131,132]
2,2,4-Trimethylpentane + carbon tetrachloride	6	303.15	34.817	0.2301	19.168	[131,132]
Benzene + n-hexane	11	298.15	23.108	-0.3511	19.381	[69]
Benzene + n-heptane	33	298.15-328.15	43.948	0.2868	16.586	[23,69,136,137]
Benzene + cyclohexane	56	298.15-333.15	25.030	0.0628	4.7114	[136,137]
Toluene + cyclohexane	65	298.15-328.15	33.309	0.0881	20.041	[98,130,136,137]
Toluene + benzene	22	298.15-313.15	36.041	0.0545	14.543	[136,137]
				Total AAD	17.204%	

*Note: the correlation (5.31) is not suitable for heavy alkanes. See Figure 4-7 for explanation.

Table 5.7b: Parameters and deviations of the concentration and temperature dependence of the diffusion coefficients for binary mixtures of polar components, with SRK EoS (MHV1-UNIFAC mixing rule), and predicted penetration volumes from Table 5.5c.

System (component 1 + component 2)	Data points	Temp. range (K)	Parameters for the penetration length		AAD (%)	References
			$A \cdot 10^{11}$, (m)	$B_{12} \cdot 10^{8}$, (m^3/mole)		
Non-polar + polar						
Acetone + benzene	33	298.15	33.876	0.0761	6.6975	[27,98]
Acetone + carbon tetrachloride	12	298.15-298.30	29.661	0.1430	24.014	[9,27]
Acetone + cumene	12	283.15-303.15	46.120	0.1762	20.674	[101]
Acetone + cyclohexane	11	298.15	30.189	0.2747	20.717	[155]
Methyl ethyl ketone + carbon tetrachloride	7	298.15	30.381	0.1099	24.336	[11]
Acetic acid + carbon tetrachloride	9	298.15	21.046	0.0773	21.600	[11]
Isobutyric acid + cumene	12	298.15-303.15	44.982	0.0280	17.745	[101]
Methanol + benzene	8	313.15	28.777	0.1387	25.792	[9]
Benzene + ethanol	17	298.30-313.13	31.474	0.1672	21.060	[9]
Methanol + carbon tetrachloride	12	293.15	17.873	0.0848	48.802	[135]
n-Propanol + carbon tetrachloride	12	293.15	13.488	0.0399	25.636	[135]
n-Butanol + carbon tetrachloride	12	293.15	15.755	0.0503	29.884	[135]
n-Propanol + toluene	15	298.15	24.712	0.1385	13.410	[135]
Polar + polar						
Diethyl ether + chloroform	8	298.15	31.428	-0.0714	8.5474	[10]
Acetone + chloroform	48	298.15-328.15	31.208	-0.0572	7.3643	[158]
Acetone + 1,2 dichlorobenzene	13	283.15-303.15	37.593	0.0954	14.070	[101]
Chloroform + acetic acid	28	298.15	26.567	0.0027	14.602	[163]
Acetic acid + 5-methyl-2-hexanone	19	283.15-303.15	29.861	0.0276	10.174	[101]
Acetic acid + methyl isobutyl ketone	20	283.15-303.15	29.495	0.0030	7.9281	[101]
Acetic acid + n-butyl acetate	18	283.15-303.15	28.908	0.0069	6.3103	[101]
Acetic acid + water	19	283.15-303.15	18.735	0.0106	32.576	[101]
Isobutyric acid + water	12	283.15-303.15	16.349	0.0288	58.689	[101]
Methyl isopropyl ketone + water	8	293.15-298.15	20.064	0.0105	29.422	[119]
Methanol + water	18	278.15-313.13	21.349	0.0104	26.967	[91]
Ethanol + water	70	313.15-358.15	16.739	0.0204	32.578	[158]
n-Butanol + water	37	298.15	27.435	0.0663	28.506	[119]
n,n-Dimethylformamide + water	12	278.15	28.476	0.0069	15.520	[63]
n-Methylpyrrolidone + water	12	278.15	360.95	0.0139	46.937	[63]
				Total AAD	22.877%	

5.3.1. Sensitivity of the Model

In this subsection we analyze why deviations from experimental data obtained on the basis of the model with fitted diffusion coefficients are significantly larger compared to deviations obtained on the basis of the "real" penetration lengths.

The diffusion coefficients demonstrate high sensitivity to slight variations of the penetration volumes with both exponential and quadratic dependence. The 2% error in the correlation of penetration volumes (Table 5.5c) results in an error of prediction of 12% (Table 5.6b). While in the case of exponential dependence the sensitivity is mainly due to the form of the dependence (Table 5.2), in the case of the quadratic dependence the reason is in the very small numerical value of the fraction of free volume ζ. This value varies between 0.05 and 0.15 for all the binary mixtures considered, depending on the concentration and temperature (as in Figure 5.9). Usually it is less than 0.1. Thus, a small absolute difference in the values of the penetration volumes results in high relative deviations of the penetration lengths and, therefore, of the diffusion coefficients.

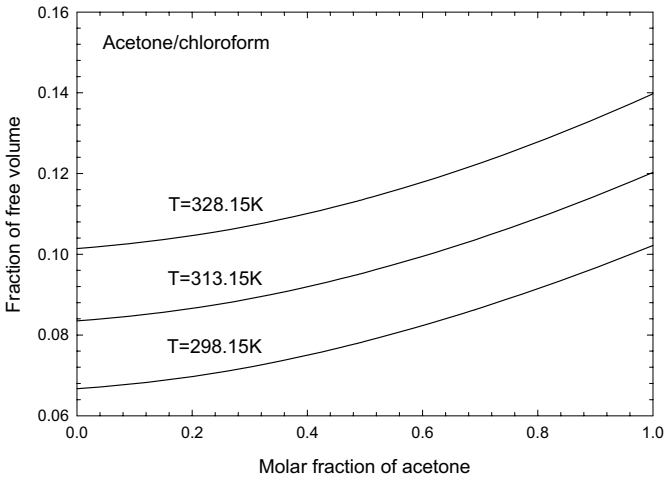

Figure 5.9: Concentration dependence of fraction of free volume ζ for the mixture acetone/chloroform. The penetration parameters are listed in Table 5-5c.

Typical values of ζ are in a good agreement with the usual behavior of the free volume in liquids. According to Wesselingh and Bollen [168], the free volume of less than 0.03 is characteristic of a glass. The values between 0.03 and 0.15 correspond to highly viscous fluids. Mobility of the fluids increases with increase of the free volume. It looks as if the fraction of free volume defined in the current study is lower than the values of the free volume defined from viscosities of the fluids. Figure 5.9 demonstrates that for the pure

chloroform at room temperature the fraction of free volume is around 0.06, which, according to [168], corresponds to a highly viscous fluid. The fact that the fraction of free volume is generally smaller than the free volume defined by Cohen [26] can be explained by the difference between the linear and the exponential probability distributions of the 'holes' (see Eq. (5.29) and (5.21)). Indeed, the linear probability distribution implies even distribution of the holes of all sizes, while according to exponential distribution the large holes are rare. A higher probability to meet a 'hole' large enough results in the smaller fraction of free volume needed for penetration. As a result, the quadratic dependence is also highly sensitive to the penetration parameters, but in a different way than the exponential dependence.

To the best of our knowledge, similar problems arise in other models for diffusion coefficients in liquids based on the free volume concept [168] and, more generally, in many problems related to the equilibrium and transport properties of the condensed phase [133], [94]. This does not seem to be an artificial problem of the chosen model, but the problem produced by the physics of the process considered. Indeed, the mechanism of diffusion in liquids may be described as squeezing of the molecules between other molecules, and the rate of such squeezing is strongly dependent on the actual amount of the empty space. In practical cases, there is always a compromise between better accuracy and better predictivity of the model.

5.4. Summary

The recently developed fluctuation theory for diffusion coefficients was tested on the description of experimental data for diffusion coefficients in binary mixtures of polar components. It was shown that with a proper expression for the penetration lengths the fluctuation theory is capable of describing the diffusion coefficients for both non-polar and polar substances. The choice of a thermodynamic model for a mixture being studied mainly affects the values of the adjusted penetration parameters, while the accuracy of description is not sensitive to the applied EoS.

The results of the model adjustment on the available sets of experimental data are presented. Generally, the developed model gives a very good approximation of the experimental data with four parameters. The absolute average deviation is usually within 2-5%, depending upon the mixtures studied, the expression for the penetration length and the thermodynamic model.

The diffusion coefficients, obtained on a basis of the exponential expression for penetration lengths are much more sensitive to the penetration volumes than to the penetration amplitudes, since the penetration volumes stay under the exponent. If only the multi-temperature data sets are considered, one observes a rather regular behavior of the

penetration volumes and penetration amplitudes as functions of the individual component properties (Table 5.1). Behavior of the penetration parameters for the mixtures where data for only one temperature are available is less regular.

The exponential penetration parameters are not individual properties of the components and no simple correlation between values of the parameters and individual physical properties of the components can be established. This fact, together with the high sensitivity of the diffusion coefficients upon the values of the penetration parameters makes it very difficult to propose a predictive equation for the exponential penetration parameters, capable of predicting diffusion coefficients with a reasonable degree of accuracy.

Application of the quadratic expression for penetration lengths results in penetration volumes exhibiting individual behavior which can be correlated with the co-volume parameters of an applied EoS. This reduces the number of independent penetration parameters to two parameters for strongly non-ideal binary mixtures and to only parameter for binary mixtures with a more regular behavior. Application of the individual values of the penetration volumes improves the prediction capabilities of the developed model and just slightly reduces the quality of description. However, experimental data on both the temperature and the concentration dependencies of diffusion coefficients is required to obtain individual values of the penetration volumes.

The penetration volumes can be predicted with a reasonable accuracy from the correlation with the b-parameters of the cubic equations of state. This makes it possible to interpret them as irreducible volumes, not available for molecular transport. However, direct application of the correlation of the penetration volumes from the co-volume parameters of the cubic EoS may produce high deviations in some cases. Despite a rather high accuracy of both averaging the individual penetration volumes (around 1.5%) and correlation of penetration volumes (around 2-2.5%) the reduction of the number of independent penetration parameters results in a significant increase of the error. This is due to high sensitivity of the values of the diffusion coefficients to the space available for free molecular motion.

The analysis of the sources of error demonstrates that the main reason is in a very low value of the fraction of the free volume available for penetration in liquid mixtures. The problem of high sensitivity on the volumetric properties occurs in many transport and thermodynamic properties in the condensed liquid state.

Additional research will be required to predict diffusion coefficients by phenomenological methods with a reasonable accuracy.

6. Molecular Dynamics Simulations of Penetration Lengths

As it was shown in the previous chapter the penetration lengths can be directly extracted from the experimental data available on the diffusion coefficients. Comparison of the penetration lengths computed in this way with those obtained by MD simulations and comparison of diffusion coefficients obtained by substitution of the penetration lengths from the MD simulations in the FT expressions can serve as a good validation test for the fluctuation theory and FT approach. If successful, this may provide a predictive method for evaluation of diffusion coefficients. Such a combination of macro- and micro-considerations has proven to be fruitful with regard to diffusion [45].

The goal of the current chapter is to investigate the concept of a penetration length at the microlevel and to develop evaluation of penetration lengths by molecular dynamics simulations. This will make it possible to predict the mutual diffusion coefficients by application of the coupled FT and MD approaches. Such an approach may become an alternative to the discussed phenomenological approach (Chapter 5).

Only initial verification of the approach is considered here. Therefore, the simplest possible assumptions about the modeled mixtures are applied: a cubic equation of state (although with advanced mixing rules) for thermodynamic modeling, and the Lennard-Jones potential as a model for microscopic interactions between the molecules in the mixtures. In view of the simplicity of the models, high precision in correlation of the experimental data cannot be expected. However, the modeling is fully predictive, and the simplicity of the models makes it possible to avoid artifacts, which might arise if more complex models would be applied. Even with such simple models, a surprisingly good agreement with experimental data is demonstrated. Perfection of the approach and application of more sophisticated models are subjects of future work.

All the quantities defined with respect to the MD simulations in this chapter correspond to the quantities averaged over all the particles in a system and over the whole time of a simulation.

6.1. Theoretical Background

The penetration length was defined in [143, 144] as an average traveling distance, after which a molecule having an initial x-component of the velocity “forgets” its initial velocity. It was also shown in [143, 144] that the penetration length Z_i can be defined as a product of a given distance h along the x-axis and an average probability that a particle of a species i will cross a plane at a distance h instead of coming back to the initial plane.

These two original definitions lead to two different possible schemes for computation of the penetration lengths by molecular dynamics: the velocity autocorrelation (VA) and the probability (P) approaches.

The essence of the VA approach is to compute an average distance along a direction which a particle has covered, while its velocity autocorrelation function, along the same direction, is essentially non-zero. The probability (P) approach is based upon the definition of a probability Λ_i that a particle of species i crosses a plane at a given distance h before coming back to the initial plane. The product of the average probability Λ_i by h is equal to the penetration length.

6.1.1. The Velocity Autocorrelation Approach

In the VA approach, the average penetration length is expressed in the following way:

$$Z_i = \left| r_{x_i}\left(t_{corr.} + t_0\right) - r_{x_i}\left(t_0\right) \right|. \tag{6.1}$$

Here t_0 is the initial time and t_{corr} is the velocity autocorrelation time along the x-direction, which is determined from the relation:

$$\left\langle u_{x_i}\left(t_{corr} + t_0\right) u_{x_i}\left(t_0\right) \right\rangle = 0. \tag{6.2}$$

If the system is perfectly isotropic, which is the case in the simulations here, the velocity autocorrelation functions along x-, y- and z- directions are equal. Hence the velocity autocorrelation times are, on average, equal for the three directions. This conclusion was directly confirmed by the simulations.

In view of isotropy, the following relation was applied to estimate t_{corr}:

$$\left\langle \mathbf{u}_i\left(t_{corr} + t_0\right) \mathbf{u}_i\left(t_0\right) \right\rangle = 0, \tag{6.3}$$

which significantly improves the statistical evaluation of the velocity autocorrelation time. An additional consequence of isotropy is:

$$\left| r_{x_i}\left(t_{corr} + t_0\right) - r_{x_i}\left(t_0\right) \right| = \left| r_{y_i}\left(t_{corr} + t_0\right) - r_{y_i}\left(t_0\right) \right| = \left| r_{z_i}\left(t_{corr} + t_0\right) - r_{z_i}\left(t_0\right) \right|. \tag{6.4}$$

Thus, to improve the statistics, an average penetration length was computed as follows:

$$Z_i = \frac{1}{3}\left(\left| r_{x_i}\left(t_{corr} + t_0\right) - r_{x_i}\left(t_0\right) \right| + \left| r_{y_i}\left(t_{corr} + t_0\right) - r_{y_i}\left(t_0\right) \right| + \left| r_{z_i}\left(t_{corr} + t_0\right) - r_{z_i}\left(t_0\right) \right| \right). \tag{6.5}$$

It should be stressed that the length expressed by Eq. (6.5) is not equal to the following expression:

$$\left| \mathbf{r}_i\left(t_{corr} + t_0\right) - \mathbf{r}_i\left(t_0\right) \right| / \sqrt{3}, \tag{6.6}$$

since in the last expression the quadratic mean is used instead of the linear average in Eq.(6.5).

6.1.2. The Probability Approach

As stated above, in this approach the penetration length is proportional to the average probability Λ_i that a particle crosses a plane at a distance h earlier than it comes back:

$$Z_i = \Lambda_i \times h . \tag{6.7}$$

Computations show that Eq.(6.7) should be understood asymptotically: If $h>Z_i$, then the measured probabilities Λ_i progressively increase with h towards asymptotic values. Checking the convergence may be problematic, due to possible statistical errors. To reduce this problem, we introduced an additional plane at the distance $-l$ (Figure 6.1) and counted the number of particles coming back to that plane, instead of the particles which come back to the "zero level". This has improved the statistical evaluation of the probability Λ_i and, therefore, of the penetration length Z_i. According to the concept of [143], the probability that a particle crosses a plane at a distance h instead of crossing a plane at a distance $-l$ is:

$$\Lambda_i = \frac{Z_i + l}{h + l} . \tag{6.8}$$

To compute Λ_i, the numbers of particles crossing the plane at the distance h and the plane at the distance $-l$ were computed. Then the probability was estimated by the following expression:

$$\Lambda_i = \frac{N_{d_x^i > h}}{N_{d_x^i < -l} + N_{d_x^i > h}} , \tag{6.9}$$

where

$$d_x^i = \lim_{t \to \infty} \left[\left(r_{x_i}(t + t_0) - r_{x_i}(t_0) \right) \times sign\left(v_{x_i} \right) \right]. \tag{6.10}$$

If the simulation time is long enough, then probabilities defined in Eq.(6.9) should converge on Λ_i. The final result should be independent of both distances l and h. The computations have shown, however, that the penetration lengths computed in this way are dependent on l, and only the approach with $l=0$ is applicable. A more detailed analysis and explanation of this fact will be presented below.

Similarly to the VA approach, the statistical evaluation may be improved by using isotropy of the system:

$$\Lambda_i = \frac{N_{d_x^i > h} + N_{d_y^i > h} + N_{d_z^i > h}}{N_{d_x^i < -l} + N_{d_x^i > h} + N_{d_y^i < -l} + N_{d_y^i > h} + N_{d_z^i < -l} + N_{d_z^i > h}} . \tag{6.11}$$

Then, on average:

$$Z_i = \Lambda_i \times (h + l) - l . \tag{6.12}$$

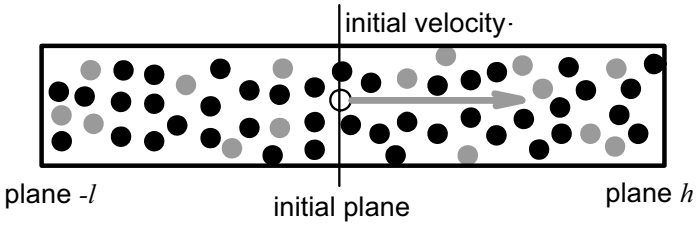

Figure 6.1: Illustration of the probability approach to estimate penetration lengths

6.2. Details of Computations

6.2.1. Phenomenological Approach

The phenomenological model based on fluctuation theory for diffusion coefficients was described in the previous chapter. In the current chapter we make use of results for a few relatively simple binary mixtures of non-polar components: cyclohexane/carbon tetrachloride, cyclohexane/toluene, benzene/toluene and benzene/heptane. Experimental values of the Fick diffusion coefficients for the listed mixtures are reported in [136] and [137]. The experimental diffusion coefficients were described by application of the quadratic expression for the penetration lengths. The thermodynamic factor was computed using the Soave-Redlich-Kwong equation of state with the modified Huron-Vidal (Version 1, MHV1) mixing rules, based upon the UNIFAC activity coefficient model [103]. The binary interaction parameters were set to zero.

The resulting average absolute deviations of description for these mixtures, as well as the values of the adjusted penetration parameters have been already presented in the previous chapter. For convenience, they are repeated in Table 6.1.

Table 6.1: Penetration parameters, extracted from experimental data, and the accuracy of the description of the experimental diffusion coefficients by the FT model with the quadratic expression for the penetration lengths.

Mixture (comp.1 + comp.2)	Parameters for the penetration length				AAD (%)
	$A \cdot 10^{11}$, (m)	$B_1 \cdot 10^4$, (m^3/mole)	$B_2 \cdot 10^4$, (m^3/mole)	$B_{12} \cdot 10^8$, (m^3/mole)	
Cyclohexane + carbon tetrachloride	25.432	1.0872	0.9896	0.0067	1.2896
Benzene + n-heptane	31.659	0.9211	1.4597	0.2651	3.4449
Toluene + cyclohexane	32.588	1.1058	1.1146	0.0348	2.6735
Toluene + benzene	36.983	1.1191	0.9323	0.0167	1.2341

6.2.2. Molecular Dynamics Approach

This work is focused on testing the capability of the approach to estimate penetration lengths. A simple MD computer code was used in the simulations. The molecules of the mixture were represented as spheres. Their interactions were modeled by a classical effective Lennard-Jones (LJ) 12-6 potential:

$$U_{ij} = 4\varepsilon_{ij}\left(\left(\frac{\sigma_{ij}}{r_{ij}}\right)^{12} - \left(\frac{\sigma_{ij}}{r_{ij}}\right)^{6}\right), \tag{6.13}$$

where ε_{ij} is the potential strength, σ_{ij} is the atomic diameter and r_{ij} is the intermolecular separation. The cutoff radius was taken to be equal to 2.5 [50].

This simple model has shown to provide good results for thermodynamic properties in pure fluids and in mixtures [152] and for dynamic properties such as mass diffusion [175] or viscosity [174]. Nevertheless, in liquid phase, the results can be very sensitive to molecular parameters, especially to the atomic diameters. For instance, in a liquid phase, an increase of σ_{ij} by 0.5% leads to an increase of the viscosity and decrease of the self-diffusion coefficient by approximately 10% [94, 133]. This fact is also in a good agreement with the previously observed sensitivity of the diffusion coefficients on the values of the penetration volumes (Chapter 5).

To find the parameters of the Lennard-Jones potentials for mixtures, we have used the classical Lorentz-Berthelot (LB) combining rules, which provide satisfactory results for the mixtures of not too different components:

$$\begin{aligned} \sigma_{ij} &= \left(\frac{\sigma_i + \sigma_j}{2}\right), \\ \varepsilon_{ij} &= \left(\varepsilon_i \varepsilon_j\right)^{1/2}. \end{aligned} \tag{6.14}$$

The diffusion coefficients are sensitive to the cross parameters. In some cases the LB combining rules do not give good values of the cross parameters [149]. Two other combining rules which provide better results for static properties [35] were tested. These combining rules are from Kong (KG) [83] and Waldman and Hagler (WH) [164]. Each mixing rule contains two relations for the potential strength and for the atomic diameter. The first relation is the same for both rules:

$$\varepsilon_{ij}\sigma_{ij}^{6} = \left(\varepsilon_{ii}\sigma_{ii}^{6}\varepsilon_{jj}\sigma_{jj}^{6}\right)^{1/2}. \tag{6.15}$$

The second relation for the WH approach is:

$$\sigma_{ij} = \left(\frac{\sigma_{ii}^{6} + \sigma_{jj}^{6}}{2}\right)^{1/6}, \tag{6.16}$$

and for the KG model it is:

$$\varepsilon_{ij}\sigma_{ij}^{12} = \frac{\varepsilon_{ii}\sigma_{ii}^{12}}{2^{13}}\left[1+\left(\frac{\varepsilon_{jj}\sigma_{jj}^{12}}{\varepsilon_{ii}\sigma_{ii}^{12}}\right)^{1/13}\right]^{13}. \qquad (6.17)$$

The influence of the mixing rules upon the estimation of the penetration lengths was investigated. The results of such tests are considered below.

6.3. Preliminary Test of the Model

6.3.1. Velocity Autocorrelation Approach

To carry out preliminary tests of the model, an equimolar benzene/toluene mixture at T=313.15 K and P=1 atm was considered. The mutual diffusion coefficient and the density of this mixture were studied experimentally in [136] and [137].

The simulations were performed in the NVT ensemble. A system consisting of 1500 particles was simulated. The reduced time step of the calculation in real units was equal to 2.555 fs. The sensitivity to the number of simulated particles and the value of the time step is discussed in the following sections.

It was found that the velocity correlation time for the selected mixture is 296 fs for benzene and 319 fs for toluene. Thus, the velocity autocorrelation time, defined by Eq.(6.3), is extremely short in liquids under selected thermodynamic conditions, corresponding to a rather dense system.

After a transient state, the two penetration lengths computed by Eq.(6.5) converge towards finite values. These values were found to be 0.3667±0.1%Å for benzene and 0.3631±0.1%Å for toluene. The penetration lengths, deduced from the experimental results [136] in the previous chapter are 0.3806Å for benzene and 0.4133Å for toluene in the corresponding equimolar mixture. Thus, molecular simulations slightly underestimate the penetration lengths obtained in the framework of the FT model.

Convergence of the penetration lengths towards final values is extremely fast due to very small values of t_{corr}. After only 1000 time steps, the computed values are within 2% of the final values. The observed time of convergence is much shorter than the time required for proper estimation of the mutual diffusion coefficients in classical MD schemes.

In conclusion, the penetration lengths computed by the VA approach converge quickly and are consistent with those deduced from experiments by the FT model, with a deviation of 4% and 14% for benzene and toluene respectively.

6.3.2. Probability Approach

In this approach, simulations have been carried out during four million time steps.

The penetration lengths were computed for various plane distances h by application of Eq. (6.11). Moreover, in order to evaluate the validity of this relation, cases with different values of l (Figure 6.1) were tested as well.

If distance h is much larger than the value of the penetration length, then the penetration length should be independent of the choice of plane distance h [143]. The simulations only partly confirm this statement. The dependence of penetration lengths upon the distance h is rather strong, although for high values of h the penetration lengths seem to converge to those predicted by the VA method. More precisely, the values obtained for h=8Å are slightly lower than the VA values. This can possibly be explained by bad convergence or numerical problems. Another possible explanation is the so-called “cage effect”, according to which the velocity correlation between the molecules in liquids at certain distances from each other may become negative [20].

The value of the l distance also has a strong influence on the computed penetration lengths. Therefore, improvement of the statistics by introducing the additional plane at the distance $-l$ cannot be achieved [51].

The dependence of the penetration length upon the value of l can possibly be explained as follows. There are many particles which, starting from plane 0, go back immediately after the first collision. Such particles have “negative penetration lengths”. When the initial plane is located at zero, but not $-l$, the particles with only positive penetration lengths are counted in the statistics, while the remaining particles make a zero contribution. In other words, we do not have a reflecting, but an absorbing boundary at zero. However, if this boundary moves to $-l$, some of these particles start contributing to the statistics. This may also partly serve as an explanation for the influence of h (which is also an absorbing boundary) on the values of the penetration lengths, which disappears only asymptotically.

It may be concluded that both methods are able to provide mutually consistent results. However, the VA method provides a much faster and more reliable way for obtaining the penetration lengths. The probability approach can in some cases provide wrong evaluation of the lengths. It is more affected by fluctuations and requires much larger computational times to reach convergence. Therefore the VA method is applied in further MD simulations.

Influence of the numerical parameters and mixing rules

As shown in [149] the combining rules used to define cross-molecular parameters can affect the evaluation of mutual diffusion coefficients. It may be expected that these rules affect the penetration lengths as well. However, since the mixtures which are studied here are composed of not too dissimilar molecules, the influence of the combining rules is expected to be insignificant.

The study of the effect of the combining rules was carried out for the same mixture, benzene/toluene, as previously, but for three different concentrations. Various mixing rules defined by Eqs. (6.14) to Eq. (6.17) were applied.

As expected, the results of the simulation have demonstrated that in this mixture the values of penetration lengths are not much affected by the combining rules. The difference reaches at most 0.35% for an equimolar mixture. So, even if the evaluation of the mutual diffusion coefficients is very sensitive to the penetration lengths, it can be assumed that for the tested mixture the choice of the combining rules does not strongly affect the results [51].

The classical Lorenz-Berthelot combining rules were applied for the following calculations.

6.4. Results

Based on the results of the previous section, all the MD simulations were performed on for a 1500-particle system with a 2.555 fs time step with two millions time steps, and using the LB combining rules. The penetration lengths were computed by the VA approach.

Four binary mixtures of non-polar components were analyzed: cyclohexane/carbon tetrachloride, cyclohexane/toluene, benzene/toluene and benzene/heptane. The molecules for such mixtures allow for simple modeling as spherical LJ particles [94, 175].

The molar fraction and temperature dependencies of the penetration lengths for the four mixtures were computed in the MD simulations. Computations were carried out for two temperatures, 298.15 K and 313.15 K, and for five molar fractions at each temperature. The computed dependencies were fitted by the quadratic expression for the penetration lengths and introduced into the FT model for the diffusion coefficients. The obtained diffusion coefficients obtained were compared to the experimental data. Additionally, the penetration lengths extracted by fitting the FT diffusion coefficients from the experimental data were compared with the penetration lengths obtained directly by the MD simulations.

The last comparison is shown in Figures 6.2 and 6.3. It is seen that the orders of magnitude of the values computed by the MD simulations are consistent with the FT penetration lengths. Moreover, general trends of concentration and temperature are consistent as well. Nevertheless, there are non-negligible differences between these values. For all the investigated mixtures, the penetration lengths obtained by the MD simulations vary less with composition than the FT penetration lengths. Also, at constant molar fractions the MD penetration lengths are less temperature dependent than the FT ones. (It might seem that quadratic dependence for penetration lengths is temperature independent, however, since the expression for penetration lengths is expressed in terms of the molar densities, the penetration lengths are implicitly temperature dependent due to the temperature dependence of the molar volume).

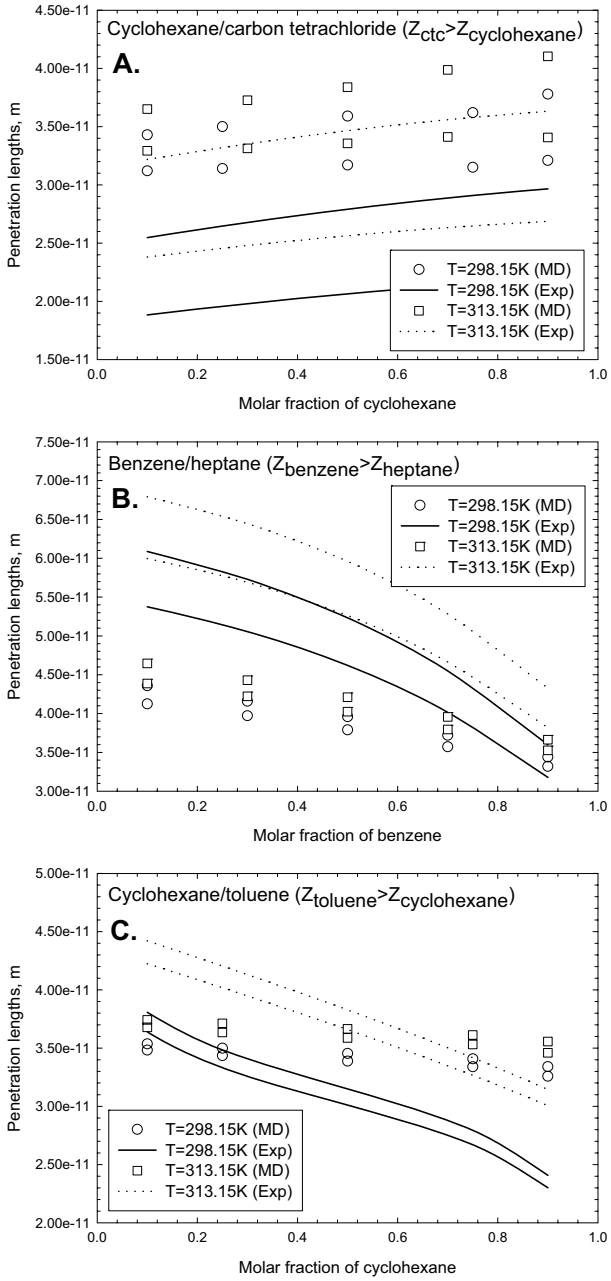

Figure 6.2: Penetration lengths computed by MD compared with those, obtained from modeling experimental data by the FTCode. Figure A: [136, 137]; figure B: [136]; figure C: [136, 137].

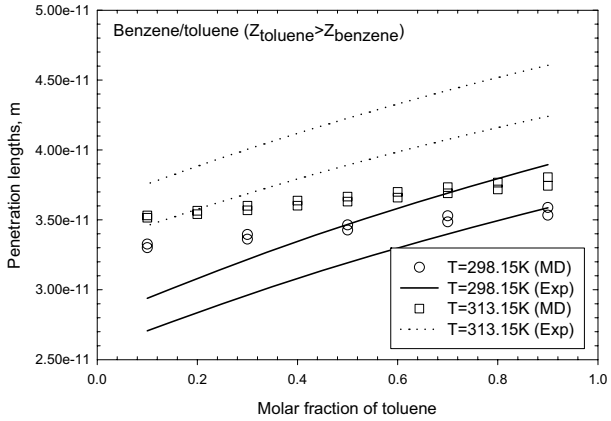

Figure 6.3: Penetration lengths computed by MD compared with those, obtained from modeling experimental data by the FTCode for the mixture of benzene/toluene [136].

Concerning the relative values of the penetration lengths of the individual compounds, it can be noticed that, typically, the heavier and the smaller a particle is, the larger its penetration length is. This trend is physically reasonable.

Comparison of the penetration lengths for the two mixtures, cyclohexane/toluene and benzene/toluene, demonstrates good qualitative and quantitative agreement of the FT and the MD approaches, especially in the dilute limits. For the mixture benzene/heptane essential disagreement is observed only at the dilute solution limit close to pure heptane, while for the mixture cyclohexane/carbon tetrachloride systematic disagreement is observed over the whole concentration range. A less accurate description of pure heptane is to be expected, since this relatively long linear molecule cannot be adequately modeled by the simple LJ model described here. However, the disagreement in descriptions of such a simple symmetric molecule as carbon tetrachloride cannot be explained by the fact that the molecular hard-sphere volume is neglected in the LJ model. Here we must assume that fitting the molecular parameters to the viscosity data is insufficient for diffusion modeling with regard to this particular substance.

The penetration lengths obtained by the MD simulations were used for computation of the mutual diffusion coefficients within the FT framework. A comparison of the experimental values of the mutual Fick diffusion coefficients and the values estimated by the coupled FT theory with the MD simulated penetration lengths is presented in Figures 6.4 to 6.5. The computed values of the Fickian diffusion coefficients are pure predictions, since the only adjustment that was carried out was tuning the LJ potential parameters to the viscosity data of pure components. The values of the diffusion coefficients predicted from the coupled MD-FT scheme are consistent with the experimental values. The deviations are around 20% for

the mixtures of benzene/heptane and cyclohexane/carbon tetrachloride and around 10% for the mixtures of cyclohexane/toluene and benzene/toluene.

Apart from the benzene/heptane mixture, the tendencies of the diffusion coefficients with mole fraction and temperature are in agreement with the experiments, although, generally, the predicted diffusion coefficients vary less with temperature and mole fraction than the experimental coefficients.

All in all, a fairly satisfactory agreement between the FT, MD approaches and the experimental data was observed (taking into account the roughness of the approximation). Let us discuss in more detail the reasons for the discrepancies between the approaches.

The first reason has to do with the intrinsic weakness of the simple LJ sphere description to handle the mass diffusion process correctly. The sizes and shapes of the molecules (especially, of long linear ones) can strongly influence the rate of penetration and, therefore, the diffusion.

The second reason is connected with the manner of describing cross interactions in MD simulations. The choice of mixing/combining rules acts on thermodynamic and dynamic properties. We demonstrated, however, that this choice should be of no importance to the mixtures considered, since application of different combining rules has resulted in deviations of less than one percent in the values of the penetration lengths.

The third reason is connected with the way the optimum penetration lengths are deduced from the experiments. The optimum penetration lengths are linked to the chosen equation of state for a mixture, which determines the thermodynamic matrix and the thermodynamic factors. Almost all the existing thermodynamic models (including that used in the present study) are fitted to predict phase equilibria, but can exhibit large deviations when applied to prediction of the thermodynamic properties. This imperfection of the models can contribute to the errors in the penetration lengths. Another source of errors is that the LJ mixtures used in molecular dynamics simulations do not obey the same equation of state as applied in the FT computations. As shown in [77], the thermodynamic behavior of the LJ mixtures cannot be properly represented by a cubic EoS.

If the considerations above are taken into account, it can be concluded that the observed discrepancies between the FT and the MD approaches are to be expected and are physically reasonable. Even with these discrepancies, the developed MD-FT approach is of acceptable accuracy for most of the studied cases. Therefore, it can be recommended for practical applications in cases where experimental information on the diffusion coefficients is missing or insufficient.

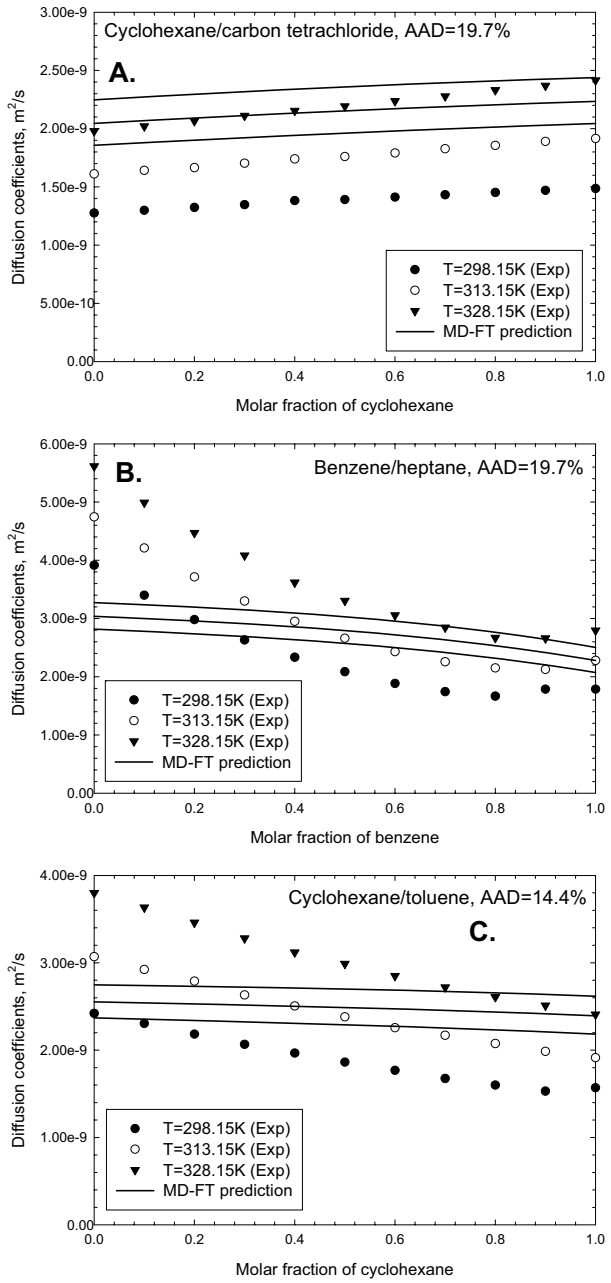

Figure 6.4: Experimental values of mutual diffusion coefficients compared with values predicted by MD simulations, coupled with the FT approach.

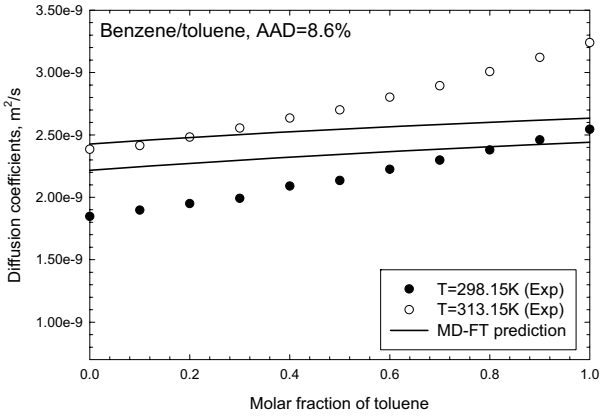

Figure 6.5: Experimental values of mutual diffusion coefficients compared with values predicted by MD simulations, coupled with the FT approach.

6.5. Summary

This chapter provides a scheme for computation of the penetration lengths in liquid mixtures based on the MD simulations. This makes it possible to verify the applicability of the fluctuation theory developed in [143] and [144] and developed in the previous chapter for prediction of diffusion coefficients in non-ideal binary mixtures, and to combine this approach with molecular dynamics simulations.

The results presented have shown that MD simulations are capable of providing consistent penetration lengths in liquid mixtures. The predicted values of diffusion coefficients for four different mixtures based on the coupled FT-MD scheme are in agreement with experiments, with typical average deviations of 10 to 20%. The computed results exhibit less pronounced temperature and concentration dependencies of the diffusion coefficients and the penetration lengths, than those deduced from the experiments, which can be explained by the roughness of the proposed approach: the combination of the cubic equations of state (although with advanced mixing rules) with a simple LJ model of the mixture.

Apart from the clear theoretical interest of the current study in verification of both FT and MD approaches, the suggested method for evaluation of the diffusion coefficients is quick and simple to implement and therefore requires much less computation time than other MD approaches, which are commonly applied to computation of mutual diffusion coefficients.

7. Diffusion Coefficients in Ternary Mixtures

Diffusion in an n-component mixture is determined by $n\cdot(n\text{-}1)/2$ independent coefficients, by the number of interactions between individual fluxes of different components. This large amount of possible interactions makes it difficult to provide exact description of diffusion. While the theory of diffusion mass transfer is well developed, the values of the diffusion coefficients in realistic multicomponent mixtures remain a problem.

Several models for the diffusion coefficients in multicomponent mixtures can be found in the literature [75, 87, 120, 134]. However, as they are mainly based on empirical considerations, their extrapolation and predictive capabilities are limited. Experimental determination of the diffusion coefficients in multicomponent mixtures is difficult. To the best of our knowledge, there are only few studies, where data on diffusivities in ternary mixtures are reported, and only one study of diffusivities in a quaternary mixture [121]. The current chapter mainly discusses modeling of ternary diffusion coefficients. However, the considerations presented can easily be extended to the multicomponent case. A procedure facilitating the analysis of the available experimental information on ternary diffusivities is presented. Then the existing empirical models for modeling of mutual diffusion coefficients in the ternary mixtures are discussed. The possibility of application of fluctuation theory to estimate diffusion coefficients is also discussed.

7.1. Analyzing Ternary Diffusion Coefficients

As was discussed in Chapter 3, the accuracy of measuring ternary diffusion coefficients is (in most cases) close to the accuracy for binary diffusion coefficients. However, the cross-terms in the matrix of ternary diffusivities are usually several times smaller than the main terms. If the cross diffusion coefficients are very small, multicomponent diffusion may be treated as several independent binary processes. However, this is not always the case. For most non-electrolyte systems and for almost all electrolyte systems cross-term diffusivities are around 20-30% of the main-term diffusivities [32, 134]. In such cases the effect of the cross diffusion can be significant compared to the main (principal) diffusion. Moreover, it is well known that the values of the Fick diffusion coefficients in ternary mixtures significantly depend upon the choice of the solvent [108, 169]. Hence, it is necessary to properly model the cross-term diffusion coefficients.

A common set of measured diffusion coefficients for a three-component mixture consists of four Fickian diffusion coefficients, each being reported separately. However, the Onsager theory predicts the existence of only three independent coefficients, as one of them disappears due to the symmetry requirement. Transforming the Fickian diffusion coefficients into Onsager coefficients for a non-ideal mixture involves derivatives of the chemical

potentials and, thus, should be based on a certain thermodynamic model (cubic equation of state, an activity coefficient model, etc.). Transformation of the Fickian diffusion coefficients into Onsager coefficients and a subsequent symmetry check make it possible to evaluate different thermodynamic models with regard to their possibility of being used to predict of the transport properties. Moreover, it allows verification of experimental information and a reduction of the number of the independent diffusion coefficients required in ternary mixtures.

In this section we will apply the Onsager reciprocal relations to verify the available experimental data on diffusion coefficients and thermodynamic models for multicomponent mixtures. A few similar studies were reported previously [105, 106] with simplified assumptions about the thermodynamics of the mixtures under study. In the current section the symmetry of the Onsager coefficients is verified for more experiments applying modern models and computational tools of equilibrium thermodynamics.

7.1.1. Theoretical Background

As was discussed in the Chapter 2, the matrix of Fickian multicomponent diffusion coefficients is not necessarily symmetric:

$$D_{ij} \neq D_{ji}. \tag{7.1}$$

Hence, in the Fickian approach diffusion in n-component mixture is determined by $(n\text{-}1)^2$ diffusion coefficients, which gives four coefficients for a ternary mixture.

As was proven by Onsager [116] and extended to continuous systems by Casimir [25], the phenomenological Onsager coefficients L_{ik} form a symmetric matrix:

$$L_{ik} = L_{ki}. \tag{7.2}$$

We will apply the system of thermodynamic coordinates, which was already considered in Chapter 2:

$$\begin{aligned} &\mathbf{I} = \mathbf{L}\nabla\boldsymbol{\mu}/z_n T, \\ &I_i = z_n J_i - z_i J_n \left(i = 1,\ldots,n-1\right). \end{aligned} \tag{7.3}$$

The connection between the usual Fick diffusion flux and relative flux, defined in Eq. (7.3) is the following [142]:

$$\mathbf{J} = \mathbf{A}\mathbf{I}, \tag{7.4}$$

where the transformation matrix is defined as follows:

$$\mathbf{A} = \frac{1}{z_n}\begin{bmatrix} 1-z_1 & -z_1 & \ldots & -z_1 \\ -z_2 & 1-z_2 & \ldots & -z_2 \\ \vdots & \vdots & \ddots & \vdots \\ -z_{n-1} & -z_{n-1} & \ldots & 1-z_{n-1} \end{bmatrix}. \tag{7.5}$$

Thus, the connection between Fickian diffusion coefficients and phenomenological coefficients for the chosen system of thermodynamic variables (Eq. (7.3)) is:

$$\mathbf{D} = \frac{1}{z_n T}\mathbf{A}\mathbf{L}\frac{\partial \boldsymbol{\mu}}{\partial \mathbf{c}} = \frac{1}{z_n nT}\mathbf{A}\mathbf{L}\frac{\partial \boldsymbol{\mu}}{\partial \mathbf{z}}. \tag{7.6}$$

By expanding Eq. (7.6) for the ternary mixtures, the following system of linear equations can be obtained:

$$\left.\begin{aligned}
D_{11} &= \frac{1}{z_n^2 nT}\left[\left(L_{11}\frac{\partial \mu_1}{\partial z_1} + L_{12}\frac{\partial \mu_2}{\partial z_1}\right)(1-z_1) - z_1\left(L_{21}\frac{\partial \mu_1}{\partial z_1} + L_{22}\frac{\partial \mu_2}{\partial z_1}\right)\right] \\
D_{12} &= \frac{1}{z_n^2 nT}\left[\left(L_{11}\frac{\partial \mu_1}{\partial z_2} + L_{12}\frac{\partial \mu_2}{\partial z_2}\right)(1-z_1) - z_1\left(L_{21}\frac{\partial \mu_1}{\partial z_2} + L_{22}\frac{\partial \mu_2}{\partial z_2}\right)\right] \\
D_{21} &= \frac{1}{z_n^2 nT}\left[-z_2\left(L_{11}\frac{\partial \mu_1}{\partial z_1} + L_{12}\frac{\partial \mu_2}{\partial z_1}\right) + (1-z_2)\left(L_{21}\frac{\partial \mu_1}{\partial z_1} + L_{22}\frac{\partial \mu_2}{\partial z_1}\right)\right] \\
D_{22} &= \frac{1}{z_n^2 nT}\left[-z_2\left(L_{11}\frac{\partial \mu_1}{\partial z_2} + L_{12}\frac{\partial \mu_2}{\partial z_2}\right) + (1-z_2)\left(L_{21}\frac{\partial \mu_1}{\partial z_2} + L_{22}\frac{\partial \mu_2}{\partial z_2}\right)\right]
\end{aligned}\right\}. \tag{7.7}$$

The system of equations, Eq.(7.7), provides a connection between the experimentally measured matrix of Fickian coefficients and the matrix of phenomenological coefficients. Solving this system with regard to L_{ij} should, in principle, give equal values of L_{12} and L_{21}. The values found are not normally equal due to two kinds of errors: imprecision of the measured values of D_{ij} and the approximation introduced by a thermodynamic model for the chemical potential μ. The discrepancies between L_{21} and L_{12} are analyzed in the following. The error of estimation of the number of moles n does not influence the equality (7.2), so that the accuracy of a thermodynamic model with regard to prediction of the molar density cannot be checked.

7.1.2. Details of Computations

Experimental data

The experimental methods and available data for ternary diffusion coefficients were analyzed in Chapter 3. We analysed data on ternary diffusion in non-electrolyte mixtures, reported in the following studies: [6, 21, 27, 79, 114, 148] and [159]. Analysis of the diffusion in electrolytes requires specific thermodynamic modelling, and will not be considered here.

The data, presented in studies [21], [148] and [27] was obtained by a modified diaphragm cell method. The authors of all the three works used the same four diaphragm cells calibrated on the same experimental data. Diffusion coefficients in the following systems were measured: toluene-chlorobenzene-bromobenzene, methanol-propanol-isobutanol and acetone-benzene-carbon tetrachloride.

The optical diffusiometer technique was used by the authors of [79] for measuring the diffusion coefficients in the ternary mixture of dodecane-hexadecane-hexane.

The authors of [6] used the birefringent interferometric technique for measuring the diffusion coefficients in the ternary mixture of acetone-benzene-methanol. Measurements for the ternary system acetone-benzene-carbon tetrachloride were also carried out and compared with the measurements performed in [27].

The rotating diaphragm cell technique was used for the study of the temperature dependence of multicomponent isothermal diffusion coefficients of the system 2,2-dichloropropane - 1,1,1-trichloroethane - carbon tetrachloride [114].

The chromatographic method was applied for the determination of the ternary Fickian diffusion coefficients in [159]. The method is similar to the Taylor dispersion method described in Chapter 3. An experimental setup contains a cycle with a long capillary tube connected by one side to the chromatograph, capable of measuring the composition. There is a constant laminar flow of one of the components of the ternary mixture through this tube. At a certain moment a small sample of the binary mixture is injected into the flowing third component. A problem for such an experimental technique is that it is only possible to measure the composition of the injected binary mixture, while the fraction of the third flowing component remains unknown [159]. The procedure developed here makes it possible to determine the unknown fraction of the third component by minimizing the difference between the Onsager cross-coefficients.

Thermodynamic models

Thermodynamic modelling required for transformation of the Fick diffusion coefficients into the Onsager coefficients is simpler than that described in Chapter 5, describing application of the FT approach, since the only thermodynamic property required is the compositional derivative of the chemical potential.

Different thermodynamic models are available for each of the mixtures studied experimentally. In the present work, we apply the following models:

- *UNIFAC.* The UNIFAC model [33, 120] was applied to prediction of the activity coefficients for all the mixtures considered.
- *Cubic Plus Association (CPA) or SRK*. The CPA model is a combination of a cubic EoS and an additional term, developed for associating fluids. We used this term for the systems with alcohols [173]. In other cases the CPA was reduced to the common Soave–Redlich–Kwong EoS. The binary interaction parameters for the CPA/SRK model were obtained by regression of the experimental binary VLE and LLE data [85].

- *PC-SAFT.* The perturbed-chain statistical associating fluid theory (PC-SAFT) [62] was used for the system of the alkanes, as well as for the system of toluene-chlorobenzene-bromobenzene. Application of this model is limited by the availability of the necessary parameters.

The computations on the basis of the models described have been carried out by application of computer code developed in the IVC-SEP Center, Technical University of Denmark. The computational part of the in-house software SPECS has been re-developed and adjusted for the modelling.

The result of all computations was formulated, in terms of the deviation from symmetry, d, determined as:

$$d(\%) = \frac{L_{12} - L_{21}}{L_{12}} \times 100$$

7.1.3. Results and Discussion

The equality of cross-coefficients in the systems containing associating fluids is verified by application of the UNIFAC and the CPA models (Figure 7.1). Both models perform similarly. In terms of absolute deviations from symmetry, the system of alcohols is modeled slightly better by the UNIFAC model, while the CPA EoS shows better results for the strongly non-ideal system of acetone-benzene-methanol (Figure 7.1b). However, the character of deviations for this system may be interpreted in such a way that the measurements contain a systematic experimental error. This can especially be seen from the character of the deviations shown by the UNIFAC model, which generally produces more uniform results than the CPA model.

A single available experimental point for the ternary mixture of alkanes [79] was simulated using three different thermodynamic models: UNIFAC, SRK and PC-SAFT (Figure 6-2a). The UNIFAC model shows slightly better results, while the SRK and the PC-SAFT models perform similarly. The two percent deviation for the best model confirms the consistency of the experimental points. The same models were applied to the system of toluene-chlorobenzene-bromobenzene (Figure 7.2b). As for the previous system, application of the UNIFAC model provides results that are closer to symmetry than the other models, while the SRK and PC-SAFT models show similar behaviour. Good performance of the best-fit model demonstrates the consistency of all experimental points.

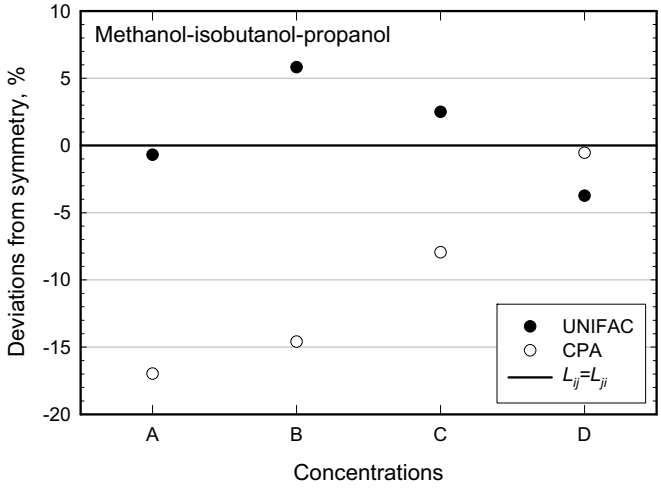

Concentrations: A - (0.2941; 0.3533); B - (0.1487; 0.1493); C - (0.1478; 0.7016); D - (0.6995; 0.1504)

Figure 7.1a: Deviations from the Onsager reciprocal relations for the systems containing associating fluids. Experimental data from [148].

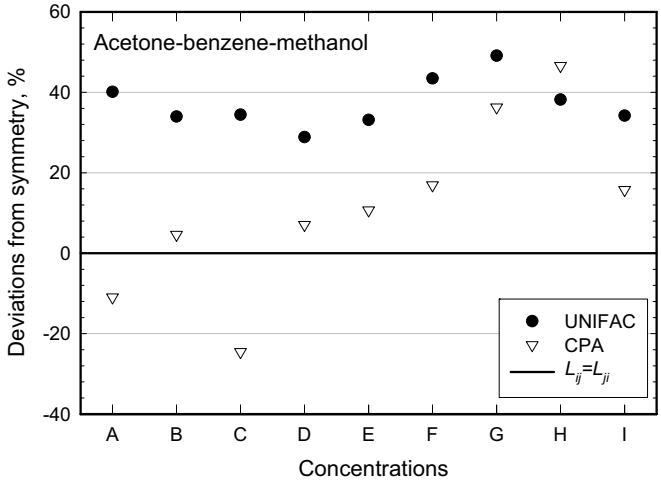

Concentrations: A - (0.350; 0.302); B - (0.766; 0.114); C - (0.553; 0.193); D - (0.400; 0.500); E - (0.299; 0.150); F - (0.206; 0.548); G - (0.102; 0.795); H - (0.120; 0.132); I - (0.150; 0.298)

Figure 7.1b: Deviations from the Onsager reciprocal relations for the systems containing associating fluids. Experimental data from [6].

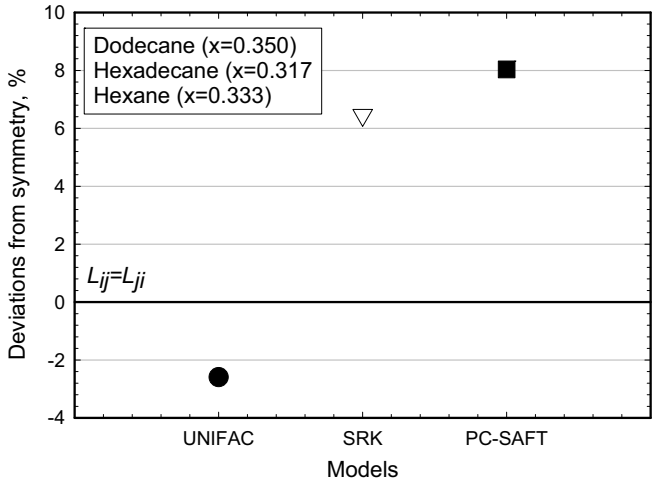

Figure 7.2a: Deviations from the Onsager reciprocal relations for the systems modelled by the three thermodynamic models. Experimental data from [79].

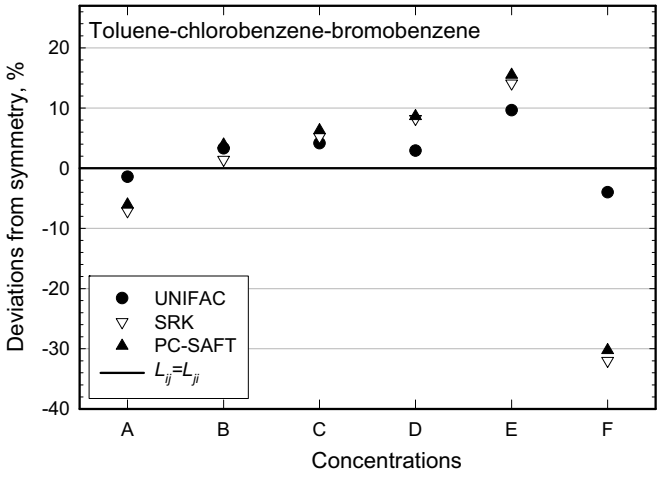

Concentrations: A - (0.250; 0.500); B - (0.260; 0.030); C - (0.700; 0.150); D - (0.150; 0.700); E - (0.450; 0.250); F - (0.180; 0.280)

Figure 7.2b: Deviations from the Onsager reciprocal relations for the systems modelled by the three thermodynamic models. Experimental data from [21].

The results for the mixture of acetone-benzene-carbon tetrachloride are rather good for both UNIFAC and SRK models (Figure 7.3a). Some (random) experimental data points seem to contain an error, since both thermodynamic models were unable to produce the symmetry.

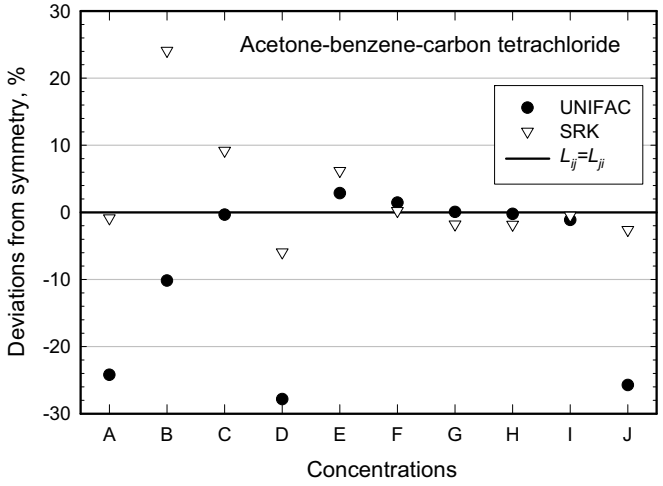

Concentrations: A - (0.2989; 0.3490); B - (0.1496; 0.1499); C - (0.1497; 0.6984); D - (0.6999; 0.1497); E - (0.0933; 0.8967); F - (0.2415; 0.7484); G - (0.4924; 0.4972); H - (0.7432; 0.2466); I - (0.8954; 0.0948); J - (0.3000; 0.3500);

Figure 7.3a: Deviations from the Onsager reciprocal relations for the systems modelled by the UNIFAC and SRK models. Experimental data from [6, 27].

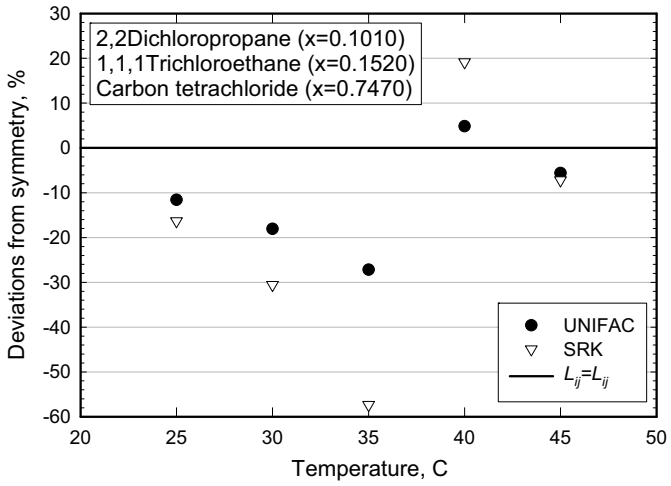

Figure 7.3b: Deviations from the Onsager reciprocal relations for the systems modelled by the UNIFAC and SRK models. Experimental data from [6, 27, 114].

The diffusion coefficients for the system 2,2dichloropropane – 1,1,1trichloroethane – carbon tetrachloride were measured at different temperatures. Thus, it was possible to see

the ability of the different models to reproduce the temperature dependence of the reciprocal relations. For the three experimental points both tested models (UNIFAC, SRK) give small deviations from symmetry (Figure 7.3b), while UNIFAC provides slightly better results. However, for the two middle points (at 30^{o} and 35^{o} C) the deviations from symmetry with the two models are too high in the case of both tested models, which probably indicates some errors in the experimental data.

Table 7.1: Mole fractions corresponding to the minimum deviations from symmetry of Onsager cross-phenomenological coefficients. Experimental data, reported in [159].

a) acetone-carbon tetrachloride-chloroform

	Fractions*		
	1	2	3
UNIFAC	0.0550	0.0275	0.9175
SRK (zero kij)	0.3871	0.1932	0.4197
SRK (non-zero)	0.0645	0.0322	0.9033
UNIFAC	0.0527	0.0296	0.9177
SRK (zero kij)	0.3128	0.1759	0.5113
SRK (non-zero)	0.0598	0.0337	0.9065

b) hexane-acetone-chloroform

	Fractions		
	1	2	3
UNIFAC	0.1287	0.0642	0.8071
SRK (zero kij)	0.1846	0.0921	0.7233
SRK (non-zero)	0.0974	0.0486	0.8540
UNIFAC	0.0453	0.0255	0.9292
SRK (zero kij)	0.0804	0.0452	0.8744
SRK (non-zero)	0.0403	0.0226	0.9371

c) methanol-acetone-chloroform

	Fractions		
	1	2	3
UNIFAC	0.1287	0.0642	0.8071
CPA (zero kij)	0.1846	0.0921	0.7233
CPA (non-zero)	0.0974	0.0486	0.8540
UNIFAC	0.0453	0.0255	0.9292
CPA (zero kij)	0.0804	0.0452	0.8744
CPA (non-zero)	0.0403	0.0226	0.9371

d) methanol-isopropanol-chloroform

	Fractions		
	1	2	3
UNIFAC	0.0805	0.0402	0.8793
CPA (zero kij)	0.1127	0.0562	0.8311
CPA (non-zero)	0.0760	0.0380	0.8860
UNIFAC	0.0640	0.0360	0.9000
CPA (zero kij)	0.0098	0.0055	0.9847
CPA (non-zero)	0.0677	0.0381	0.8942

e) heptane-acetone-chloroform

	Fractions		
	1	2	3
UNIFAC	0.1400	0.0699	0.7901
SRK (zero kij)	0.5998	0.2994	0.1008
SRK (non-zero)	0.1397	0.0697	0.7906
UNIFAC	0.3450	0.1940	0.4610
SRK (zero kij)	0.3658	0.2057	0.4285
SRK (non-zero)	0.0320	0.0180	0.9500
UNIFAC	0.2117	0.1191	0.6692
SRK (zero kij)	0.5334	0.3000	0.1666
SRK (non-zero)	0.0909	0.0511	0.8580

*Remark: compositions of the binary mixture 1+2 have been reported in [159]. The fraction of the third component is obtained from minimization of the deviation from symmetry of Onsager coefficients. And the corresponding normalization of mole fractions in ternary mixture 1+2+3 was performed.

The experimental results analyzed in Table 7.1 were obtained by application of the chromatographic technique. As discussed above, the problem of using such an experimental technique is that the fraction of one component (the flowing solvent) remains unknown. We used the system of equations (7.7) for evaluation of the fraction of the solvent by minimizing the deviations from symmetry of the matrix of Onsager phenomenological coefficients. For all the systems presented in the tables, it was possible to reduce the deviation from symmetry to zero. This, of course, does not provide the exact value of the third mole fraction due to possible experimental errors. However, the obtained values of this fraction can be considered as good approximations. These values are high, which looks physically reasonable since, according to the experimental procedure, there is an excess of the third component with the injection of the small samples of the binary mixtures. It is seen that for all systems considered the results are similar for the UNIFAC and SRK models.

7.1.4. Discussion

It is shown in this section that checking the symmetry of Onsager coefficients is necessary and nontrivial. Of the data tested, the most problematic system is that of acetone-benzene-methanol. This system exhibits high non-ideality, and abnormally high cross-diffusion coefficients are reported for it. Both thermodynamic models applied to this system produce high and different deviations from symmetry. The nature of these deviations requires further analysis.

Apart from this system, all the models considered behave similarly, UNIFAC being slightly (but uniformly) better. An important fact is that the thermodynamic models are either consistent or fail simultaneously on the same points. This shows that verification of symmetry is a good method for checking the consistency of experimental data on ternary diffusion.

It should be noted that most of the thermodynamic models have been designed for and fitted to problems of phase equilibria. However, verification of the symmetry requires such “exotic” properties as derivatives of chemical potentials. The analysis carried probably indicates that the existing thermodynamic models (especially UNIFAC) can calculate these properties also. It again proves that when both the knowledge of chemical potential and molar volume are required, the combination of cubic EoS with the activity coefficients model (such as, e.g., SRK+MHV1/UNIFAC) can provide more consistent results than a simple cubic EoS. However, further work on improvement of the existing thermodynamic models is required for a more reliable prediction of the partial molar properties, in connection with transport-related problems.

7.2. Overview of Existing Models for Diffusion Coefficients in Multicomponent Mixtures

Existing models for estimation of the diffusion coefficients in the multicomponent mixtures can roughly be divided into three main groups:

- reduction techniques, which are trying to reduce the number of independent diffusion coefficients by "lumping" the components of the mixture into pseudocomponents, or by other assumptions;
- different interpolation schemes, similar to the schemes described for binary mixtures and based upon the values of the infinite dilution diffusion coefficients;
- application of free volume/activation energy methods.

Additionally, in the previous chapter the coupled FT+MD approach was proposed, . A possibility for its extension to the prediction of diffusivities in multicomponent mixtures is discussed in this section.

7.2.1. Reduction of the Number of Independent Coefficients

Several approaches have been developed to reduce the problem of multicomponent mass transfer to binary diffusion [145].

The first approach attempts to select an effective value of the binary diffusion coefficient for a selected component, which will be capable of representing its diffusion in a multicomponent mixture. Two different models have been proposed in [153, 154], which differ in the underlying assumptions. Under assumption that the concentration of the second component does not change in the experiment, the effective Fickian diffusion coefficient for the first component in a ternary mixture is expressed as [154]:

$$D_{11}^{eff} = D_{11}\left(1-\frac{D_{12}D_{21}}{D_{11}D_{22}}\right). \tag{7.8}$$

A model based on more sophisticated assumptions was proposed in [153]. It defines the effective value of the diffusion coefficients for the first component as follows:

$$\begin{aligned} &D_{11}^{eff} = D_{11}\cdot p\frac{2q(r+\sqrt{p})}{(1+q\sqrt{p})^2}, \\ &q^2=\frac{D_{11}}{D_{22}},\ r=\frac{D_{11}+D_{22}}{2\sqrt{D_{11}D_{22}}},\ p=1-\frac{D_{12}D_{21}}{D_{11}D_{22}}. \end{aligned} \tag{7.9}$$

The validity of the pseudo-binary approach described by Eqs. (7.8) and (7.9) depends upon the process studied. Later Subramanian [151] proposed a rather universal approach for "lumping" the diffusion coefficients in a multicomponent mixture to an effective binary diffusion coefficient. The approach is based on the minimization of the deviations between real and effective solutions of the systems of diffusion equations in a given process.

The effective diffusivities for separate components in the multicomponent mixtures do not necessarily follow the empirical mixing rules or other correlations, developed for the Fickian or the MS diffusion coefficients. Thus, estimation of these diffusivities requires conducting an experiment under conditions corresponding to the assumptions, which were introduced in order to derive the approximation. In this sense, the advantage of lumping schemes for the task of prediction of the diffusion coefficients in multicomponent mixtures is questionable.

A more rigorous approach to reduce the number of the independent diffusion coefficients is based on the concepts of the thermodynamics of irreversible processes and different definitions of the Onsager coefficients. A general idea is to select such specific system of thermodynamic coordinates, in which the fluxes of different components become independent, and the matrix of the Onsager phenomenological coefficients becomes diagonal. This makes it possible to reduce the number of independent diffusion coefficients from $(n\text{-}1)^2$ independent Fickian or $n(n\text{-}1)/2$ independent Onsager coefficients to n-1 or n independent diagonal coefficients.

One of the examples of such transformation is the system of thermodynamic coordinates, proposed by Kett and Anderson [80]. They assumed that in a system of coordinates related to the volumetric flow of a mixture each component is driven by its own "driving force" $\nabla\mu_i$. This is equilibrated by the "friction force" $\sigma_i\eta\mathbf{u}_i$, where σ_i is an individual friction coefficient, η is viscosity, and $\mathbf{u}_i$ is individual velocity of component i.

This assumption leads to the following expression for the molar diffusion flux:

$$\mathbf{J}_i = -\frac{z_i v}{\sigma_i \eta}\nabla\mu_i . \tag{7.10}$$

The corresponding expression for the phenomenological coefficient is as follows:

$$L_{ij} = \frac{z_i v T}{\sigma_i \eta}\left\{\delta_{ij} - z_j\left[\frac{\sigma_i}{\sigma_j} + 1 - \sum_{k=1}^{n} z_k \frac{\sigma_i}{\sigma_k}\right]\right\}. \tag{7.11}$$

A resulting expression for the Fickian diffusion coefficients is

$$D_{ij} = \frac{z_i}{\eta}\left[\frac{1 - V_i z_i}{\sigma_i} + \frac{z_i V_n}{\sigma_n}\right] + \sum_{k,k\neq i}^{n-1}\frac{z_i z_k}{\eta}\left(\frac{V_n}{\sigma_n} - \frac{V_k}{\sigma_k}\right), \left(i, j = 1, ..., n-1\right). \tag{7.12}$$

In this approach, the Onsager coefficients and Fickian diffusion coefficients are expressed in terms of n unknown friction coefficients.

Another system of thermodynamic coordinates is proposed by Cussler [32]. Cussler suggests the following system of thermodynamic forces, conjugate to the molar diffusion fluxes, with regard to the volume average velocity:

$$\mathbf{X}_i = \frac{1}{T}\sum_{j=1}^{n-1}\alpha_{ij}\nabla\mu_j,\ \ \alpha_{ij} = \delta_{ij} + \frac{z_j V_i}{z_n V_n}\ \ (i = 1,...,n-1). \tag{7.13}$$

Cussler assumes that in such system of thermodynamic coordinates the matrix of Onsager phenomenological coefficients becomes diagonal. The corresponding expression for the Fickian diffusion coefficients is

$$D_{ij} = \sum_{l=1}^{n}\left(\frac{D_i z_i \nu}{RT}\right)\left(\delta_{il} + \frac{z_l V_i}{z_n V_n}\right)\frac{\partial\mu_i}{\partial z_j}. \tag{7.14}$$

In both described models, the diagonal Fickian diffusion coefficients, related to the friction coefficients, are assumed to contain unknown constants which have to be determined experimentally.

The above described approaches reduce the number of the independent diffusion coefficients. However, they do not provide any model for estimation of the effective diffusivities or friction coefficients. As shown by Shapiro et al. [145], some of the diagonalization procedures clearly violate the Onsager reciprocal relations [177]. It is always recommended to verify the validity of the symmetry of the Onsager or the MS diffusivities, when applying such kind of approaches.

7.2.2. Interpolation schemes

The next branch of models for estimation of the multicomponent diffusion coefficients is based on the interpolation schemes and infinite dilution diffusion coefficients, as was already discussed for binary mixtures in Chapter 4. There are few major problems preventing straightforward extension of the existing models from binary to multicomponent mixtures. First, the concentration dependence of the MS and the Fickian diffusion coefficients in multicomponent mixtures is more complicated than that in the binary mixtures [168]. For many mixtures, viscosity data, and, correspondingly, the viscosity contribution to the mixing rules, are not available. Nevertheless, Rutten [134] states that available experimental data on ternary diffusion coefficients indicate that the concentration dependence of the MS diffusivities in a majority of non-associating ternary mixtures is close to the Vignes- or Darken-like type of behavior. However, a major problem, preventing straightforward application of interpolation schemes, is related to the estimation of the infinite dilution diffusion coefficients.

An attempt to extend the binary interpolation schemes to multicomponent mixtures was done by Krishna [86]:

$$\begin{aligned} &\text{Đ}_{ij} = \left(\text{Đ}_{ij}^{i\to 1}\right)^{Z_i}\left(\text{Đ}_{ij}^{j\to 1}\right)^{Z_j}, \\ &Z_i = \frac{z_1}{z_1 + z_2};\ Z_j = 1 - Z_i. \end{aligned} \tag{7.15}$$

Eq. (7.15) has the same form for all three MS diffusion coefficients in ternary mixtures, with corresponding different values of limiting diffusivities. Eq. (7.15) is the Vignes-like mixing rule, with the actual mole fractions replaced by their equivalent binary compositions. It can easily be shown that Eq. (7.15) predicts two different values of the limiting diffusion coefficient at the limit of pure component 3.

$$\lim_{z_j \to 0} \mathcal{D}_{ij} = \mathcal{D}_{ij}^{j \to 1}, \text{ at } z_i = 0. \tag{7.16}$$

And correspondingly if we approach infinite dilution limit from other side:

$$\lim_{z_i \to 0} \mathcal{D}_{ij} = \mathcal{D}_{ij}^{i \to 1}, \text{ at } z_j = 0. \tag{7.17}$$

Hence the mixing rule (7.15) is not geometrically consistent [84].

A more consistent mixing rule was proposed by Cullinan and Cusick [28]. It is exactly the extension of the Vignes rule to a ternary mixture:

$$\mathcal{D}_{ij} = \left(\mathcal{D}_{ij}^{i \to 1}\right)^{z_i} \left(\mathcal{D}_{ij}^{j \to 1}\right)^{z_j} \left(\mathcal{D}_{ij}^{k \to 1}\right)^{z_k}. \tag{7.18}$$

As for binary mixtures, Eq. (7.18) is capable of describing a monotonous concave behavior of diffusion coefficients. As it is explained below, it should be supplemented with an additional model for estimation of the infinite dilution diffusion coefficients.

Eq. (7.18) involves three infinite dilution diffusion coefficients for each of the ternary diffusion coefficients. The two first infinite dilution diffusion coefficients in Eq. (7.18) are equal to the infinite dilution diffusivities in binary mixtures. However, the third coefficient is not. It is rather problematic to measure the third term in Eq.(7.18), since it is the diffusivity of the component i with regard to the component j, where both fractions of i and j are infinitely small. Hence, this value needs to be modeled. There is an attempt to derive the expression for the infinite dilution diffusion coefficients from the transition state theory [134]. However, this leads to an inconsistent expression, which does not always provide symmetric and positive values of the MS diffusivities [84, 134].

Several requirements with regard to the consistency of the models for the infinite-dilution diffusivities in multicomponent mixtures have been formulated. First, the MS diffusivities must be symmetric. Second, there should be no discontinuities of the type, in Eqs. (7.16), (7.17) [84]:

$$\lim_{i \to 0}\left(\mathcal{D}_{ij}^{j \to 0}\right) = \lim_{j \to 0}\left(\mathcal{D}_{ij}^{i \to 0}\right). \tag{7.19}$$

A final requirement is the reduction of Eq. (7.18) to the ordinary Vignes rule for binary mixtures, if the fraction of component k is infinitesimal. For Eq.(5.16), this condition is obeyed, since the two first infinite dilution diffusivities are equal to binary diffusion coefficients.

In accordance to these conditions, a simple geometrical rule was proposed by Wesselingh and Krishna [167]:

$$\mathcal{Đ}_{ij}^{k\to 1} = \sqrt{\mathcal{Đ}_{ij}^{i\to 1}\mathcal{Đ}_{ij}^{j\to 1}} \,. \tag{7.20}$$

Substitution of Eq. (7.20) into Eq. (7.18) results in the following expression for the multicomponent diffusion coefficient:

$$\mathcal{Đ}_{ij} = \left(\mathcal{Đ}_{ij}^{i\to 1}\right)^{\left(1+z_i-z_j\right)/2}\left(\mathcal{Đ}_{ij}^{j\to 1}\right)^{\left(1+z_j-z_i\right)/2} . \tag{7.21}$$

Eq. (7.21) suggests that, if diffusivities at "i" and "j" limits are equal, the MS diffusion coefficients are independent of composition. Rutten [134] indicates that Eq. (7.20) obviously fails for mixtures with significant differences between the components. Indeed, if components i and j have rather low limiting diffusion coefficients (and component k does not), then the estimate according to Eq. (7.20) will be very inaccurate. To correct this failure of the model, the following viscosity correction can be introduced [134]:

$$\mathcal{Đ}_{ij}^{k\to 1} = \sqrt{\mathcal{Đ}_{ij}^{i\to 1}\frac{\eta_i}{\eta_k}\mathcal{Đ}_{ij}^{j\to 1}\frac{\eta_j}{\eta_k}} \,. \tag{7.22}$$

Kooijman and Taylor [84] carried out an extensive research, focused on adjusting and testing different geometric mixing rules for estimation of the infinite dilution diffusion coefficients in multicomponent mixtures. On the basis of this analysis, they proposed the following mixing rule:

$$\mathcal{Đ}_{ij}^{k\to 1} = \sqrt{\mathcal{Đ}_{ik}^{k\to 1}\mathcal{Đ}_{jk}^{k\to 1}} \,. \tag{7.23}$$

This expression was compared with the experimental data for methanol-isobutanol-propanol [148] and for acetone-benzene-methanol [6]. The mutual ternary diffusion coefficients were predicted applying the interpolation scheme, Eq. (7.18), with known infinite dilution diffusivities from a binary mixture, and with estimating the unknown limiting diffusivity by Eqs. (7.20), (7.23) or similar. The research performed in [84] indicates that, generally, the best description of the concentration dependence is achieved by application of the combination of the interpolation scheme (7.18) and the expression (7.23) for infinite dilution diffusivities. Estimation of the infinite dilution diffusion coefficient by the rule (7.20) provides slightly worse results.

It was also reported in [84] that prediction of the concentration dependence of the Fick diffusion coefficients by Eqs. (7.18), (7.20) and (7.23) is better than prediction for the MS diffusivities. This contradicts the statement that the concentration dependence of MS diffusion coefficients is generally simpler than of the Fick diffusivities [169]. The reason is, probably, that the calculated concentration dependence of the MS diffusivities is dependent upon the selected thermodynamic model.

In sum, the interpolation schemes of the Vignes type for ternary mixtures involve nine infinite dilution diffusion coefficients (three per each of MS diffusion coefficients). Six of these are binary diffusion coefficients, which may be obtained either from experiment or from a proper model for binary diffusivities. The other three infinite dilution diffusion coefficients $\mathcal{D}_{ij}^{k\to 1}$ are difficult both to measure and to model. Existing empirical and geometrical models for their prediction can only be applied to mixtures with simple behavior of the diffusion coefficients [84, 134].

7.2.3. Free Volume and Activation Energy Models

Application of free volume and activation energy models to the estimation of binary diffusion coefficients was discussed in Chapter 3. In this section, possibilities for extension of this approach to estimation of ternary and multicomponent diffusivities are considered.

Wesselingh and Bollen [168] proposed mixing rules, which make it possible to extend the free volume approach, developed for the binary mixtures, to the multicomponent mixtures. The expression, proposed in [168] for self-diffusion coefficient in a multicomponent mixture, is similar to the expression, proposed for a binary mixture (Chapter 4):

$$\begin{aligned} \mathcal{D}_{i\#,i}^{0} &\simeq \frac{1}{6}\sqrt{\frac{3kT}{\rho^{*} d_i}} \\ \mathcal{D}_{i\#,i} &= \mathcal{D}_{i\#,i}^{0} \exp\left(-0.7\frac{V_i^{*}}{V_i^{f,mix}}\right) \end{aligned} . \qquad (7.24)$$

The mixing rules for the parameters, entering Eq. (7.24) are discussed below.

It is assumed that the individual free volumes of the components, as well as the compressed volumes and densities of the components and the molecular diameters are known. The diameters, however, can be related to the compressed volumes [168].

The linear mixing rule for the free volume of the mixture is proposed:

$$V^{f,mix} = \sum_{i=1}^{n} z_i V_i^{f} \ . \qquad (7.25)$$

Obviously, the individual free volumes differ from the free volumes of the pure components. The last free volumes may be estimated using the Guggenheim expression [120, 124] or other possible definitions of the free volume [18, 19]. Wesselingh and Bollen [168] assume that free volume, accessible for a molecule of a given component i in the mixture is proportional to its surface fraction σ_i:

$$V_i^{f,mix} = \frac{\sigma_i}{z_i} V^f,$$
$$\sigma_i = \frac{z_i \left(V_i^*\right)^{2/3}}{\sum z_j \left(V_j^*\right)^{2/3}}. \tag{7.26}$$

Eq. (7.26), together with the already known individual compressed volumes of the components, makes it possible to estimate the exponential term, entering the equation for self-diffusion coefficient, Eq. (7.24).

The pre-multiplier in Eq.(7.24), which has the physical meaning of the non-impeded diffusion (friction) coefficient, involves the total compressed density of the mixture. A mixing rule for this property is also required. The total compressed density of the mixture is assumed to obey the linear mixing rule:

$$\rho^* = \sum_{i=1}^{n} z_i \rho_i^* . \tag{7.27}$$

For the sake of relation of the self-diffusion coefficients to the mutual diffusivities, it is convenient to derive the expression for tracer friction coefficients. This expression has a form similar to the expression for the self-diffusion coefficient, Eq. (7.24). The non-impeded friction coefficient is defined in the following way:

$$\xi_{i\#,i}^0 = 2N_A \sqrt{3kT\rho^* d_i} . \tag{7.28}$$

The corresponding equation for the friction coefficients of the tracer amount of a component in the mixture as a whole is the following:

$$\xi_{i\#,i} = \xi_{i\#,i}^0 \exp\left(-0.7 \frac{V_i^*}{V_i^{f,mix}}\right). \tag{7.29}$$

The mixing rules described above make it possible to estimate the effective friction coefficients of the components, Eq. (7.29). It is now necessary to relate them to the mutual friction coefficients, to obtain the mutual diffusion coefficients.

The authors [168] propose a geometric mixing rule to relate the effective tracer friction coefficients to the mutual friction coefficients:

$$\xi_{ij} = \frac{\xi_{i\#,i}\xi_{j\#,j}}{\sum_{k=1}^{n} z_k \xi_{k\#,k}}, (i, j = 1, ..., n;\ i \neq j) . \tag{7.30}$$

Summarizing, extension of the free volume approach to multicomponent mixtures, according to [168] requires knowledge of the individual free volumes of the components, compressed volumes and densities of the components.

Wesselingh and Bollen [168] have also proposed a way of estimation of the free volumes different from direct estimation by the Guggenheim expression. If the data on

viscosity of a multicomponent mixture is available, the free volumes can be extracted by fitting the free volume expression to the viscosity data. Once the required values of the free volume, the compressed density and the molecular diameters are obtained the application of Eqs. (7.25)-(7.30) makes it possible to calculate mutual diffusivities. Despite its complexity, such a scheme is easy to program and can provide a good agreement with the experimental values for multicomponent mixtures [168], provided that viscosity data are available.

An application of the activation energy theory to the estimation of multicomponent diffusion coefficients was proposed by Mortimer and Clark [113]. The authors considered a quasi-lattice model of the liquid and assumed that there are holes, or vacancies, in the lattice. Mortimer and Clark consider a number of molecules making transition over the activation energy barrier in a given direction. Substitution of the Eyring expression for the rate constant makes it possible to obtain a explicit expressions for the Onsager phenomenological coefficients, based on the rate constant and the geometric properties of the lattice. The authors have successfully adjusted the developed model to the diagonal terms of the experimentally measured ternary diffusion coefficients in the ternary mixture of toluene-chlorobenzene-bromobenzene [21]. On the basis of the adjusted parameters, they predicted the cross-values of the diffusion coefficients with a reasonable accuracy (10%). Despite a number of strong assumptions the model has good prediction capabilities, especially combined with the prediction estimates for the main-term diffusion coefficients, described in section 6.2.1.

As it was already mentioned, the authors of [93] conducted an extensive research, focused on relating the free volume and the activation energy parameters to the thermodynamic properties, estimated by a cubic EoS. This direction of research could be fruitful for development of a predictive model, based on the free volume and the activation energy approach.

Discussion of the application of the free volume theory to prediction of the diffusion coefficients in polymer solutions can be found in [145].

7.2.4. The FT Approach

This section is a recommendation for future work, on the FT approach described in the two previous chapters for estimation of multicomponent diffusion coefficients.

One recommendation is to investigate another expression for the penetration lengths, constructed in the same way as for the diffusion and the friction coefficients in the free volume theory, Eq. (7.29):

$$Z_i = Z_i^0 \exp\left(-\gamma \frac{V_i^*}{V_i^{f,mix}} \right). \qquad (7.31)$$

Application of mixing rules, similar to those, proposed in [168], can make it possible to estimate the compressed and the free volume of a component in a mixture.

From the considerations of [168] for non-impeded diffusion coefficients, it may be derived that the penetration amplitude will be related to the non-impeded self-diffusion coefficient.

Recent developments of the free volume theory and the relation demonstrated between the concept of penetration lengths and free volume make it possible to combine these two approaches in a natural way. However, we believe that problem of the sensitivity of the transport properties to the size of the molecules in the liquid state, observed in [94, 133, 168], makes it difficult to create a really predictive approach, based on pure phenomenological considerations. This needs to be further investigated.

Possibly, a more promising approach to modeling of the diffusion coefficients in multicomponent mixtures is the combination of the FT approach and molecular dynamics described in the previous chapter. Compared to conventional molecular dynamics simulations [66, 77, 94, 175], it provides more accurate results in an essentially smaller time of simulation. What is more important, it provides the results directly in the form of mutual diffusion coefficients. The results presented in the previous chapter shown that even with a rather simple spherical LJ potential as a model for intermolecular interactions [51] the combined FT+MD model is capable of predicting diffusion coefficients with a good accuracy. An extension of this combined model to prediction of diffusion coefficients in multicomponent mixtures is straightforward. The only difference is an increased time of calculation, since the number of particles in the simulation needs to be increased.

7.3. Summary

Experimental measurement of the diffusion coefficients in multicomponent mixtures is a difficult task. There is a necessity for predictive approaches to estimate the diffusivities in ternary and multicomponent mixtures.

There are a few empirical or semi-empirical approaches to modeling the diffusion coefficients. The first is based on determination or modeling of the infinite dilution diffusion coefficients and interpolating these values over the whole concentration range by simple “mixing rules”. This is the simplest of the consistent approaches, and it may works for relatively simple mixture according to the rather insufficient amount of experimental data. Besides the problems described in Chapter 4, an additional difficulty of this approach is in the description of the infinite dilution diffusion coefficients.

Models based on the free volume/activation energy theory are well developed for multicomponent mixtures [72, 93, 113, 168]. They have better foundation than the interpolation methods described above. Recent developments in this area have significantly

increased the prediction capabilities of these methods. The universal character of the free volume and activation energy theory provides great possibilities to relate the parameters of these models to physical and thermodynamic properties [93]. However, a weakness of these methods is that they operate in terms of self- and tracer diffusion coefficients. The relation between these properties and the mutual diffusivities is essentially empirical and not-accurate. The application of transition state theory for diffusion coefficients, combined with assumptions about liquid structure makes it possible to obtain directly mutual diffusion coefficients [113]; however such an approach is not fully predictive and accurate.

Another method, the UNIDIF [74, 75], which was also described in Chapter 4, is in principle designed for modeling of multicomponent mixtures. However so far it has been applied only for binaries.

Development of a rigorous theoretical approach, based on the fluctuation theory for diffusion, provides wide possibilities for prediction of diffusion coefficients in multicomponent mixtures. As was shown in the previous chapter, the phenomenological approach to calculation of the penetration lengths is not very predictive, due to the high sensitivity to the values of the constituting parameters. Recent developments of the free volume theory and attempts of its extension to the multicomponent mixtures make it possible to combine the free volume theory with the FT approach.

The combination of MD and FT proved to be a successful, predictive and fast (compared to conventional MD simulations) approach to estimation of the mutual diffusion coefficients in binary mixtures [51]. Extension of the MD-FT approach to multicomponent mixtures is straightforward. Application of a more advanced molecular dynamics code, capable of proper description of complex molecules may make it possible to predict the penetration lengths and the diffusion coefficients in multicomponent mixtures.

Additional research is required to evaluate the applicability of the combined free volume and FT approaches, as well as MD+FT model, to predict diffusion coefficients in multicomponent mixtures.

8. Conclusions and Future Work

The purpose of the present study was to develop framework, capable of describing and predicting diffusion coefficients in binary and multicomponent mixtures. The background of the developed framework was the recently developed fluctuation theory (FT), based on rigorous theoretical considerations of statistical mechanics and non-equilibrium thermodynamics. Practical application of the fluctuation theory to modeling the diffusion coefficients requires a model for estimation of the thermodynamic factor (the thermodynamic matrix), as well as a model for computation of the key parameters of the fluctuation theory, the penetration lengths.

A procedure for estimation the thermodynamic factor was developed. It allows straightforward application of existing thermodynamic simulators for estimation of the thermodynamic matrix. A flexible computational code for estimation of the diffusion coefficients in the framework of fluctuation theory was developed. It can serve as a basis for modeling of other transport properties in the FT framework, such as heat conductivity and thermodiffusion coefficient. A procedure for the estimation of the thermodynamic matrix was verified by application of the condition of symmetry of cross compositional derivatives.

Two different models for estimation of the penetration lengths were proposed and verified to describe diffusion coefficients in binary mixtures. Both expressions demonstrate excellent description of binary diffusion coefficients over the whole concentration and wide temperature ranges with only four adjustment parameters. They are capable of describing all the known forms of the concentration dependence for the mutual diffusion coefficients, such as convex/concave functions with strong/weak minima/maxima. The influence of different thermodynamic models on the quality of description of the experimental data was analyzed. It was shown that choice of a thermodynamic model influences the values of the penetration parameters, while the quality of description changes only little.

The prediction capabilities of different expressions for the penetration lengths were tested. It was shown that an exponential dependence of the penetration lengths on the molar concentrations gives a high sensitivity of the diffusion coefficients on the values of the penetration parameters. The source for such sensitivity is both in the form of the dependence and in the value of the fraction of free volume, available for penetration. Moreover, the penetration parameters, entering the exponential expression for penetration lengths, are not individual properties of the components, but the properties of a mixture as a whole.

On the contrary, the values of the penetration volumes, entering the second, quadratic expression for the penetration lengths, are individual properties of the components. The averaged individual values of the penetration volumes for a large number of the substances were obtained. It was shown that application of a more advanced thermodynamic model,

such as the Soave-Redlich-Kwong equation of state with MHV1 mixing rule or the UNIFAC activity coefficient model, provides better individual behavior of the penetration volumes.

Further analysis of the averaged individual penetration volumes made it possible to establish a correlation between the penetration volumes and the co-volume parameters of the cubic equations of state. The fact that the penetration volumes are very close to the co-volume parameters in EoS shows a clear physical interpretation of the proposed quadratic expression for the penetration lengths.

Re-adjustment of the available experimental data on binary diffusion coefficients was carried out, assuming that penetration volumes are equal to: a) the average individual values, and b) the co-volume parameters from cubic EoS. Despite the fact that the penetration volumes can be considered as individual properties with a high degree of accuracy, both assumptions result in an essentially worse description of the experimental data, compared to the case where the penetration volumes are also adjusted. A high sensitivity to the value of the penetration volumes is connected to the very low values of the volume available for penetration in liquids. This is in a good agreement with the free volume theory, which also predicts a low value of the free volume, that is, the volume available for molecular penetration in the liquid state.

A different approach to evaluation of the penetration lengths and, therefore, of the diffusion coefficients, is proposed in Chapter 6. The approach combines the fluctuation theory framework with molecular dynamics simulations, applied to prediction of the penetration lengths. Such an application of molecular dynamics simulations is straightforward. It is based on the original definition of the penetration lengths. The values of the penetration lengths, produced by molecular dynamics are in excellent qualitative and good quantitative agreement with the penetration lengths, obtained by adjustment of the diffusion coefficients to the experimental data. This substantiates correctness of the FT methodology, as well as its suitability for practical applications. A new possibility arises, consisting in determining the diffusion coefficients by combination of the FT and MD formalisms. Such diffusion coefficients, evaluated with the penetration lengths from the MD simulations, are in good agreement with the experimental values. The accuracy of prediction of the diffusion coefficients over the whole concentration range at several temperatures for the simple mixture of benzene/toluene is less than 9%, which is excellent, taking into account that no fitting is involved. The accuracy of prediction of diffusion coefficients for three other investigated mixtures is fair and lies within 15-20%. The deviations can be explained by the fact that the MD simulations are performed on the basis of the simple spherical Lennard-Jones model of molecular interactions. Further research, with application of a more advanced MD code is required in order to test the area of applicability of the MD+FT approach.

Chapter 8. Conclusions and Future Work

Chapter 7 of the thesis presents a procedure for verification of the diffusion coefficients in ternary mixtures. The procedure is based upon transformation of the Fick diffusion coefficients into phenomenological coefficients and subsequent verification of the Onsager reciprocal relations. Transformation of the Fick diffusion coefficients into Onsager coefficients requires a thermodynamic model for estimation of the compositional derivatives of the chemical potentials. Different thermodynamic models are applied. Based on the symmetry of cross-terms in the matrix of ternary phenomenological coefficients conclusions about quality of the experimental data, as well as accuracy of the applied thermodynamic model are formulated. It is shown that majority of the investigated experimental data obeys the Onsager reciprocal relations with a fair accuracy for all the applied thermodynamic models. Generally, application of the UNIFAC model provides better performance, compared to cubic equations of state.

Possibilities for extension of the approaches developed in Chapters 5 and 6 for modeling diffusion coefficients in binary mixtures, to multicomponent diffusion coefficient, are discussed in Chapter 7.

Suggestions for future work

An evident direction for further research is better validation of the combined FT+MD approach, using more sophisticated models for molecular interactions, and its extension to prediction of diffusion coefficients in ternary mixtures.

The description of experimental ternary diffusion coefficients by the “pure” FT approach with a quadratic dependence of the penetration lengths requires investigation of different mixing rules for the penetration amplitudes. It is worth checking whether the penetration interaction parameters for the ternary diffusion coefficients are equal to the parameters for binaries.

The penetration amplitudes are not individual parameters of the components. Search for their correlation with mixture properties is required, to produce a fully predictive FT model for diffusion coefficients.

Since the proposed models for the penetration lengths are essentially empirical, further investigation of different expressions for the penetration lengths is required. A combination of the free volume approach and the fluctuation theory may be productive with regard to this goal, since it has been demonstrated that the concept of penetration length is related to the concept of free volume. Thus, the application of the recent developments of the free volume theory to prediction of the penetration lengths may be fruitful.

Nomenclature

$\mathbf{A}$	transformation matrix
A	penetration amplitude
$\mathbf{B}$	transition matrices for solvent-solvent transformations
B_i	penetration volume of species i
C_i	average molecular velocity of species i
C_p^j	specific heat capacity of component j
c_t	overall molar density
c_i	molar concentration of species i
$\mathbf{D}$	matrix of Fick diffusion coefficients (molar reference frame)
D_{ij}	Fick diffusion coefficient of species i with respect to species j (molar reference frame)
$\mathbf{\mathit{Đ}}$	matrix of Maxwell-Stefan diffusion coefficients (molar reference frame)
$Đ_{ij}$	Maxwell-Stefan diffusion coefficient of species i with respect to species j (molar reference frame)
$Đ_{i\#,j}$	Maxwell-Stefan tracer diffusion coefficient of tracer i with respect to species j
$\mathbf{d}_i^{chem}$	chemical driving force, exerted on species i
$\mathbf{d}_i^{friction}$	friction force, exerted on species i
$\mathbf{d}_i$	generalized driving force
d_i	molecular diameter of species i
E_D	dispersion coefficient
E_{ij}	potential energy of interaction between species i and species j
F_f	hydrodynamic friction force
$\mathbf{G}, \mathbf{g}$	transformation matrices
ΔG^a	activation Gibbs energy
H	fraction of the diaphragm, available for diffusion
h	Planck constant, $6.6261 \cdot 10^{-23}$ J s^{-1}
h_i^0	standard state enthalpy of component i

Nomenclature

$\mathbf{I}_i$	relative diffusion flux of species i
$\mathbf{J}_i$	molar diffusion flux of species i (molar reference frame)
$\mathbf{J}_S$	flux of specific entropy
k	Boltzmann constant, $1.38065 \cdot 10^{-23}$ J K^{-1}
k_{rate}	specific rate constant in Eyring theory of rate processes
$\mathbf{L}$	matrix of Onsager phenomenological coefficients
L_{ij}	Onsager coefficient of species i with regard to species j
L	length of the tube
$\mathbf{l}$	transformation matrix, inverse of $\mathbf{L}$
l_D	effective thickness of the diaphragm
M_i	molar mass of species i
m_i	molality of species i per mass of solvent or mass of the particle of species i
$\mathbf{N}_i$	absolute diffusion flux of species i
N_i	molar density of the component i
N	overall molar density
N_A	Avogadro constant, $6.0221 \cdot 10^{23}$ mol^{-1}
n	number of moles in the mixture
n_i	number of moles of component i
P	pressure
Pe	Peclet number
Q	molar flow of the solute
R	universal gas constant, 8.314 J mol^{-1} K^{-1}
R_i	radius of the molecule of species i
Re	Reynolds number
r	radial distance, coordinate
r_0	radius of the tube
S	entropy
$\dot{S}$	specific entropy production
S_D	surface area of the diaphragm
T	temperature
$T_{1,2,3}$	numerical criteria

Nomenclature

t	time
t_{corr}	time of the velocity autocorrelation
U_0	total flow velocity
U	internal energy
U_{ij}	energy of intermolecular interaction in *i-j* pair
$\bar{U}$	average flow velocity
$\mathbf{u}_i$	velocity of the species i
$\bar{\mathbf{u}}$	average velocity
V_i	partial molar volume of species i
w_i	mass fraction of species i
$\mathbf{X}, \dot{\mathbf{x}}$	conjugate thermodynamic forces and fluxes, correspondingly
X	Langevin stochastic force
x	distance coordinate
$\mathbf{Y}, \dot{\mathbf{y}}$	conjugate thermodynamic forces and fluxes, correspondingly
Z_i	penetration length of species i
z_i	molar fraction of species i

Greek letters

α^R	weighting factor, depending upon the choice of reference frame R
β	diaphragm constant
Γ	thermodynamic correction factor
γ	activity coefficient
δ	Kronecker's delta function
Λ_i	probability of a particle of species i to cross a plane at given distance
η	kinematic viscosity
κ	transmission coefficient
μ	molar chemical potential
ν_i	number of the molecules of species i per unit of volume of liquid
ξ_{ij}	friction coefficient of *i-j* pair
Ω	angular velocity
Π	generalized potential in molar units
ρ	mass density

Nomenclature

ς_i	fraction of free volume
ε_{ij}	potential strength
σ_{ij}	atomic diameter
σ_t^2	variance of the average molar concentration
υ_i	volume fraction of species i
ϕ_i	fugacity coefficients
Φ	Faraday constant, 96484 C mol^{-1}
χ_i	stoichiometric coefficients of species i in the chemical reaction
$\mathbf{\Psi}_i$	external forces, acting per mole of species i
ψ	association coefficient in Wilke-Chang equation
ζ	fraction of free volume, available for penetration

Superscripts

*	property related to the compressed state
(1),(2)	properties, related to different systems of thermodynamic coordinates
eff	effective value
EX	excess property
H	Hittorf reference frame
id	ideal propery
m	mass property or mass reference frame
REF	reference state property
RES, r	residual property
V	volumetric property or volume reference frame

Subscripts

0	property at initial moment of time or at zero coordinate
C	property at critical point
K	denotes kinetic contribution
mix	overall property of the mixture
lower	property related to the lower compartment of the diffusion cell
R	denotes resistance contribution
t	total property of the mixture
T	denotes thermodynamic contribution
upper	property related to the upper compartment of the diffusion cell

Bibliography

1. Adamson A.W., “Physical Chemistry of Surfaces”, 3rd ed., John Wiley & Son, New York, 1976.

2. AIChE, Design Institute for Physical Properties, “DIPPR 801 Database”, web-site: http://dippr.byu.edu.

3. AIChE Journal, “The 100 Most Cited Articles in AIChE Journal History”, *AIChE J.*, **50** (2004) 4.

4. Albright J.G. and Mills R., **“**A Study of Diffusion in the Ternary System, Labeled Urea-Urea-Water, at 25° by Measurements of the Intradiffusion Coefficients[1] of Urea[2]” *J. Phys. Chem.,* **69** (1965) 3120.

5. Albright J.G., Gillespie S.M., Rard J.A. and Miller D.G., “Ternary Solution Mutual Diffusion Coefficients and Densities of Aqueous Mixtures of NaCl and Na_2SO_4 at 298.15 K for Six Different Solute Fractions at a Total Molarity of 1.000 mol·dm^{-3}”, *J. Chem. Eng. Data*, **43** (1998) 668.

6. Alimadadian A. and Colver C.P., “A New Technique for the Measurement of Ternary Molecular Diffusion Coefficients in Liquid Systems”, *Can. J. Chem. Eng.,* 54 (1976) 208.

7. Alizadeh A., Nieto de Castro C.A., Wakeham W.A., “The theory of the Taylor dispersion for technique for liquid diffusivity measurements”, *Int. J. Thermophys.*, **1** (1980) 243.

8. Aminabhavi T.M. and Munk P., “Diffusion Coefficients of Some Nonideal Liquid Mixtures”, *J. Phys. Chem.*, **84** (1980) 442.

9. Anderson D.K., Hall J.R. and Babb A.L., “Mutual Diffusion in Non-Ideal Binary Liquid Mixtures”, *J. Phys. Chem.*, **62** (1958) 404.

10. Anderson D.K. and Babb A.L., “Mutual Diffusion in Non-Ideal Liquid Mixtures. II. Diethyl Ether-Chloroform”, *J. Phys. Chem.*, **65** (1961) 1281.

11. Anderson D.K. and Babb A.L., “Mutual Diffusion in Non-Ideal Liquid Mixtures. III. Methyl Ethyl Ketone-Carbon Tetrachloride and Acetic Acid-Carbon Tetrachloride”, *J. Phys. Chem.*, **66** (1962) 899.

12. Aris R., “On the Dispersion of a Solute in a Fluid Flowing through a Tube”, *Proceed. Royal Soc. of London, Series A*, **235** (1956) 67.

13. Bailey H.R. and Gogarty W.B., “Diffusion Coefficients from Capillary Flow”, *SPE J.,* SPE302 (1963) 256.

14. Baldauf W. and Knapp H., “Measurements of diffusivities in liquids by the dispersion method”, *Chem. Eng. Sci.,* **38** (1983) 1031.

15. Bardow A., Marguardt W., Goke V., Koss H.-J. and Lucas K., “Model-Based Measurement of Diffusion Using Raman Spectroscopy”, *AIChE J.,* **49** (2003) 323.

16. Barnes C., “Measurements of Diffusion Coefficients by Diaphragm Cell Method”, *J. Appl. Phys.,* **5** (1934) 4.

17. Bidlack D.L. and Anderson D.K., “Mutual Diffusion in the Liquid System Hexane-Hexadecane”, *J. Phys. Chem.*, **68** (1964) 206.

18. Bondi A., “van der Waals Volumes and Radii”, *J. Phys. Chem.,* **68** (1964) 441.

19. Bondi A., “Physical Properties of Molecular Crystals, Liquids, and Glasses”, Wiley, New York, 1968.

20. Boon J.P. and Yip S., “Molecular Hydrodynamics”, Dover, New York, 1991.

21. Burchard J.K. and Toor H.L., “Diffusion in an Ideal Mixture of Three Completely Miscible Non-Electrolytic Liquids-Toluene, Chlorobenzene, Bromobenzene”, *J. Phys. Chem.,* **66** (1962) 2015.

22. Burchard J.K. and Toor H.L., “Diffusion in the Three Component Liquid System Methyl Alcohol-*n*-Propyl Alcohol-Isobutyl Alcohol”, *J. Phys. Chem.,* **67** (1963) 540.

23. Calus W.F. and Tyn M.T., “Temperature and Concentration Dependence of Diffusion Coefficient in Benzene-n-Heptane Mixtures”, *J. Chem. Eng. Data,* **18** (1973) 377.

24. Carrington A. and McLachlan A.D., “Introduction to Magnetic Resonance”, Chapman and Hall, London, 1967.

25. Casimir H.B.G., ”On Onsager's Principle of Microscopic Reversibility”, *Rev. Mod. Phys.*, **17** (1945) 343

26. Cohen M.H. and Turnbull D., “Molecular Transport in Liquids and Gases”, *J. Chem. Phys.*, **31** (1959) 1164.

27. Cullinan H.T. and Toor H.L., “Diffusion in the Three-Component Liquid System Acetone-Benzene-Carbon Tetrachloride”, *J. Phys. Chem*., **69** (1965) 3941.

28. Cullinan H.T., Cusick M.R., “Predictive Theory for Multicomponent Diffusion Coefficients”, *Ind. Eng. Chem. Fundam.,* **6** (1967) 73.

29. Cummings P.T., Evans D.J., “Nonequilibrium molecular dynamics approaches to transport properties and non-Newtonian fluid rheology”, *Ind. Eng. Chem. Res.,* **31** (1992) 1237.

30. Cussler E.L., Jr. and Lightfoot E.N., “Multicomponent Diffusion Involving High Polymers. I. Diffusion of Monodisperse Polystyrene in Mixed Solvents” and “Multicomponent Diffusion Involving High Polymers. III. Ternary Diffusion in the System Polystyrene 1-Polystyrene 2-Toluene”, *J. Phys. Chem.,* **69** (1965) 1135 and 2875.

31. Cussler E.L., Jr. and Dunlop P.J., ”An Experimental Comparison of the Gouy and the Diaphragm Cell Methods for Studying Isothermal Ternary Diffusion”, *J. Phys. Chem.,* **70** (1966) 1880.

32. Cussler E.L., “Diffusion mass transfer in fluid systems”, Cambridge University Press, Cambridge, 1997.

33. Danner R.P. and High M.S., “Polymer Solution Handbook”, Design Institute for Physical Property Data, American Institute of Chemical Engineers, 1992

34. Darken L.S., "Diffusion, Mobility and Their Interrelation through Free Energy in Binary Metallic Systems”, *Trans. Am. Inst. Mining Met. Eng.,* **175** (1948) 184.

35. Delhommelle J. and Milli'e P., ”Inadequacy of the Lorentz-Berthelot combining rules for accurate predictions of equilibrium properties by molecular simulation.”, *Mol. Phys.*, **99** (2001) 619.

36. Derlacki Z.J., Easteal A.J., Edge A.V.J., Woolf L.A. and Roksandic Z., “Diffusion Coefficients of Methanol and Water and the Mutual Diffusion Coefficient in Methanol-Water Solutions at 278 and 298 K”, *J. Phys. Chem.*, **89** (1985) 5318.

37. Douglass D.C. and McCall D.W., “Diffusion in Paraffin Hydrocarbons”, *J. Phys. Chem.,* **62** (1958) 1102.

38. Duda J.L., Ni J.L. and Vrentas J.S., “An Equation Relating Self-Diffusion and Mutual Diffusion Coefficients in Polymer-Solvent Systems“, *Macromolecules*, **12** (1979) 459.

39. Dullien F.A.L., PhD thesis, University of British Columbia, Vancouver, Canada, 1961.

40. Dullien F.A.L., “Porous Media: Fluid Transport and Pore Structure”, Academic Press, Inc., New York, 1979.

41. Dullien F.A.L. and Asfour A.-F., “Concentration Dependence of Mutual Diffusion Coefficients in Regular Binary Solutions: A New Predictive Equation”, *Ind. Eng. Chem. Fundam.,* **24** (1985) 1.

42. Dunlop P.J. and Gosting L.J., “Interacting Flows in Liquid Diffusion: Expressions for the Solute Concentration Curves in Free Diffusion, and their Use in Interpreting Gouy Diffusiometer Data for Aqueous Three-component Systems”, *J. Am. Chem. Soc.,* **77** (1955) 5238.

43. Dunlop P.J., “A Study of Interacting Flows in Diffusion of the System Raffinose-KCl-H_20 at 25°”, and “Interacting Flows in Diffusion of the System Raffinose–Urea–Water“, *J. Phys. Chem.,* **61** (1957) 994, 1619.

44. Dunlop P.J., “Data for Diffusion in Concentrated Solution of the System NaCl–KCl–H_2O at 25°: A Test of the Onsager Reciprocal Relation for this Composition”, *J. Phys. Chem.,* **63** (1959) 612.

45. Dzugutov M., “A Universal Scaling Law for Atomic Diffusion in Condensed Matter”, *Letters to Nature*, **381** (1996) 137.

46. Einstein A., “Über die von der molekularkinetischen Theorie der Wärme geforderte Bewegung von in ruhenden Flüssigkeiten suspendierten Teilchen (On the motion of small particles suspended in liquids at rest required by the molecular-kinetic theory of heat)”, *Annalen der Physik und Chemie, IV. Folge,* **17** (1905) 549 (in German).

47. Fei W. and Bart H.-J., “Prediction of Diffusivities in Liquids”, *Chem. Eng. Technol.,* **21** (1998) 659

48. Fick A. E., “Uber Diusion (Super Diffusion)”, *Annalen der Physik und Chemie von J.C. Poggendor,* **94** (1855) 59 (in German).

49. H. Fujita and L.J. Gosting, “A New Procedure for Calculating the Four Diffusion Coefficients of Three-Component Systems From Gouy Diffusiometer Data”, *J. Phys. Chem.,* **64** (1960) 1256.

50. Galliero G., Duguay B., Caltagirone J.-P. and Montel F., “Thermal diffusion sensitivity to the molecular parameters of a binary equimolar mixture, a non-equilibrium molecular dynamics approach”, *Fluid Phase Equil.*, **208** (2003) 171.

51. Galliero G., Medvedev O.O. and Shapiro A.A., ”Molecular Dynamics Simulations of the Penetration Lengths: Application within the Fluctuation Theory for Diffusion Coefficients”, *Physica A*, (2005) *in press*.

52. Gardiner C.W., “Handbook of Stochastic Methods”, Springer-Verlag, 2004

53. van Geet A.L. and Adamson A.W., “Diffusion in Liquid Hydrocarbon Mixtures”, *J. Phys. Chem.*, **68** (1964) 238.

54. Ghai R.K. and Dullien F.A.L., “Diffusivities and Viscosities of Some Binary Liquid Nonelectrolytes at 25 C”, *J. Phys. Chem.,* **78** (1974) 2283.

55. Glasstone S., Ladier K.J. and Eyring H., “The Theory of Rate Processes”, McGraw-Hill, New York, 1941.

56. Gollings A.F., Hall D.C., Mills R. and Woolf L.A., “A conductance-monitored diaphragm cell for diffusion measurements”, *J. Phys. E: Sci. Instrum.,* **4** (1971) 425.

57. Gosting L.J., Hanson E.M., Kegeles G., Morris M.S., “The theory of an interference method for the study of diffusion“, *Rev. Sci. Instr.,* **20** (1949) 209.

58. Graham T., “On the Law of Diffusion of Gases”, *Philosophical Magazine,* **2** (1833) 175, 269, 351.

59. Graham T., “On the motion of gases”, *Phil. Trans.*, **140** (1850) 805.

60. Green M.S., “Markoff random processes and the statistical mechanics of time-dependent phenomena. II. Irreversible processes in fluids”, *J. Chem. Phys.,* **22** (1954) 398.

61. de Groot S.R. and Mazur P., “Non-Equilibrium Thermodynamics”, Amsterdam: North Holland, 1962.

62. Gross J. and Sadowski G., “Perturbed-Chain SAFT: An Equation of State Based on a Perturbation Theory for Chain Molecules”, *Ind. Eng. Chem. Res.*, **40** (2001) 1244.

63. Guarino G., Ortona O., Sartorio R. and Vitagliano V., “Diffusion, Viscosity, and Refractivity Data on the Systems Dimethylformamide-Water and N-Methylpyrrolidone-Water at 5C”, *J. Chem. Eng. Data*, **30** (1985) 366.

64. Haase R., “Thermodynamics of Irreversible Processes”, London: Addison-Wesley, 1969.

65. Hahn E.L., “Spin Echoes”, *Phys. Rev.,* **80** (1950) 580.

66. Haile J.M., “Molecular Dynamics Simulation: Elementary Methods”, John Wiley & Sons, New York, 1992.

67. Hammond B.R. and Stokes R.H., *Trans. Faraday Soc.,* 49 (1953) 890.

68. Hampe M.J., Shermuly W. and Blaβ E., "Decrease of diffusion coefficients near binodal states of liquid-liquid systems", *Chem. Eng. Techn.,* **14** (1991) 219.

69. Harris K.R., Pua C.K.N. and Dunlop P.J., "Mutual and Tracer Diffusion Coefficients and Frictional Coefficients for the Systems Benzene-Chlorobenzene, Benzene-n-Hexane, and Benzene-n-Heptane at 25 C", *J. Phys. Chem.*, **74** (1970) 3518.

70. Hartley G.S. and Crank J., *Trans. Faraday Soc.,* **52** (1956) 619

71. Heyes D.M., "Molecular dynamics simulation of liquid binary mixtures: partial properties of mixing and transport coefficients", *J. Chem. Phys.,* **96** (1992) 2217.

72. Hirschfelder J.O., Curtiss C.F. and Bird R.B., "Molecular Theory of Gases and Liquids", Wiley, New York, 1954.

73. Hoheisel C., "Transport Properties of Molecular Liquids", *Phys. Rep.,* **245** (1994) 111.

74. Hsu Y.-D. and Chen Y.-P., "Correlation of the Mutual Diffusion Coefficients of Binary Liquid Mixtures", *Fluid Phas. Equil.,* **152** (1998) 149.

75. Hsu Y.-D. and Chen Y.-P., "A Group Contribution Correlation of the Mutual Diffusion Coefficients of Binary Liquid Mixtures", *Fluid Phas. Equil.,* **173** (2000) 1.

76. IVC-SEP, Department of Chemical Engineering, Technical University of Denmark, "SPECS project", web-site: http://www.ivc-sep.kt.dtu.dk/research/specs.htm

77. Keffer D.J. and Adhangale P., "The Composition Dependence of Self and Transport Diffusivities from Molecular Dynamics Simulations", *Chem. Eng. J.*, **100** (2004) 51.

78. Kelly C.M., Wirth G.B. and Anderson D.K., "Tracer and Mutual Diffusivities in the System Chloroform-Carbon Tetrachloride at 25C", *J. Phys. Chem.,* **75** (1971) 3293.

79. Kett T.K. and Anderson D.K., "Multicomponent Diffusion in Nonassociating, Nonelectrolyte Solutions", *J. Phys. Chem.,* **73** (1969) 1262.

80. Kett T.K. and Anderson D.K., "Ternary Isothermal Diffusion and the Validity of the Onsager Reciprocal Relations in Nonassociating Systems", *J. Phys. Chem.,* **73** (1969) 1268.

81. King C.J., Hsueh L. and Mao K.-W., "Liquid Phase Diffusion of Non-electrolytes at High Dilution.", *J. Chem. Eng. Data.,* **10** (1965) 348.

82. Kirkwood J.G., Baldwin R.L., Dunlop P.J., Gosting L.J. and Kegeles G, *J. Chem. Phys.*, **33** (1960) 1505.

83. Kong C.L., “Combining rules for intermolecular potential parameters. II. Rules for the Lennard-Jones (12-6) potential and the Morse potential”, *J. Chem. Phys.*, **59** (1973) 2464.

84. Kooijman H.A. and Taylor R., “Estimation of Diffusion Coefficients in Multicomponent Liquid Systems”, *Ind. Eng. Chem. Res.,* **30** (1991) 1217.

85. Korean Thermophysical Properties Databank, web-site: http://infosys.korea.ac.kr/kdb/

86. Krishna R., “Ternary Mass Transfer in a Wetted Wall Column. Significance of Diffusional Interactions. Part II: Equimolar diffusion”, *Trans. Inst. Chem. Eng.,* **59** (1981) 44.

87. Krishna R. and Wesselingh J.A., “The Maxwell-Stefan Approach to Mass Transfer”, *Chem. Eng. Sci.*, **52** (1997) 861.

88. Kubo R., “Statistical-mechanical theory of irreversible processes. I. General theory and simple applications to magnetic and conduction problems”, *J. Phys. Soc. Japan*, **12** (1957) 570.

89. Kubo R., “The fluctuation-dissipation theorem”, *Rep. Prog. Phys.*, **29** (1966) 255.

90. Kulkarni M.V., Allen G.F. and Lyons P.A., “Diffusion in Carbon Tetrachloride-Cyclohexane Solutions”, *J. Phys. Chem.*, **69** (1965) 2491.

91. Lee Y.E. and Li S.F.Y., “Binary Diffusion Coefficients of the Methanol/Water System in the Temperature range 30-40 C”, *J. Chem. Eng. Data*, **36** (1991) 240.

92. Leffler J. and Cullinan H.T. Jr., “Variation of Liquid Diffusion Coefficients with Composition”, *I&EC Fundamentals,* **9** (1970) 84.

93. Liu H., Silva C.M. and Macedo E.A., “Generalized Free Volume Theory for Transport Properties and New Trends About the Relationship between Free Volume and Equations of State”, *Fluid Phas. Equil.,* **202** (2002) 89.

94. Liu H., Silva C.M. and Macedo E.A., “Unified approach to the self-diffusion coefficients of dense fluids over wide ranges of temperature and pressure--hard-sphere, square-well, Lennard-Jones and real substances”, *Chem. Eng. Sci.*, **53** (1998) 2403.

95. Lo H.Y., “Diffusion Coefficients in Binary Liquid n-Alkane Systems”, *J. Chem. Eng. Data*, **19** (1974) 236.

96. Lo P.Y. and Myerson A.S., “Ternary diffusion coefficients in metastable solutions of glycine-valine-H20.” *AIChE J.,* **35** (1989) 676.

97. Maxwell J.C., “Illustrations of the Dynamical Theory of Gases”*,*1859.

98. McCall D.W. and Douglas D.D., “Diffusion in Binary Solutions” *J. Phys. Chem.*, **71** (1967) 987.

99. Medvedev O.O. and Shapiro A.A., “Verifying Reciprocal Relations for Experimental Diffusion Coefficients in Multicomponent Mixtures“, *Fluid Phase Equil.*, **208** (2003) 291.

100. Medvedev O.O. and Shapiro A.A., “Modeling Diffusion Coefficients in Binary Mixtures”, *Fluid Phase Equil.*, **225C** (2004) 13.

101. Melzer W.-M., Baldauf W. and Knapp H., ”Measurement of Diffusivitiy, Viscosity, Density and Refractivity of Eight Binary Liquid Mixtures”, *Chem. Eng. Proc.*, **26** (1989) 71.

102. Mewes B., Bauer G. and Brueggemann D., “Remote Sensing - Fuel vapor measurements by linear Raman spectroscopy using spectral discrimination from droplet interferences”, *Appl. Opt.,* **38** (1999) 1040.

103. Michelsen M.L., “A method for incorporating excess Gibbs energy models in equations of state” and “A modified Huron-Vidal mixing rule for cubic equations of state”, *Fluid Phase Equil.*, **60** (1990) 47, 213.

104. Michelsen M.L., Mollerup J.M., “Thermodynamic Models: Fundamentals & Computational Aspects”, Tie-Line Publications, Copenhagen, 2004.

105. Miller D.G., “Ternary Isothermal Diffusion and the Validity of the Onsager Reciprocity Relations”, *J. Phys. Chem.*, **63** (1959) 570.

106. Miller D.G., ”Definitive Test of the Onsager Reciprocal Relations in Isothermal Ternary Diffusion of Water--Sodium Chloride--Potassium Chloride”, *J. Phys. Chem.*, **69** (1965) 3374.

107. Miller D.G., *J. Solut. Chem.,* **10** (1981) 831.

108. Miller D.G, Vitagliano V. and Sartorio R., “Some Comments on Multicomponent Diffusion: Negative Main Term Diffusion Coefficients, Second Law Constraints, Solvent Choices, and Reference Frame Transformations”, *J. Phys. Chem.*, **90** (1986) 1509.

109. Miller D.G., “A method for obtaining multicomponent diffusion coefficients directly from Rayleigh and Gouy fringe position data”, *J. Phys. Chem.,* **92** (1988) 4222.

110. Mills R., Woolf L.A. and Watts R.O., *AIChE J.*, **14** (1968) 671.

111. Modell M. and Reid R.C., “Thermodynamics and Its Applications”, Prentice-Hall, Englewood Cliffs, NJ, 1974.

112. Mori H., “A Continued-Fraction Representation of the Time-Correlation Functions” and “Transport, Collective Motion, and Brownian Motion”, *Progr of Theor. Physics,* **34** (1965) 399 and 423.

113. Mortimer R.G. and Clark N.H., “Transitions State Theory for Diffusion Coefficients in Multicomponent Liquids”, *Ind. Eng. Chem. Fundam.,* **10** (1971) 604.

114. Mortimer R.G. and Hicks B.C., “Experimental study of the temperature dependence of multicomponent isothermal diffusion coefficients”, *J. Phys. Chem.,* **80** (1976) 1376.

115. Nelder J.A. and Mead R., “A simplex method for function minimization”, *Computer Journal,* **7** (1965) 308.

116. Onsager L., “Reciprocal Relations in Irreversible Processes. I.”, *Phys. Rev.*, **37** (1931) 405 and “Reciprocal Relations in Irreversible Processes. II.“, *idem*, **38** (1931) 2265.

117. Onsager L., “Theories and problems of liquid diffusion”, *Ann. N.Y. Acad. Sci.*, **46** (1945) 241.

118. Padrel de Oliviera C.M., Fareleira J.M.N.A. and Nieto de Castro C.A., “Mutual Diffusivity in Binary Mixtures of n-Heptane with n-Hexane Isomers”, *Int. J. Thermophys*., **10** (1989) 973.

119. Pertler M., Blass E. and Stevens G.W., “Fickian Diffusion in Binary Mixtures That Form Two Liquid Phases”, *AIChE J.*, **42** (1996) 910.

120. Poling B.E., Prausnitz J.M. and O' Connell J., ”The Properties of Gases and Liquids”, McGraw-Hill Higher Education, Fifth Edition, New York, 2000.

121. Rai G.P. and Cullinan H.T., “Diffusion Coefficients of Quaternary Liquid System Acetone-Benzene-Carbon Tetrachloride-n-Hexane at 25 C”, *J. Chem. Eng. Data,* **18** (1973) 213.

122. Ramakanth C., Mukherjee A.K. and Das T.R., “Diffusion Coefficients for Selected Binary Liquid Systems: Cyclohexanes and n-Alkyl Alcohols”, *J. Chem. Eng. Data*, **36** (1991) 384.

123. Ramprasad G., Mukherjee A.K. and Das T.R., “Mutual Diffusion Coefficients of Some Binary Liquid Systems: Benzene-n-Alkyl Alcohol”, *J. Chem. Eng. Data*, **36** (1991) 124.

124. Reid R.C., Prausntiz J.M. and Poling B.E., “The Properties of Gases and Liquids”, Fourth Edition, McGraw-Hill Book Company, New York, 1987

125. Revzin A., “New procedure for calculating the four diffusion coefficients for ternary systems from Gouy optical data. Application to data for the system potassium bromide-hydrobromic acid-water”, *J. Phys. Chem.,* **76** (1972) 3419.

126. Riede Th. and Shlunder E.-U., “Diffusivities of the ternary liquid mixture 2-propanol—water—glycerol and three-component mass transfer in liquids”, *Chem. Eng. Sci*., **46** (1991) 609.

127. Rigby S.P. and Gladden L.F., “The prediction of transport properties of porous media using fractal models and NMR experimental techniques”, *Chem. Eng. Sci.*, **54** (1999) 3503.

128. Robinson R.A. and Stokes R.H., “Electrolyte Solutions”, Butterworth, London, UK, 1960.

129. Robinson R.L., Edmister W.G. and Dullien F.A.L., “Calculation of Diffusion Coefficients from Diaphragm Cell Diffusion Data”, *J. Phys. Chem.*, **69** (1965) 258.

130. Rodwin L., Harpst J.A. and Lyons P.A., “Diffusion in the System Cyclohexane-Benzene”, *J.Phys.Chem.*, **69** (1965) 2783.

131. Rowley R.L., Yi S.C., Gubler V. and Stoker J.M., “Mutual Diffusivity, Thermal Conductivity, and Heat of Transport in Binary Liquid Mixtures of Alkanes in Carbon Tetrachloride”, *Fluid Phase Equil*., **36** (1987) 219.

132. Rowley R.L., Yi S.C., Gubler V. and Stoker J.M., “Mutual Diffusivity, Thermal Conductivity, and Heat of Transport in Binary Liquid Mixtures of Alkanes in Chloroform”, *J. Chem. Eng. Data*, **33** (1988) 362.

133. Rowley R.L. and Painter M.M., “Diffusion and Viscosity Equations of State for a Lennard-Jones Fluid Obtained from Molecular Dynamics Simulations”, *Int. J. Thermophys*., **18** (1997) 1109.

134. Rutten W.M., “Diffusion in Liquids”, PhD thesis, Delft: Delft University Press, The Netherlands, 1992.

135. Sanchez V. and Cliffton M., “Mutual Diffusion Coefficients in Binary Mixtures of Carbon Tetrachloride and Alcohols at 20 C”, *J. Chem. Eng. Data*, **23** (1978) 209.

136. Sanni S.A., Fell C.J.D. and Hutchison H.P., “Diffusion Coefficients and Densities for Binary Organic Liquid Mixtures”, *J. Chem. Eng. Data*, **16** (1971) 424.

137. Sanni S.A. and Hutchison P., “Diffusivities and Densities for Binary Liquid Mixtures”, *J. Chem. Eng. Data*, **18** (1973) 317.

138. Schanik H.M., Luo H., and Hoheisel C., “Molecular Dynamics Calculation of the Transport Coefficients of Liquid Benzene+Cyclohexane Mixtures Using Six-Center Lennard-Jones potentials”, *J. Chem. Phys.,* **99** (1993) 9912.

139. Schmoll J. and Hertz H.G., *Zeitschrift fur Physikalische Chemie*, 194 (1996) 193.

140. Sen P.N., Schwartz L.M., Mitra P.P. and Halperin B.I., “Surface relaxation and the long-time diffusion coefficient in porous media:Periodic geometries”, *Phys. Rev. B*, **49** (1994) 215.

141. Shapiro A.A. and Stenby E.H., “Factorization of Transport Coefficients in Macroporous Media”, *Transp. Porous Media,* **16** (2000) 305.

142. Shapiro A.A. and Stenby E.H., “Diagonal Non-Equilibrium Thermodynamic and Modeling Transport Coefficients”, in: W. Kohler, S. Wiegand (Eds.), “Thermal Nonequilibrium Phenomena in Fluid Mixtures”, Lecture Notes on Physics, Heidelberg: Springer, 2001.

143. Shapiro A.A., “Evaluation of Diffusion Coefficients in Multicomponent Mixtures by Means of the Fluctuation Theory”, *Physica A*, **320** (2003) 211.

144. Shapiro A.A., “Fluctuation Theory for Transport Properties in Multicomponent Mixtures: Thermodiffusion and Heat Conductivity”, *Physica A*, **322** (2004) 151.

145. Shapiro A.A., Davis P.K. and Duda J.L., “Diffusion in multicomponent mixtures”, in: R. Gani and G.K. Kontogeorgis (Eds.), “Computer Aided Property Estimation”, Amsterdam: Elsevier, 2004.

146. Shieh J.C. and Lyons P.A., “Transport Properties of Liquid n-Alkanes”, *J. Phys. Chem.*, **17** (1969) 3258.

147. Shroff G.H. and Shemilt L.W., “Liquid Diffusivities for the System n-Propanol-Toluene”, *J. Chem. Eng. Data*, **11** (1966) 183.

148. Shuck F.O. and Toor H.L., ”Diffusion in the Three Component Liquid System Methyl Alcohol-n-Propyl Alcohol-Isobutyl Alcohol”, *Chem. Eng. Sci.*, **67** (1963) 540.

149. Stocker J.M. and Rowley R.L., *J. Chem. Phys.*, **91** (1989) 3670.

150. Stokes G.G., "On the effect of the internal friction of fluids on the motion of pendulums", *Trans. Cambridge Phil. Soc.*, **9** (1850) 5.

151. Subramanian S., “Minimum Error Fickian Diffusion Coefficients for Mass Diffusion in Multicomponent Gas Mixtures”, *J. Non-Equilib. Thermodyn.*, **24**, 1 (1999).

152. Sun T. and Teja A.S., ”Vapor-Liquid and Solid-Fluid Equilibrium Calculations Using a Lennard-Jones Equation of State”, *Ind. Eng. Chem. Res.*, **37** (1998) 3151.

153. Sundelöf L.-O., Acosta R. and Nyström B., “Sedimentation in Multicomponent Systems. II. Sedimentation of Blue Dextran in Aqueous Solutions of Dextran and of Hydroxypropyl Cellulose.”, *Chemica Scripta* **18** (1981) 7.

154. [Sun81] Sundelöf L.-O., *J. Chem. Soc., Faraday Trans. 2*, **77**, 1779 (1981).

155. Tasic A.Z., Djordjevic B.D., Serbanovic S.P., Grozdanic D.K., “Diffusion coefficients for the liquid system acetone-cyclohexane at 298.15 K”, *J. Chem. Eng. Data*, **26** (1981) 118.

156. Taylor G.I., “Dispersion of Soluble Matter in Solvent Flowing Slowly through a Tube”, *Proc. Royal Soc. of London, Series A*, **219** (1953) 186.

157. Taylor R., Krishna R., “Multicomponent Mass Transfer”, Wiley-Interscience, 1993.

158. Tyn M.T. and Calus W.F., “Temperature and Concentration Dependence of Mutual Diffusion Coefficients of Some Binary Liquid Systems”, *J. Chem. Eng. Data*, **20** (1975) 310.

159. Usmanova A.A., Vostretsov M.N., Bickbulatov A.S. and Diakonov S.G., “Thermophysical Properties of the Substances”, USSR State Bureau on the Standard Reference Data, **17** (1982) 122 (*in Russian*).

160. Vergara A., Paduano L. and Sartorio R., “Multicomponent Diffusion in Systems Containing Molecules of Different Size. 4. Mutual Diffusion in the Ternary System Tetra(ethylene glycol)-Di(ethylene glycol)-Water”, *J. Phys. Chem.,* **105** (2001) 328.

161. Vignes A., ”Diffusion in Binary Solution”, *Ind. Eng. Chem. Fundamentals*, **5** (1966) 189.

162. Visual Numerics™, “IMSL. Fortran Subroutines for Mathematical Applications”, version 3.0, 1997.

163. Vitagliano V, Zagari A. and Sartorio R, “Diffusion and Viscosity in $CHCl_3$-CH_3COOH System at 25 C”, *J. Chem. Eng. Data*, **18** (1973) 370.

164. Waldman M. and Hagler A.T., “New Combining Rules for Rare Gas van der Waals Parameters”, *J. Comput. Chem.*, **14** (1993) 1077.

165. Wedlake G.D. and Dullien F.A.L., “Interdiffusion and Density Measurements in Some Binary Liquid Mixtures”, *J. Chem. Eng. Data*, **19** (1974) 229.

166. Wendt R.P., “Studies of Isothermal Diffusion at 25° in the System Water-Sodium Sulfate-Sulfuric Acid and Tests of the Onsager Relation”, *J. Phys. Chem.,* **66** (1962) 1279.

167. Wesselingh J.A. and Krishna R., “Elements of Mass Transfer”, Ellis Horwood: Chichester, U.K., 1990

168. Wesselingh J.A. and Bolen A.M., “Multicomponent Diffusivities From the Free Volume Theory”, *Trans. IChemE.*, **75** (1997) 590

169. Wesselingh J.A. and Krishna R., “Mass Transfer in Multicomponent Mixtures”, Delft: Delft Academy Press, 2000.

170. Wild A., “Multicomponent Diffusion in Liquids“, Dusseldorf: VDI Verlog GmbH, 2003.

171. Wilke C.R. and Chang P.C., “Correlation of Diffusion Coefficients in Dilute Solutions”, *AIChE J.,* **1** (1955) 264.

172. Wu J., Albright J.G. and Miller D.G., “Isothermal Diffusion Coefficients for NaCl-MgCl2-H2O. 6. Concentration Ratios 3:1, 1:1, and 1:3 near Saturation at 35.degree.C”, *J. Phys. Chem.,* **98** (1994) 13054.

173. Yakoumis I.V., Kontogeorgis G.K., Voutsas E.C. and Tassios D.P., “Vapor-liquid equilibria for alcohol/hydrocarbon systems using the CPA Equation of state”, *Fluid Phase Equil.*, **130** (1997) 31

174. Zabaloy M.S., Machado J.M.V. and Macedo E.A., “A Study of Lennard-Jones Equivalent Analytical Relationships for Modeling Viscosities”, *Int. J. Thermophys.*, 22 (2001) 829.

175. Zhu Y., Xiaohua L., Zhou J., Wang Y. and Shi J., “Prediction of Diffusion Coefficients for Gas, Liquid and Supercritical Fluid: Application to Pure Real Fluids and Infinite Dilute Binary Solutions Based on the Simulation of Lennard-Jones Fluid”, *Fluid Phase Equil.*, 194 (2002) 1141.

176. Zhou Y. and Miller G.H., “Mutual diffusion in binary Ar-Kr mixtures and empirical diffusion model”, *Phys. Rev. E.,* **53** (1996) 1587.

177. Zielinski J.M. and Hanley B.F., “Practical Friction-Based Approach to Modeling Multicomponent Diffusion”, *AIChE J.,* **45** (1999) 1.

Appendix

A.1 Residual Internal Energy

he aim of this section is to derive an expression for the residual contribution to internal energy in the T,P,n_i system of coordinates.

he starting point of the derivations is the expression for internal energy in terms of the residual Helmholtz free energy and entropy

$$U^r\left(T,P,n_i\right)=A^r\left(T,P,n_i\right)+TS^r\left(T,P,n_i\right). \tag{A.1.1}$$

he residual Helmholtz free energy is expressed as follows [104]

$$A^r\left(T,P,n_i\right)=G^r\left(T,P,n_i\right)-PV+nRT\,. \tag{A.1.2}$$

he residual entropy is expressed as

$$S^r\left(T,P,n_i\right)=\left(H^r\left(T,P,n_i\right)-G^r\left(T,P,n_i\right)\right)/T\,. \tag{A.1.3}$$

he residual Gibbs energy and the enthalpy are expressed in the terms of the fugacity coefficients [104]

$$\begin{aligned} G^r\left(T,P,n_i\right)&=RT\sum n_i\ln\phi_i \\ H^r\left(T,P,n_i\right)&=-RT^2\sum n_i\left(\frac{\partial\ln\phi_i}{\partial T}\right)_{P,n} \end{aligned}\,. \tag{A.1.4}$$

Substitution of Eq. (A.1.4) in Eq. (A.1.2) results in the following expression for the residual Helmholtz energy and entropy

$$A^r\left(T,P,n_i\right)=RT\sum n_i\ln\phi_i-PV+nRT\,, \tag{A.1.5}$$

$$S^r\left(T,P,n_i\right)=-RT\sum n_i\left(\frac{\partial\ln\phi_i}{\partial T}\right)_{P,n}-R\sum n_i\ln\phi_i\,. \tag{A.1.6}$$

he residual internal energy is

$$U^r\left(T,P,n_i\right)=-PV+nRT-RT^2\sum n_i\left(\frac{\partial\ln\phi_i}{\partial T}\right)_{P,n}\,. \tag{A.1. }$$

ransformation to the specific residual energy is carried out by dividing the final expression (A.1.) by the molar volume (change of the system of coordinates)

$$U^r\left(T,P,N_i\right)=-P+NRT-RT^2\sum N_i\left(\frac{\partial\ln\phi_i}{\partial T}\right)_{P,n}\,. \tag{A.1.8}$$

A.2 Derivatives of Residual Internal Energy

he specific internal residual energy is expressed in variables T,P,N_i., according to the previous appendix. We wish to estimate the following derivatives of internal energy

$\partial U/\partial N_i\big|_{T,V,\mathbf{N}}$ and $\partial U/\partial T\big|_{T,V,\mathbf{N}}$.

he solution to this problem is as follows.

he full derivative of the internal energy is

$$dU\left(T,P,\mathbf{N}\right)=\left.\frac{\partial U}{\partial T}\right|_{T,P,\mathbf{N}}dT+\left.\frac{\partial U}{\partial P}\right|_{T,P,\mathbf{N}}dP+\left.\frac{\partial U}{\partial N_i}\right|_{T,P,\mathbf{N}}dN_i$$

he full derivative of pressure in coordinates T,V,N_i is

$$dP=\left.\frac{\partial P}{\partial T}\right|_{T,V,\mathbf{N}}dT+\left.\frac{\partial P}{\partial V}\right|_{T,V,\mathbf{N}}dV+\left.\frac{\partial P}{\partial N_i}\right|_{T,V,\mathbf{N}}dN_i$$

Hence, correspondingly

$$\left.\frac{\partial U}{\partial T}\right|_{T,V,\mathbf{N}}=\left.\frac{\partial U}{\partial T}\right|_{T,P,\mathbf{N}}-\left.\frac{\partial U}{\partial P}\right|_{T,P,\mathbf{N}}\left.\frac{\partial P}{\partial T}\right|_{T,V,\mathbf{N}}. \qquad \text{(A.2.1)}$$

$$\left.\frac{\partial U}{\partial N_i}\right|_{T,V,\mathbf{N}}=\left.\frac{\partial U}{\partial N_i}\right|_{T,P,\mathbf{N}}-\left.\frac{\partial U}{\partial P}\right|_{T,P,\mathbf{N}}\left.\frac{\partial P}{\partial N_i}\right|_{T,V,\mathbf{N}}. \qquad \text{(A.2.2)}$$

he derivatives in coordinates T,V,N_i in Eqs. (A.2.1), (A.2.2) are easily estimated with the help of thermodynamic simulator or from straightforward differentiation of a thermodynamic EoS.

A.3 Verifying the Approach for Estimating the Thermodynamic Matrix

he method developed for estimation of the thermodynamic matrix (Chapter 5, section 5.1) must be verified to check its consistency and consistency of its implementation into the code for modeling diffusion coefficients.

Possible consistency checks for the thermodynamic quantities (such as fugacity coefficients and their derivatives) [104] are not considered in this study, since all the thermodynamic properties are estimated by the SPECS code, which have proved to be precise and robust [6] and have been tested many times. he only possible errors in the estimation of thermodynamic matrix may either be due to errors in the derivations (see section 5.1) or due to errors in their implementation in the program.

Let us consider the equation for thermodynamic matrix, derived in Chapter 5

$$
\begin{aligned}
&F_{ij} = -\left.\frac{\partial\left(\mu^j/T\right)}{\partial N_i}\right|_{U,V,\mathbf{N}} = -\frac{1}{T}\left.\frac{\partial\mu^j}{\partial N_i}\right|_{U,V,\mathbf{N}} + \frac{\mu^j}{T^2}\left.\frac{\partial T}{\partial N_i}\right|_{U,V,\mathbf{N}}, \left(i,j=1,...,n\right);\\
&F_{i,n+1} = F_{n+1,i} = \left.\frac{\partial\left(1/T\right)}{\partial N_i}\right|_{U,V,\mathbf{N}} = -\frac{1}{T^2}\left.\frac{\partial T}{\partial N_i}\right|_{U,V,\mathbf{N}}, \left(i=1,...,n\right);\\
&F_{n+1,n+1} = \left.\frac{\partial\left(1/T\right)}{\partial U}\right|_{U,V,\mathbf{N}} = -\frac{1}{T^2}\left.\frac{\partial T}{\partial U}\right|_{U,V,\mathbf{N}}
\end{aligned}
\qquad \text{(A.3.1)}
$$

Eq. (A.3.1) involves the derivatives defined in Chapter 5

$$
\begin{aligned}
&\left.\frac{\partial\mu^j}{\partial N_i}\right|_{U,V,\mathbf{N}} = \left.\frac{\partial\mu^j}{\partial N_i}\right|_{T,P,\mathbf{N}} + \left.\frac{\partial\mu^j}{\partial T}\right|_{T,P,\mathbf{N}}\left.\frac{\partial T}{\partial N_i}\right|_{U,V,\mathbf{N}} + \left.\frac{\partial\mu^j}{\partial P}\right|_{T,P,\mathbf{N}}\left.\frac{\partial P}{\partial N_i}\right|_{U,V,\mathbf{N}},\\
&\left.\frac{\partial P}{\partial N_i}\right|_{U,V,\mathbf{N}} = \left.\frac{\partial P}{\partial N_i}\right|_{T,V,\mathbf{N}} + \left.\frac{\partial P}{\partial T}\right|_{T,V,\mathbf{N}}\left.\frac{\partial T}{\partial N_i}\right|_{U,V,\mathbf{N}},\\
&\left.\frac{\partial T}{\partial N_i}\right|_{U,V,\mathbf{N}} = -\frac{\left.\partial U/\partial N_i\right|_{T,V,\mathbf{N}}}{\left.\partial U/\partial T\right|_{T,V,\mathbf{N}}},\\
&\left.\frac{\partial T}{\partial U}\right|_{U,V,\mathbf{N}} = \frac{1}{\left.\partial U/\partial T\right|_{T,V,\mathbf{N}}}.
\end{aligned}
\qquad \text{(A.3.2)}
$$

he condition of symmetry of the cross-terms in the thermodynamic matrix can be considered as a good test of the proposed method. his symmetry cannot be immediately seen from the formulae for the cross-term coefficients. he achieved difference between the cross-terms is of the order of 10^{-14} for all the modeled mixtures over the whole concentration range, including dilute limits. t was possible to achieve such a high degree of symmetry only due to the fact that all the derivatives involved in the estimation of the thermodynamic matrix are analytical. Numerical differentiation resulted in a noticeable inaccuracy, especially in the dilute limits, since the Onsager phenomenological coefficients tend to zero at their limits.

Appendix

An example of the values involved in the estimation of the thermodynamic matrix is presented in able A.3.1. t can be seen that the final symmetry of the cross-terms arises from the balance of all the properties involved in the calculation. his indicates the applicability of the proposed approach to estimation of the thermodynamic factor.

able A.3.1 alues of properties, involved in the estimation of the cross-terms in the thermodynamic matrix. Mixture acetone chloroform (molar fractions 0.2 0.8), =298.15K.

Property	*i=1, j=2*	*i=2, j=1*	Symmetry
F_{ij}	-3.712172483835415E-002	-3.712172483835457E-002	10^{-14}
$-\frac{1}{T}\frac{\partial \mu^j}{\partial N_i}\Big\|_{U,V,\mathbf{N}}$	-3.576401564351944E-002	-3.457495352870717E-002	-
$\frac{\mu^j}{T^2}\frac{\partial T}{\partial N_i}\Big\|_{U,V,\mathbf{N}}$	-1.357709194834707E-003	-2.546771309647404E-003	-
$\frac{\partial \mu^j}{\partial N_i}\Big\|_{T,P,\mathbf{N}}$	-0.298623170805454	-0.298623170805454	-
$\frac{\partial \mu^j}{\partial T}\Big\|_{T,P,\mathbf{N}}\frac{\partial T}{\partial N_i}\Big\|_{U,V,\mathbf{N}}$	2.74685335824742	2.45456605968561	-
$\frac{\partial \mu^j}{\partial P}\Big\|_{T,P,\mathbf{N}}\frac{\partial P}{\partial N_i}\Big\|_{U,V,\mathbf{N}}$	8.21481107667335	8.15257950570389	-

A.4 Computational Background

For the purpose of modeling diffusion coefficients a computational FORTRAN95 code was developed, further referred to as the *FTCode*. The structure of the FTCode can be described in the following way:

- Input of all the required data is from a given working folder. The working folders have a unique name and contain a set of text files (Figure A.4.1) consisting of all the required data for estimation of the diffusion coefficients in the given mixture. The only manual input required is specifying the name of the working mixture and the corresponding name of the working folder;
- The kinetic, thermodynamic and coordinate matrices, as well as thermodynamic factor (Chapter 5), for each data point, listed in the file "diffile.txt" are estimated directly and stored;
- The resistance matrix on the basis of the selected expression for the penetration lengths and penetration coefficients, listed in the file "lenfile.txt" is estimated;
- The matrix of the Onsager coefficients is calculated and matrix of the Fick diffusion coefficients estimated for each data point. The total average deviation of the calculated Fick coefficients from the experimental values is then calculated.
- This is followed by multi-parameter optimization of adjusting the penetration coefficients, to achieve the best match of the experimental values. Optimization is carried out using the direct search polytope algorithm [115], incorporated in the IMSL mathematical library [162].
- The optimization results are output into the file in the working folder. For debugging purposes, the information about the matrices and the thermodynamic factor for each data point can also be stored in the working folder.

The developed FTCode is adjustable. It is written in a transparent manner and thoroughly commented. Thus, it is easy to extend and to modify this code. The code for calculation of each matrix is written in a separate file, with local variables defined in the corresponding module file. The computer code is optimized for easy "reading", rather than for maximum performance. A typical time of the optimization run (3 subsequent optimization cycles) for a binary mixture with around 70 experimental data points is 10-20 seconds on a PC with Pentium 4, 2.8GHz processor and 512Mb of RAM. The main time costs are due to the large amount of data being stored for debugging purposes and due to the procedure of calling the SPECS computational subroutines.

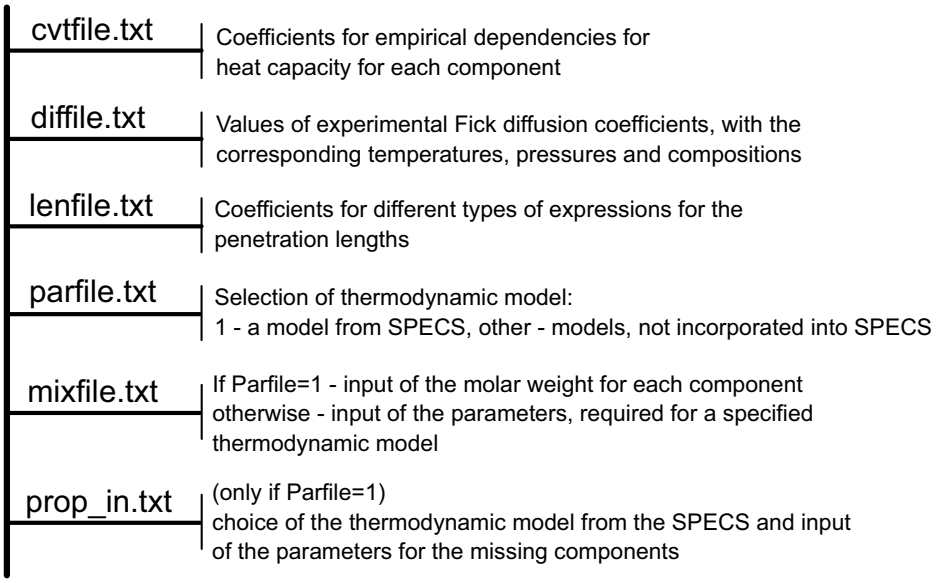

Figure A.4.1: Data, required for estimation of the diffusion coefficients for a given mixture.

The FTCode with slight modifications was applied to modeling the thermodiffusion coefficients within the framework of the fluctuation theory [143]. This proves the fact that the code is adjustable and can be used as a basis for future modeling of the transport properties within the FT framework [144].

A.5 Influence of the Thermodynamic Model

As discussed in Chapter 5 a thermodynamic model is required for estimation of the thermodynamic matrix and the thermodynamic factor, required for transforming of the Onsager coefficients into Fick diffusion coefficients.

The current appendix demonstrates the sensitivity of the diffusion coefficients upon the choice of a thermodynamic model and matrix, being applied to estimation of the thermodynamic factor.

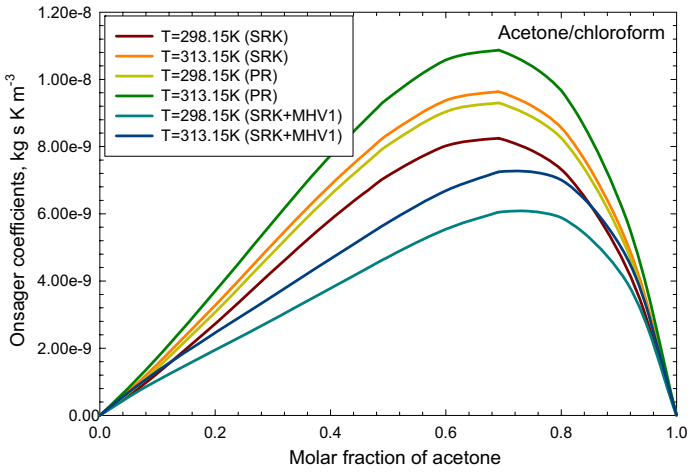

Figure A.5.1: Onsager phenomenological coefficients, estimated by application of different thermodynamic models for the mixture acetone/chloroform [158].

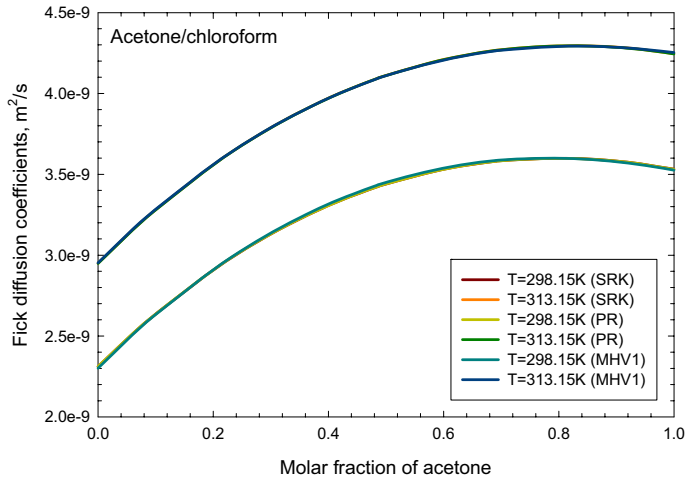

Figure A.5.2: Fick diffusion coefficients, estimated by application of different thermodynamic models for the mixture acetone/chloroform [158].

Figure A.5.2 demonstrates that although Onsager coefficients, estimated with the help of different thermodynamic models, differ essentially the resulting values of Fick diffusion coefficients coincide for different models. This is due to the difference in thermodynamic factors, used for recalculation of Onsager coefficients into the Fick diffusivities, estimated by different models (Table A.5.1).

Table A.5.1: Values of thermodynamic factor, used for recalculation of Onsager coefficients into the Fick diffusivities, estimated by different thermodynamic models

Molar fraction acetone	Thermodynamic factor, Eq. (5.10)					
	SRK EoS		PR EoS		SRK+MHV1 EoS	
	T=298.15K	T=313.15K	T=298.15K	T=313.15K	T=298.15K	T=313.15K
0.000	209670.0	213510.0	186010.0	189250.0	209690.0	213530.0
0.050	420.0	427.8	372.6	379.2	454.5	454.9
0.100	210.7	214.7	187.0	190.3	252.5	248.7
0.200	106.8	108.8	94.7	96.4	149.4	144.9
0.245	88.0	89.6	78.0	79.4	128.5	124.4
0.300	72.9	74.3	64.7	65.8	110.2	106.7
0.400	56.8	57.9	50.4	51.3	87.7	85.3
0.480	49.5	50.5	43.9	44.7	75.6	73.8
0.500	48.2	49.2	42.8	43.6	73.2	71.6
0.600	44.0	44.9	39.0	39.8	63.8	62.9
0.685	43.4	44.3	38.5	39.3	59.5	59.0
0.700	43.7	44.5	38.7	39.5	59.2	58.7
0.800	49.1	50.1	43.6	44.4	61.1	61.2
0.900	73.8	75.3	65.4	66.7	82.9	83.8
0.950	127.7	130.3	113.3	115.5	135.7	137.7
1.000	55159.0	56294.0	48910.0	49866.0	55166.0	56300.0

Oleg Medvedev

Diffusion Coefficients in Multicomponent Mixtures

ISBN: 87-90142-94-2